# Mechanistic Studies on Monocyte Migration into Multicellular Spheroids of Breast Tumor Origin


## Dissertation

Zur Erlangung des Doktorgrades der Naturwissenschaften (Dr. Rer. Nat.)
der Naturwissenschaftlichen Fakultät III –
Biologie und Vorklinische Medizin der Universität Regensburg

vorgelegt von
**Magdalena Książkiewicz**
aus Gdynia

Regensburg, 2009

Die Arbeit wurde angeleitet von: Prof. Dr. L. Kunz-Schughart

Promotionsgesuch eingereicht am: 30.10.2009

| | | |
|---|---|---|
| Prüfungsausschuss: | Vorsitzender: | Prof. Dr. R. Warth |
| | 1. Gutachter: | Prof. Dr. A. Kurtz |
| | 2. Gutachter: | Prof. Dr. L. Kunz-Schughart |
| | 3. Prüfer: | Prof. Dr. A. Göpferich |
| | Ersatzprrüfer: | Prof. Dr. E. Tamm |

# Mechanistic Studies on Monocyte Migration into Multicellular Spheroids of Breast Tumor Origin

# 1. Introduction

## 1.1 Breast cancer

### 1.1.1 Ethiology

Over 1 million breast cancer cases occur worldwide every year (Ferlay *et al*., 2001) and it is now first among cancers affecting women. Men can also develop breast cancer, however the accounts to only 1% of all breast cancers (Olivotto *et al*., 2006). With 429 900 new cases in Europe, breast cancer consisted 13.5% of all cancer occurrences in 2006 (Ferlay *et al*., 2007). Increased risk for breast cancer development includes various factors which can be grouped as fallows: hormones and reproductive factors; diet and diet related factors; ionizing radiation; family history of breast cancer; benign breast disease. Some risk factors are particularly related to reproductive life in women such as early age of menarche, late age at first birth, lack of breast feeding and oral contraceptives. Among endogenous risk factor, genetic predisposition is responsible for about 5-10% of all breast cancer incidences. The most important genes identified in this context are inherited mutations in BRCA1 and BRCA2 genes (Eeles, 1999). BRCA1 mutations appear to be responsible for 45% of breast cancers in families with multiple cases of breast cancer and BRCA2 is responsible for 35% of familiar breast cancers (National Cancer Institute 2005d)[1]. Other risks factors are listed in Fig. 1.1.

### 1.1.2 Classification

Breast cancer in most cases refers to malignancies in women that arise from the terminal ductal-lobular units of epithelial tissue (Stewart and Kleinhaus, 2003). Breast cancers can be differentiated into two main groups: non-invasive (*in situ*) and invasive breast cancer. Breast cancer *in situ* refers to a cancer where proliferation of presumably malignant epithelial cells is confined to the mammary ducts and/or lobules. Invasive breast cancer is capable of invading distant tissues – metastasizing. In both groups lobular and ductal carcinomas are distinguished. The most frequent malignant lesion of the breast (75-80%) is invasive (infiltrating) ductal carcinoma (Fig.1.2.). About 20% of infiltrating ductal carcinomas (IDC) can be categorized into histomorphological subtypes: tubular, medullar, mucinous,

[1] http://www.son.wisc.edu/ce/programs/asynch/bccd/BrCa1/BreastMod1AddlResources.pdf

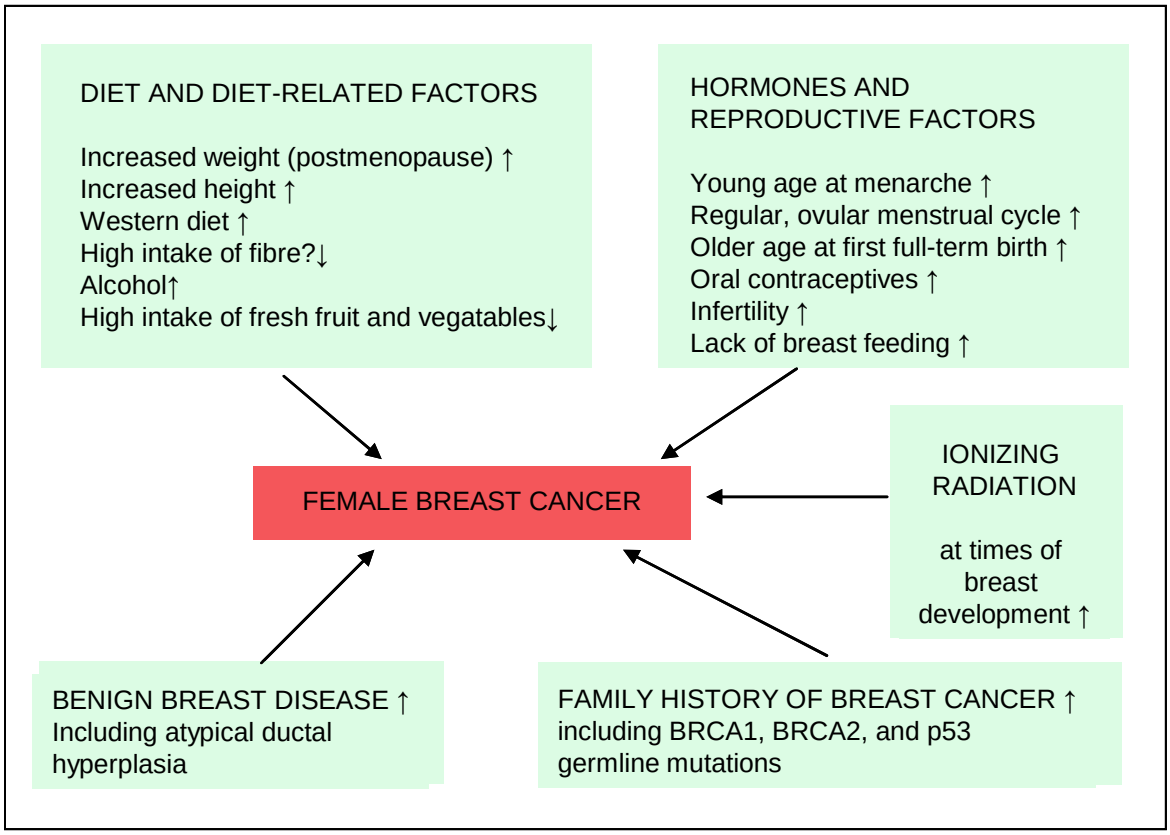


**Fig. 1.1 Risk and protective factors for breast cancer development. Factors associated with an increased (↑) or decreased (↓) risk of breast cancer (modified from Stewart B.W, Kleihues P, World Cancer Report 2003, p. 190; IARC Press, Lyon).**

papillary, micropapillary, metaplastic. The remaining 80% do not belong to any of these specific tumor sub-classes and are thus called “Not Otherwise Specified” (NOS) (Yoder *et al.*, 2007).

### 1.1.3 Invasive ductal breast cancer – desmoplastic reaction

Most invasive-ductal breast tumors develop a desmoplastic reaction, also termed scirrhous reaction. Desmoplastic response is a host mediated collagenous response and results from a complex interaction between the host and invading tumor cells. Desmoplastic regions consist of fibroblasts, inflammatory cells and vascular structures. This characteristic tumor appearance, often described as “lump”, can vary from a predominantly cellular form (fibroblasts/myofibroblasts) with little collagenous matrix to dense fibrous stroma with few stromal cells (Walker, 2001). The mechanism of desmoplasic reaction is not well understood and its role as prognostic marker for cancer is still disputed.

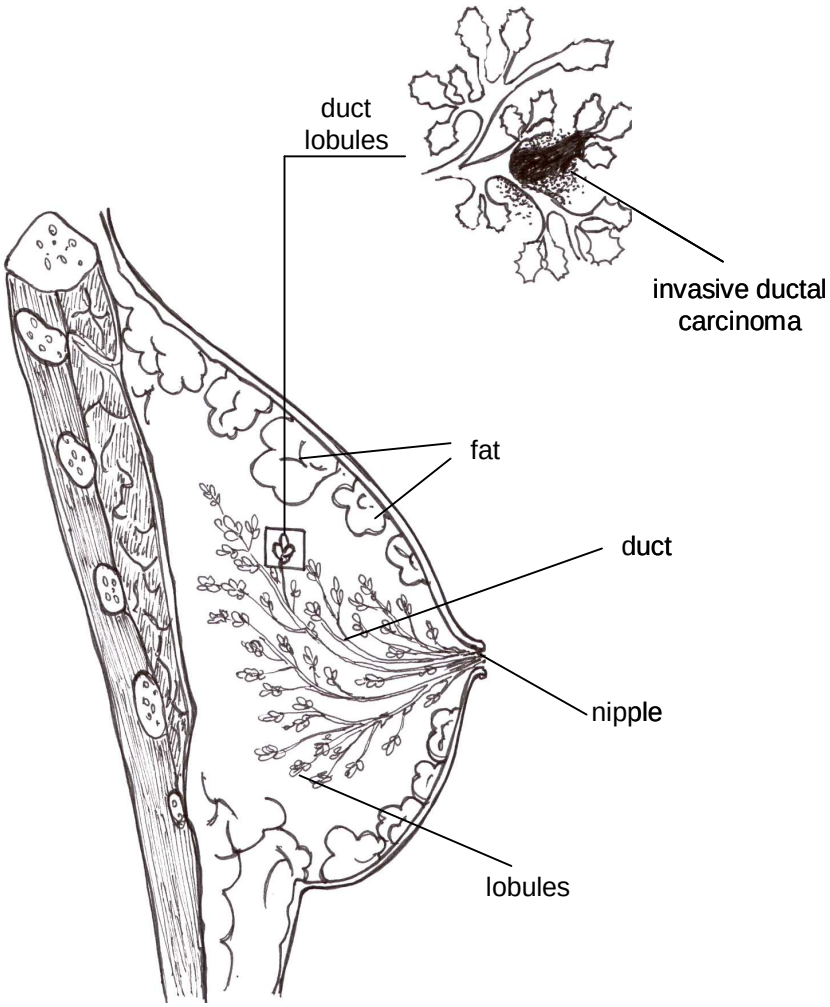


**Fig. 1.2 Diagram of the breast; enlarged is a cross-section of an invasive ductal carcinoma (modified from Meuret, 1995. Mammakarzinom. 2nd ed. Georg Thieme Verlag, Stuttgart ).**

Generally, desmoplasia in epithelial cancers is considered as a tumor promoting factor. This was proven in a variety of experimental tumor models in which an impact of stromal microenvironment on various stages of tumorigenesis was shown (Elenbaas and Weinberg, 2001). The work of Shao et al. indicated that the desmoplastic response in breast tumor carcinomas may be a substantial barrier to gene and immunotherapies (Shao *et al.*, 2000). On the other hand, such a barrier may also prevent tumor invasion (Vaage, 1992; Lieubeau *et al.*, 1994). Moreover, both carcinoma cells and stromal cells are known to secrete autocrine and paracrine factors which can be involved in growth stimulation or inhibition (Horgan *et al.*, 1987; Osborne *et al.*, 1989). Some authors report that the major initiator of tumor desmoplasia is the secretion of platelet-derived growth factor (PDGF) by breast carcinoma cells. Only tumor cells that secrete significant amounts of PDGF and at the same time lack expression of a PDGF receptor seem to exhibit a desmoplastic reaction (Shao *et al.*, 2000). Moreover, tumor progression may also be affected by other paracrine factors

released by stromal cells in the desmoplastic areas such as cytokines, ECM (Extracellular matrix) and ECM modulating molecules (Devalaraja and Richmond, 1999) as well as by direct cell-cell interactions between tumor and stromal cells such as fibroblasts (Steffen *et al.*, 1998).

## 1.2 Tumor heterogeneity

### 1.2.1 Cellular interactions in solid tumors

About 90% of human tumors arise as a consequence of genetic mutations in epithelial cells, leading to their abnormal proliferation. But these malignant cells are not isolated islands, they are surrounded by a peritumoral stroma comprised of diverse host cell types (immunocompetent cells, inflammatory cells, fibroblasts and endothelial cells) and extracellular matrix (ECM) (Hanahan and Weinberg, 2000). Tumor cells influence their microenvironment (Fig. 1.3) and for example induce a desmoplastic reaction as described earlier, and in turn the surrounding cells critically affect the multistep process of carcinogenesis and the malignant phenotype (van Roozendaal *et al.*, 1995).

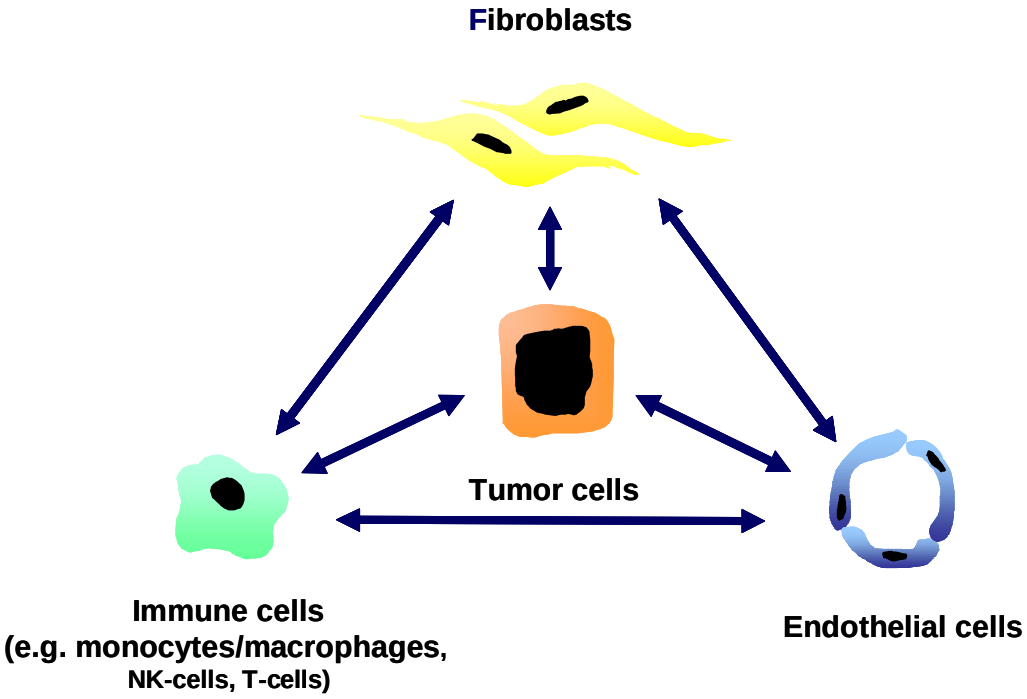


**Fig. 1.3 Heterologous cellular interactions in solid tumors (Kunz-Schughart & Knuchel, Histol. Histopathol. 2002a, 17: 599-621).**

### 1.2.2 Tumor-associated fibroblasts (TAF)

There is increasing evidence that fibroblasts, the predominant stromal cell type in tumor desmoplasia, are involved in tumor progression and can no longer be considered as passive structural elements (Wernert, 1997; Elenbaas and Weinberg, 2001; Kunz-Schughart and Knuechel, 2002a; Kunz-Schughart and Knuechel, 2002b). These fibroblasts differ phenotypically from the normal one. Hence, fibroblast contributing to the tumor stroma are termed reactive stroma, peritumoral fibroblasts, carcinoma-associated fibroblasts or, as in current thesis, tumor-derived/tumor-associated fibroblasts (TAF). At both, primary and metastatic sites of tumors, TAF are able to influence proliferation, differentiation and invasion of malignant cells (van den Hoff, 1991). Fibroblasts are an extremely heterogenous population of cells and also can give rise to different types of TAF (Schor *et al.*, 1994; Gregoire and Lieubeau, 1995).

Fibroblasts derived from breast carcinomas, as compared to those from normal breast tissue, show an altered, oncogenic and/or myofibroblastic phenotype. One special feature is the synthesis of intracellular $\alpha$-smooth muscle actin (Brouty-Boye *et al.*, 1991; Ronnov-Jessen *et al.*, 1996; Schurch, 1999). TAF can contain high levels of myofibroblasts, up to 80% of the whole population (Heimdal *et al.*, 2001). According to literature data, the presence of myofibroblast characteristics in the desmoplastic reaction of tumors is positively correlated with tumor invasiveness (De Wever and Mareel, 2002; De Wever *et al.*, 2008). TAF also differ in cell surface (integrins, cell adhesion molecules) and secretory (growth factors, cytokines/chemokines) protein expression (Kunz-Schughart and Knuechel, 2002a) that act on the epithelial tumor cells and can promote tumor growth (Elenbaas and Weinberg, 2001). However, not only TAF from invasive cancers but also fibroblasts derived from benign prostatic hyperplasia may, in contrast to normal fibroblasts, show tumor promoting ability when admixed with nontumorigenic prostate epithelial cell line (Olumi *et al.*, 1999).

Several growth factor levels have been found to be elevated in such fibroblasts. Once secreted, growth factors can stimulate growth of tumor cells by paracrine signaling, induce autocrine loops or positively impact tumor angiogenesis. Examples of such growth factors expressed in stroma are the insulin like-growth-factors (IGF-I and IGF-II) which are mitogens for different cell types including fibroblasts and epithelial cells and therefore exert probably both auto- and paracrine effects on tumor growth. IGFs are expressed in stromal fibroblasts of breast cancers and the expression of IGF-II in particular correlates with tumor progression (Yee *et al.*, 1989; Cullen *et al.*, 1992).

Epithelial tumor cells express molecular mediators such as TGF-β which interact with the surrounding cells. In breast cancers expression of high level of TGF-β1 is positively correlated with disease progression (Gorsch *et al.*, 1992). According to research performed by several groups, TGF-β1 can induce differentiation of cell-cycle arrested fibroblasts into myofibroblasts in culture and may thus relate to the of myofibroblasts presence in desmoplastic tumors which positively correlates with tumors invasiveness (Ronnov-Jessen and Petersen, 1993; Vaughan *et al.*, 2000).

### 1.2.3 Tumor-associated macrophages (TAM)

Many solid tumors are characterized by the presence of leukocytic infiltrate. Tumor-associated macrophages (TAM) are a major component of the infiltrate in tumors. They primarily arise as a result of abnormal maturation of monocytes (MO) migrated into tumor tissues from the blood stream (van Ravenswaay C *et al.*, 1992). TAM were first investigated for their role in antitumor response, later studies showed that cancer induce functional abnormalities leading to an immature macrophage phenotype that can promote tumor growth (Mantovani *et al.*, 1992; Sunderkotter *et al.*, 1994). Those findings revealed a dual role of macrophages (MAC) in cancer. Macrophages, after their activation by antibodies, LPS or IFN-γ can mediate reduction of tumor growth by non-specific anti-tumor cytotoxic mechanisms (direct cytotoxicity) or induction of specific cell lytic effects (indirect cytotoxicity) (Grabbe *et al.*, 1994; Blachere *et al.*, 1997). Activated MAC can release reactive oxygen intermediates (ROIs) (Young and Hardy, 1995), cytokines (Jones and Millar, 1989; Weiser *et al.*, 1991) and metalloproteinases (Gorrin-Rivas *et al.*, 2000), which can take part in antitumor response. On the other hand, TAM have been shown to play a key role in tumor progression by their ability to producing of various factors and employing different mechanisms as shown below in Tab. 1.1 (al-Sarireh and Eremin, 2000).

Similarly to dual role of MAC/TAM in cancer, there are conflicting data on the relevance of extensive TAM infiltration in cancer progression. The presence of TAM infiltration correlates with poor prognosis in carcinomas of the breast, cervix and bladder (Bingle *et al.*, 2002). The observations in brain, prostate and lung tumors, however, are contradictory (Bingle *et al.*, 2002). Thus may be due to the fact that TAM can inhibit tumor growth and destroy neoplastic cells, but also support tumor development, metastasis and angiogenesis (Brigati *et al.*, 2002; Tsung *et al.*, 2002; Schoppmann *et al.*, 2002). Which of these functions is dominant may depend on the differentiation status of TAM which is affected by the tumor cells, their stroma and environment. As reported by Nesbit et al., tumor tissue expressing high level of CCL2 was extensively infiltrated by MO and the tumor mass was eliminated.

Tumor tissue expressing low level of CCL2, were moderately infiltrated by MO and these tumors showed pronounced angiogenesis and rapid tumor growth (Nesbit *et al.*, 2001). These data demonstrate the contradictory role of TAM infiltrates in tumors.

**Tab. 1.1 TAM and tumor progression (Al-Sarireh & Eremin, J.R.Coll.Surg. Edinb. 2000, 45: 1-16)**

| Mechanism | Mediator(s) |
|---|---|
| Enhanced Growth | Growth factors (EGF, PDGF, TGF-β)<br><br>Cytokines (IL-6, IL-1, TNF-α)<br><br>L-arginine derived polyamine |
| Enhanced Angiogenesis | Through production of various cytokines (GM-CSF, TGF-α, TGF-β, IL-1, IL-6, IL-8) and prostanoids<br><br>Procoagulant activity |
| Invasion and Dissemination | Cytokines (TNF-α, IL-1)<br><br>Lytic enzymes (metaloproteinases and plasminogen activator) |
| Immunosuppression | Prostanoids ($PGE_2$)<br><br>Cytokines (IL-10) and other mediators (TGF-β) |

## 1.3 Classification of MO subpopulations

Monocytes (MO) are part of the human mononuclear phagocyte system and constitute three to eight percent of the leukocyte in the human blood. They play a role in processes such as antigen presentation, phagocytosis and inflammation. They secrete different molecules, including chemokines that are important in infectious processes and malignancy (Nathan, 1987; Ziegler-Heitbrock, 1989). MO derive from myelomonocytic stem cells in bone marrow which give rise to monoblasts, that develop into MO. MO circulate in the blood stream for about 1-3 days. Then they migrate into the various tissues and mature into different types of MAC depending on their location. MO are also assumed the primary and major leukocyte infiltrate in tumor tissue and the main source of TAM.

The first attempts to classify MO focused on their differences in size and density. Using gradient centrifugation and elutriation two main subsets of MO were distinguished which differed phenotypically and functionally: a major subpopulation of “regular MO” and a minor one of “intermediate MO”. The smaller and denser “regular MO” produced fewer reactive oxygen intermediates, exhibited higher antigen presenting capacity and proliferated with lower activity than “intermediate MO” (Yasaka *et al.*, 1981; Turpin *et al.*, 1986; Inamura *et al.*, 1990). Via rosetting with antibody-coated erythrocytes, Fcγ receptor positive (FcγR+) and negative (FcγR-) monocytes could be separated and the FcγR- MO were found to have a greater antigen-presenting capacity (Zembala *et al.*, 1984; Szabo *et al.*, 1990). Subpopulations were also defined on the basis of adherence to fibronectin (FN)-coated surfaces. Fn adherent cells constitute about 20% of all monocytes (Brown *et al.*, 1989). The Fn-adherent MO were found to express 20-fold more peroxidase activity as compared to the non-bound MO (Owen *et al.*, 1992). It is noted, however, that the selection methods mentioned did not lead to pure MO population and the accuracy of analyses was affected by contamination of other cell types.

A more accurate phenotypic analysis of MO is possible by the use of flow cytometry and employing two- or multi-color immunofluorescence. Ziegler-Heitbrock defined blood MO based on the expression of CD14 antigen (major receptor for bacterial lipopolisacharide) and CD16 antigen (Fcγ receptor type III) expression. This approach revealed that about 90% of all MO strongly express CD14 and are at the same time CD16-negative ($CD14^{++}CD16^{-}$). A minor population of MO co-expresses $CD14^{+}$ and $CD16^{+}$ at low level (Ziegler-Heitbrock, 1996). The same author also showed that the $CD14^{+}CD16^{+}$ subpopulation can be described as pro-inflammatory. It produces pro-inflammatory cytokines such as TNF, IL-1 and IL-6 but not anti-inflammatory IL-10. $CD14^{+}CD16^{+}$ cells

increase in number in diseases like sepsis (Fingerle *et al.*, 1993), HIV+ and AIDS (Dunne *et al.*, 1996; Zembala *et al.*, 1997), which are characterized by high cytokine production (Ziegler-Heitbrock, 1996). Using the CD14/CD16 staining and additional markers Rothe and coworkers defined six different subsets of MO ($CD14^{++}CD16^{-}$, $CD14^{+}CD16^{-}$, $CD14^{++}CD16^{+}$, $CD14^{+}CD16^{-}CD33^{dim}$, $CD14^{+}CD16^{-}CD33^{high}$, $CD14^{++}CD16^{+}CD56^{+}$) (Rothe *et al.*, 1996). The use of CD markers showed that the heterogeneity of blood MO is enormous. It is highly relevant to elucidate the functional and clinical significance of the different MO subsets in health and disease and their potential to differentiate into a tumor-promoting TAM phenotype.

## 1.4 Proinflammatory cytokines

### 1.4.1 The family of chemokines

Chemokines are small, low molecular weight (8-11 kDa) proinflammatory cytokines, which are characterized by their ability to induce migration and activation of specific leukocyte subsets (Kunkel, 1985; Baggiolini and Dahinden, 1994 ;Hedrick and Zlotnik, 1996). They play a role in inflammatory diseases (Murdoch and Finn, 2000), can act as autocrine and paracrine growth factors, induce angiogenesis, regulate metastasis, and influence tumor rejection (Wang *et al.*, 1998). The large family of chemokines, containing nearly 50 members, is divided into subfamilies based on their structural motifs. Most chemokines contain conserved cysteines residues, which are important for their secondary structure. Based on the spacing of the first two cystein residues they are classified into four groups: CXC ($\alpha$), CC ($\beta$), C ($\gamma$) and CX3C ($\delta$) where C stands for cysteine and X for any other amino acid (Rollins, 1997; Baggiolini, 1998). Considering their activities, chemokines can be divided into homeostatic chemokines which regulate traffic and activation of leukocytes, and the so-called inflammatory chemokines which trigger functional immune response (Mellado *et al.*, 2001a).

Chemokines can be produced by almost every nucleated cell type under appropriate conditions (Gale and McColl, 1999). Most chemokines are expressed in response to stimulus, but some are constitutively expressed in a tissue-specific manner and may also depend on the origin of cells. The BRAK chemokine is, for example, constitutively expressed at high levels in squamous epithelium, but require a stimulus to be expressed by inflammatory cells and certain cancers (Frederick *et al.*, 2000). The most important ones shown to affect monocyte migration are CCL2, CCL3, CCL5, CCL4, which belong to the CC group of chemokines and signal via binding to so-called CCR receptors (see Tab. 1.2).

**Tab. 1.2 The chemokine receptor family (modified from Murphy, Pharmacol. Rev. 2002, 54: 227-229)**

| Name | Main Agonists | Main Functions |
|---|---|---|
| CR subgroup | | |
| XCR1 | XCL1-2 | T cell trafficking |
| CCR subgroup | | |
| CCR1 | CCL3, CCL5, CCL7, CCL8, CCL13-16, CCL23 | T cell and monocyte migration; innate and adaptive immunity; inflammation |
| CCR2 | CCL2, CCL7, CCL8, CCL13 | T cell and monocyte migration; innate and adaptive immunity; Th1 inflammation |
| CCR3 | CCL5, CCL7, CCL8, CCL11, CCL13, CCL15, CCL24, CCL26 | Eosinophile, basophile, and T cell migration; allergic inflammation |
| CCR4 | CCL17, CCL22 | T cell and monocyte migration; allergic inflammation |
| CCR5 | CCL3, CCL4, CCL5, CCL8, CCL14 | T cell and monocyte migration; innate and adaptive immunity; HIV infection |
| CCR6 | CCL20 | Dendritic cell migration |
| CCR7 | CCL19, CCL21 | T cell and dendritic cell migration; lymphoid development; primary immune response |

| | | |
|---|---|---|
| CCR8 | CCL1, CCL4, CCL17 | T cell trafficking |
| CCR9 | CCL25 | T cell homing to gut |
| CCR10 | CCL26-28 | T cell homing to skin |
| CXCR subgroup | | |
| CXCR1 | CXCL8 | Neutrophile migration; innate immunity; acute inflammation |
| CXCR2 | CXCL1-3, CXCL5-8 | Neutrophile migration; innate immunity; acute inflammation; angiogenesis |
| CXCR3 | CXCL9-11 | T cell migration; adaptive immunity; Th1 inflammation |
| CXCR4 | CXCL12 | B cell lymphopoiesis; bone marrow myelopoiesis; central nervous system and vascular development; HIV infection |
| CXCR5 | CXCL13 | B cell trafficking; lymphoid development |
| CXCR6 | CXCL16 | T cell migration |
| CX3CR subgroup | | |
| $CX_3CR1$ | CX3CL1 | T cell and NK cell trafficking and adhesion; innate and adaptive immunity; Th1 inflammation |

### 1.4.2 Chemokine receptors and their signaling pathways

All chemokine receptors belong to the seven-transmembrane G protein-coupled receptor (GPCR) family. This receptor family contains a single polypeptide chain with an extracellular and a cytoplasmic region. The extracellular region is composed of the N-terminus and three extracellular loops, which bind the chemokine ligand. The intracellular region of receptor consists of three loops and C-terminus, which is responsible for signal transduction (Murphy, 1994). The chemokine receptors can also be grouped into four families: CR, CCR, CXCR and CX3CR, which interacts with the respective chemokines subfamilies C, CC, CXC and CX3C (Murphy *et al.*, 2000). Receptors which belong to these four subfamilies are listed in Tab. 1.2.

Chemokine receptors show a promiscuous behavior. As summarized in Tab. 1.2, many chemokine receptors bind more than one chemokine with varying affinities. CCR1, for example, bind with high affinity CCL3 (MIP-1$\alpha$), CCL5 (RANTES), CCL7 (MCP-3), CCL8 (MCP-2), CCL14 (HCC-1), CCL15 (Lkn-1) and CCL23 (MPIF-1) and with low affinity CCL4 (MIP-1$\beta$) and CCL2 (MCP-1). Moreover, individual chemokines act as ligand for different receptors. MCP-3, for example, acts as a ligand for CCR1, CCR2, CCR3 and CCR5 receptors (Murphy *et al.*, 2000; Chou *et al.*, 2002).

Chemokine signaling involves the activation of a G-protein pathway. Interaction of a chemokine with its receptor leads to exchange of GDP for GTP and the dissociation of the $\alpha$-subunit from the $\beta\gamma$-subunit. Dissociated subunits are able to activate several intracellular signaling pathways including the cAMP/protein kinase A pathway, the mitogen-activated protein kinases (MAPK) pathway, the phosphatidylinositol/calcium/protein kinase C pathway and the c-Jun N-terminal kinases (JNK) pathway (Hamm, 1998; Lefkowitz, 1998; Iacovelli *et al.*, 1999). The majority of the responses to chemokines are inhibited by pertussis toxin (PTX), due to the involvement of $G_i$ proteins in signal transduction which are affected by PTX (Mellado *et al.*, 1998; Rodriguez-Frade *et al.*, 1999b). However, several G-protein-independent pathways can be also activated as e.g. JAK/STAT (Janus kinase/signal transducer and activator of transcription) cascade (Mellado *et al.*, 1998; Williams, 1999).

The JAK/STAT cascade is activated as result of the chemokine receptor homo- or hetero-dimerization (Molino *et al.*, 2000) (Fig. 1.4). This process was first demonstrated for CCR2, receptor for CCL2 (Rodriguez-Frade *et al.*, 1999a). Today, it is well established that many chemokine receptors, if not all, must undergo a process of dimerization to become activated (Rodriguez-Frade *et al.*, 1999a; Rodriguez-Frade *et al.*, 2001; Mellado *et al.*, 2001a;

Mellado *et al.*, 2001b). A scheme of the chemokine receptor signaling pathways is given in Fig. 1.4.

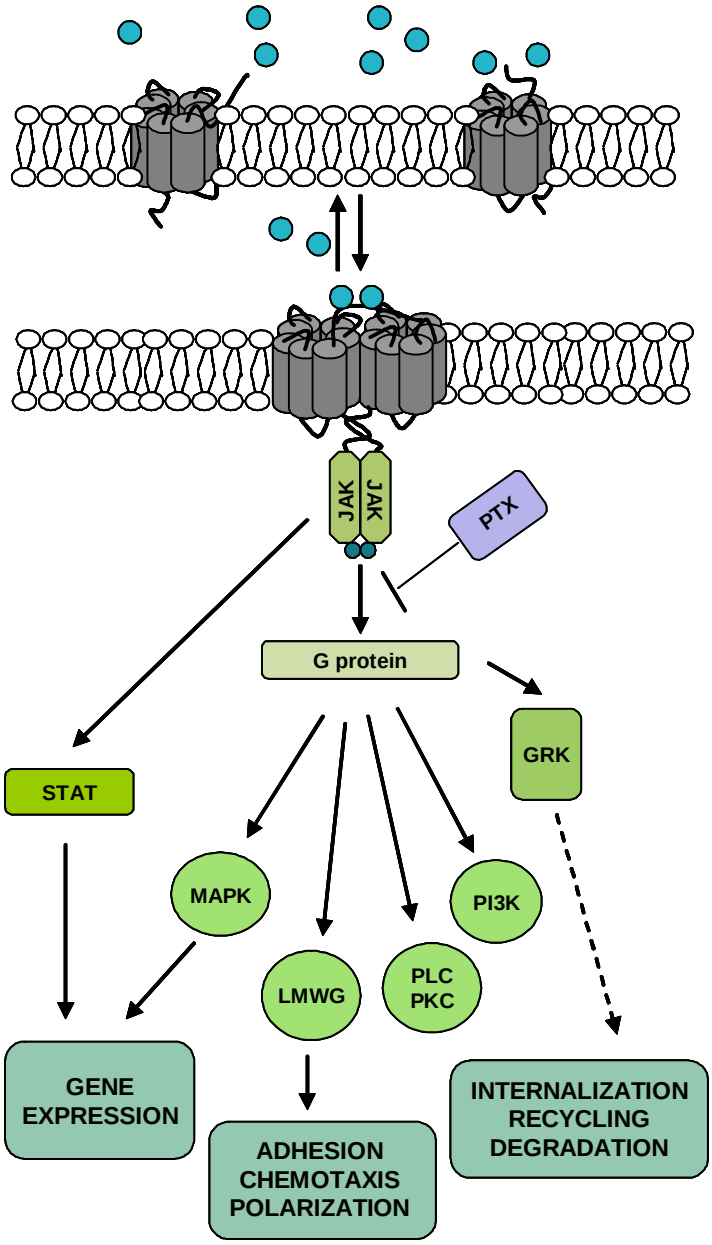


**Fig. 1.4 Schematic model of signaling pathways activated following chemokine binding to receptors. The figure shows some of the molecules involved in these pathways and the effects on cells. JAK: Janus-Kinase; STAT: Signal Transducer and Activator of Transcription; MAPK: MAP-Kinase; LMWG: Low Molecular Weight G-proteins; PLC: Phospholipase C; PKC: Proteinkinase C; PI3K: Phosphatidylinositol-3-Kinase; GRK: G-protein-coupled Receptor Kinases; PTX: Pertusis toxin (modified from M. Mellado et al. Annu. Rev. Immunol. 2001, 19: 397-421).**

### 1.4.3 CCL2 as a member of chemokine family

CCL2, also known as monocyte chemoattractant protein -1 (MCP-1), belongs to the CC subfamily of inflammatory chemokines (Bacon *et al.*, 2002). According to its biological role, it belongs to the group of inflammatory chemokines. Although it was first identified in 1989 as a substance secreted by malignant cells, that promotes monocyte migration (Yoshimura *et al.*, 1989; Van Damme *et al.*, 1989), it is also produced by non-malignant cell types. *In vitro*, constitutive secretion of human CCL2 has been reported for several solid tumor cell lines (Bokoch, 1995; Mellado *et al.*, 1998), fibroblasts (Sanchez-Madrid and del Pozo, 1999) and monocytic human cell lines (Mellado *et al.*, 2001a). It can, however, also be produced by endothelial cells following stimulation by cytokines, viruses, endotoxins and other substances like phorbol esters or lipopolisacharide (Proost *et al.*, 1998).

CCL2 induces cellular migration by binding to and activating the specific CC chemokine family receptor CCR2. The CCR2A/2B receptor exists in two isoforms named A and B. The isoforms are alternatively spliced variants of a single receptor gene that differ only in the sequence of the cytosolic carboxyl-terminal tail. The CCR2B isoform seems to be predominant one (Charo *et al*., 1994; Wong *et al*., 1997). CCR2A/2B is expressed on the surface of monocytes, activated memory T cells, B cells and basophilees (Frade *et al.*, 1997; Rabin *et al.*, 1999). CCR2A/B is important in inflammation and host defense mechanism (Kuziel *et al.*, 1997; Boring *et al.*, 1997; Gonzalo *et al.*, 1998). In addition to CCL2, CCR2A/2B can be activated by other inflammatory/inducible ligands such as CCL7 (MCP-3), CCL8 (MCP-2), CCL13 (MCP-4) (Charo *et al.*, 1994; Gong *et al.*, 1997).

CCL2 particularly attracts MO as originally described by Matsushima et al. (Matsushima *et al.*, 1989). However, it can also induce migration of other cell types such as activated CD4 positive and CD8 positive memory T-cells, lymphocytes or NK cells (Leonard and Yoshimura, 1990; Carr *et al.*, 1994). CCL2 plays a role in several physiological and pathophysiological states where MO/MAC infiltration and/or their activation is an important phenomenon. Among them are cancers, inflammatory heart disease, asthma, rheumatoidal arthritis, inflammatory skin diseases, bronchial infections, liver diseases and sepsis (Rollins and Sunday, 1991; Strieter *et al.*, 1994; Baggiolini and Dahinden, 1994; Bossink *et al.*, 1995; Schroder *et al.*, 1996).

## 1.5 Objective

In ductal breast carcinomas a high macrophage content is correlated with poor prognosis and clinical outcome (Leek *et al.*, 1996). These TAM originate from blood MO that have migrated into tumor tissue where they undergo abnormal differentiation and/or maturation. Little is known about the impact of desmoplastic fibroblast on these processes. Previous studies performed in our laboratory have shown that the proportion of MO migrating into spheroids of breast tumor-derived fibroblasts is significantly higher than in spheroids from normal skin and breast fibroblasts (Silzle *et al.*, 2003). The recorded data imply the existence of a particular subpopulation of 10 to 15% in the blood MO pool which is capable to infiltrate spheroids of tumor-derived fibroblasts. Furthermore, it was documented that MO to fibroblasts ratio in co-cultures of normal and tumor-derived fibroblasts is correlated with the CCL2 release. Neutralization of endogenous CCL2 in conditioned media from breast tumor derived fibroblast spheroids, however, led to a pronounced reduction of MO migration only in a Boyden-Chamber assay, while the same antibody was inefficient in 3-D culture. This observation could result from:

- insufficient distribution/penetration of the antibody in the spheroids
- high accumulation of CCL2 within the spheroid that cannot be blocked with the antibody concentration applied
- a CCL2 signaling pathway that does not play a significant role in MO migration into 3-D fibroblast cultures

With this background, the aim of the present thesis was:

1. to verify the relevance of paracrine factors and in particular of CCL2/CCR2 signaling for MO migration into spheroids of fibroblasts and tumor cells of breast tumor origin.
2. to identify and/or characterize the migrating blood MO subpopulation.

In order to achieve these goals a three-dimensional (3-D) cell co-culture model under well defined conditions was applied, according to the one used by T. Silzle et al. (Silzle *et al.*, 2003). The model allows to mimic and investigate interactions of fibroblasts and tumor cells, respectively, with MO *in vitro*.

MO migration into spheroids of breast-tumor derived fibroblast and also of defined breast carcinoma cell lines (MCF-7, T47D, Hs578T, BT549, BT474) was investigated and CCL2 secretion was analyzed.

The different experimental approaches to study the phenomenon of MO migration into fibroblastic tumor regions included: wash-out and addition of chemokines to modulate the

co-cultures' milieu; application of siRNA; preincubation of MO with toxins and blocking antibodies.

For studying the migratory activity of MO subpopulations, blood MO were stained for defined surface antigens and subpopulations were isolated using fluorescence-activated cell sorting (FACS) prior to spheroid exposure. Finally, gene expression profiles of migrated *vs*. non-migrated MO were compared using cDNA array analyses.

# 2. Materials and Methods

## 2.1 Materials

### 2.1.1 Cell lines and primary cells

#### 2.1.1.1 Human breast cancer cell lines

Five different breast cancer lines were used in this study. Cell lines Hs578, MCF-7 and BT549 were purchased from the ATCC, cell line T47D was from the ECACC and BT474 was from the Tumorbank Heidelberg. All cell lines were free from mycoplasm as routinely verified by luminescence based mycoplasma test systems (Myco Alert Mycoplasma Detection Kit, Cambrex).

T47D (Keydar *et al.*, 1979; Sommers *et al.*, 1994)
This cell line was isolated from a pleural effusion obtained from a 54-year-old female patient with breast infiltrating ductal carcinoma.
Hypertetraploid, ER+, PR+
*In vitro* invasion: +

Hs578 (Hackett *et al.*, 1977; Sennerstam and Auer, 1993; Sommers *et al.*, 1994)
Cell line derived from a carcinoma of the breast obtained from a mammary gland of a 74-year-old female patient (Hackett *et al.*, 1977). This line had a mixed polygonal morphology initially, but a stellate cell type was selected during passageing and cloning. Cells are tumorigenic in immunosuppressed mice.
Hyperdiploid, ER-, PR-
*In vitro* invasion: +++

MCF-7 (Sugarman *et al.*, 1985; Sommers *et al.*, 1994)
The cell line is originated from malignant mammary gland tissue of a 69-year-old female patient with a differentiated, infiltrating ductal carcinoma.
Hypertriploid to hypertetraploid, ER+, PR+
*In vitro* invasion: +

BT549 (Smith *et al.*, 1985;Sommers *et al.*, 1994; Katayose *et al.*, 1997)
This cell line was isolated from malignant mammary gland tissue of a 72-year-old female patient with a papillary, invasive ductal tumor which had metastasized into regional lymph nodes.
Hyperdiploid, ER-, PR-

*In vitro* invasion: +++

BT474 (Lasfargues *et al.*, 1978; Sommers *et al.*, 1994)
The cell line was originated from malignant mammary gland tissue of a 60-year-old female patient, with a solid, invasive ductal carcinoma. Cells are tumorigenic in athymic mice.
Hypertetraploid, ER+, PR+
*In vitro* invasion: +

#### 2.1.1.2 Primary cells

*Fibroblasts:*
VF1 – normal foreskin from child
PF27T – invasive ductal adenomatous carcinoma of mammary gland in stage G2
PF37T – invasive ductal adenomatous carcinoma of mammary gland in stage G2
PF53T – invasive ductal adenomatous carcinoma of mammary gland in stage G2

*Monocytes:*
Peripheral-blood mononuclear cells (MNC) were obtained by leukopheresis of healthy donors. Monocytes (MO) were isolated from MNC by counter current centrifugal elutriation.

### 2.1.2 Media, buffers and supplements

#### 2.1.2.1 Media and supplements

| | |
|---|---|
| Accutase | PAA Laboratories GmbH, Pasching, Austria |
| Amphotericin B | PAA Laboratories GmbH, Pasching, Austria |
| Collagenase III | PAN Biotech GmbH, Aidenbach, Germany |
| D-(+)-Glucose (45% in tissue culture grade water) | Sigma-Aldrich CHEMIE GmbH, Steinheim, Germany |
| DMEM | PAN Biotech GmbH, Aidenbach, Germany |
| FCS | PAN Biotech GmbH, Aidenbach, Germany |
| Opti-MEM I Reduced Serum Medium with GlutaMAX I | Invitrogen GmbH, Karlsrue, Germany |
| Penicillin/Streptomycin | PAN Biotech GmbH, Aidenbach, Germany |
| RPMI-1640 | PAN Biotech GmbH, Aidenbach, Germany |
| Trypsin/EDTA | PAN Biotech GmbH, Aidenbach, Germany |
| | |
| Freezing medium for MO | 70% RPMI, 20% FCS, 10% DMSO |

| | |
|---|---|
| Medium for primary fibroblast culturing | 80% DMEM, 20% FCS, 25 mM glucose, 100 U/ml penicillin, 100 µg/ml streptomycin, 25 µg/ml amphotericin B |
| Standard freezing medium | 90% FCS, 10% DMSO |
| Standard medium | 90% DMEM, 10% FCS, 100 U/ml penicillin, 100 µg/ml streptomycin |

#### 2.1.2.2 Buffers and reagents for cell culturing and flow cytometry

| | |
|---|---|
| Blocking/Wash Buffer used for FC | PBS pH 7,2-7,4<br>1% FCS |
| CASYton (dilution liquid for cell cultures) | Schärfe System GmbH, Reutlingen, Germany |
| DMSO | Merck, Darmstadt, Germany |
| PBS | PAN Biotech GmbH, Aidenbach, Germany |

#### 2.1.2.3 Buffers and reagents for immunohistochemistry

| | |
|---|---|
| DAB Chromogen | DAKO Cytomation, Glostrup, Denmark |
| Diluent buffer | DAKO Cytomation, Glostrup, Denmark |
| Entellan | Merck, Darmstadt, Germany |

#### 2.1.2.4 Reverse Transcription PCR buffers and reagents

| | |
|---|---|
| Buffer M-MuLV RT | Fermentas, St. Leon-Rot, Germany |
| DEPC-treated Water ($H_2O_{DEPC}$) | Fermentas, St. Leon-Rot, Germany |
| dNTP Mix | Invitrogen, Friesoythe, Germany |
| DTT | Invitrogen, Friesoythe, Germany |
| Random Hexamer Primer | Fermentas, St. Leon-Rot, Germany |
| ReverAid M-MuLV Reverse Transcriptase | Fermentas, St. Leon-Rot, Germany |

### 2.1.3 Antibodies

**Tab. 2.1 Primary antibodies applied in flow cytometry and immunohistochemistry**

| Antibody | Origin | Clone | Conjugate | Distributor |
|---|---|---|---|---|
| anti-human CD90 | mouse | AS02 | FITC | Dianova GmbH, Hamburg, Germany |
| anti-human CD14 | mouse | TüK 4 | PE/Cy5 | Immunotools, Friesoythe, Germany |
| anti-human CD16 | mouse | LNK16 | PE | Immunotools, Friesoythe, Germany |
| anti-human CD11a | mouse | MEM-25 | - | Immunotools, Friesoythe, Germany |
| anti-human CD11b | mouse | MEM-174 | - | Immunotools, Friesoythe, Germany |
| anti-human CD49e | mouse | SAM-1 | FITC | Acries Antibodies GmbH, Hiddenhausen, Germany |
| anti-human CD45 | mouse | HI30 | APC | Caltag Laboratories GmbH, Hamburg, Germany |
| anti-human CD45 | mouse | 2B11+PD7/26 | - | DAKO, Glostrup, Denmark |
| anti-human CKpan | mouse | KL1 | - | Immunotech, Marseille, France |
| anti-human CD31 | mouse | JC/70A | - | DAKO, Glostrup, Denmark |
| anti-human α-SML | mouse | asm-1 | - | Dianova GmbH, Hamburg, Germany |
| anti-human DOC-3 | mouse | - | - | kindly provided by Prof. Dr. Matthias Mack, Inner Medicine II, University of Regensburg, Germany |

**Tab. 2.2 Isotype control and secondary antibodies applied in flow**

| Antibody | Origin | Clone | Conjugate | Distributor |
|---|---|---|---|---|
| *Isotypes* | | | | |
| IgG1 | mouse | 203 | - | Immunotools, Friesoythe, Germany |
| IgG2 | mouse | 713 | - | Immunotools, Friesoythe, Germany |
| *Secondary Ab* | | | | |
| goat-anti-mouse | goat | polyclonal | PE | DAKO GmbH, Hamburg, Germany |
| goat-anti-mouse | goat | polyclonal | FITC | Immunotools, Friesoythe, Germany |

### 2.1.4 Nucleotides

#### 2.1.4.1 siRNA constructs

| | |
|---|---|
| Negative Control siRNA Alexa Fluor 488 | Qiagen, Hilden, Germany |
| Self-designed siRNAs | IBA GmbH Göttingen, Germany |
| Silencer Validated siRNA CCL2 (sequence not available) | Ambion/Applied Biosystems, Darmstadt, Germany |

**Tab. 2.3 Sequences of siRNA constructs for MCP-1 gene silencing**

| siRNA construct | Sequence |
|---|---|
| Alexa Fluor 488<br>(negative control) | 5’ UUC UCC GAA CGU GUC ACG UdT dT 3’--AlexaFluor488<br>3’ ACG UGA CAC GUU CGG AGA AdT dT 5’ |
| 1 ds siRNA<br>(self-designed) | 5’ GGG CUC GCU CAG CCA GAU GCA TT 3’<br>3’ TT CCC GAG CGA GUC GGU CUA CGU 5’ |
| 2 ds siRNA<br>(self-designed) | 5’ GUG GUC CCA AAG AAG CUG UGA TT 3’<br>5’ TT CAC CAG GGU UUCUUC GAC ACU 5’ |
| 2 ds siRNA (self-designed) | 5’ GGG CUC GCU CAG CCA GAU GCA TT 3’ |
| 2 se siRNA (self-designed) | 5’ GUG GUC CCA AAG AAG CUG UGA TT 3’ |

### 2.1.4.2 PCR primers for real-time PCR

CCL2 Real Time PCR primers (Muhlbauer *et al.*, 2003) — Metabion, Martinsried, Germany

Housekeeping Gene 18S Real Time PCR primers — Metabion, Martinsried, Germany

**Tab. 2.4 Sequences of primers for real-time (RT) PCR**

| Primer | Sequence |
|---|---|
| CCL2 fw | 5’ GCG GAG CTA TAG AAG AAT CAC 3’ |
| CCL2 rev | 5’ TTG GGT TGT GGA GTG AGT GT 3’ |
| 18S fw | 5’ ACC GAT TGG ATG GTT TAG TGA G 3’ |
| 18S rev | 5’ CCT ACG GAA ACC TTG TTA CGA C 3’ |

### 2.1.5 KITS for RNA isolation, real-time PCR, oligonucleotide array

| | |
|---|---|
| Agilent Low RNA input Linear Amplification Kit | Agilent Technologies, Böblingen, Germany |
| One-Color Microarray-Based Gene Expression Analysis | Agilent Technologies, Böblingen, Germany |
| QuantiTect SYBR Green PCR Kit | Qiagen, Hilden, Germany |
| RNeasy Protect Mini Kit | Qiagen, Hilden, Germany |

### 2.1.6 KITS for ELISA and immunohistochemistry

| | |
|---|---|
| Human CCL2/MCP-1 Immunoassay | R & D Systems GmbH, Wiesbaden-Nordenstadt, Germany |
| StreptAB – Complex/HRP- Duett (Mouse/Rabbit) | DAKO GmbH, Hamburg, Germany |

### 2.1.7 Reagents and chemicals

#### 2.1.7.1 Basic chemicals and reagents

| | |
|---|---|
| Acetone (100%) | Acros Organics, New Jersey, USA |
| Agarose (for Routine Use) | Sigma-Aldrich CHEMIE GmbH, Hamburg, Germany |
| BSA | Biomol GmbH, Hamburg, Germany |
| Chloroform | Carl Roth, Karlsruhe, Germany |
| Ethanol | Merck, Darmstadt, Germany |
| Hydrogen peroxide | Merck, Darmstadt, Germany |
| Methanol | Merck, Darmstadt, Germany |
| Oligofectamine | Invitrogen, Friesoythe, Germany |
| 2-Propanol | Merck, Darmstadt, Germany |
| RNase AWAY | Molecular BioProducts, San Diego, USA |
| Saint -Mix | Synvolux Therapeutics B.V., Groningen, Holland |
| TRIzol Reagent | Invitrogen, Friesoythe, Germany |

#### 2.1.7.1.1 Toxins and chemokines

| | |
|---|---|
| Cholera Toxin | Biomol GmbH, Hamburg, Germany |
| Cholera Toxin B-Subunit | Biomol GmbH, Hamburg, Germany |
| Pertussis Toxin | CALBIOCHEM, Nottingham, UK |
| Pertussis Toxin B-Oligomer | CALBIOCHEM, Nottingham, UK |
| rhMCP-1 | Immunotools |

### 2.1.8 Consumables

| | |
|---|---|
| Cell culture flasks T25 (100 ml) | BD Falcon, Heidelberg, Germany |
| Cell culture flasks T75 (250 ml) | BD Falcon, Heidelberg, Germany |
| Cell culture flasks T175 (600 ml) | BD Falcon, Heidelberg, Germany |
| Cell strainer 70 µm pores | BD Falcon, Heidelberg, Germany |
| CRYO.S 2 ml | Greiner, Solingen, Germany |
| Disposable plastic pipettes 10 ml | Bibby Sterilin, Staffordshire, UK |
| Disposable scalpels NO. 10 | PFM AG, Köln, Germany |
| Eppendorf tubes 1.5 ml | Eppendorf, Hamburg, Germany |
| Extra Volume Tip 100-1300 µl | Starlab GmbH, Ahrensberg, Germany |
| FACS tubes 5 ml | BD Falcon, Heidelberg, Germany |
| Glass Pasteur pipettes 230 mm | VWR international, Darmstadt, Germany |
| Light Cycler Capillaries 20 µl | Roche Diagnostics, Manheim, Germany |
| Latex exam gloves | Kimberly-Clark, Roswell, USA |
| Microscope slides for Paraffin-IH | R. Langenbrinck, Teningen, Germany |
| Microtest tissue culture plates, 96 well | BD Falcon, Heidelberg, Germany |
| Needles 0.9x40 mm | Becton Dickinson S.A., Fraga, Spain |
| Nitrile exam gloves | Semperit Technische Produkte, Vienna, Austria |
| Petri dishes 94/16 ml | Greiner, Solingen, Germany |
| Pipette tips 1000 µl | Greiner, Solingen, Germany |
| Pipette tips 200 µl | Greiner, Solingen, Germany |
| Pipette tips 10 µl | Greiner, Solingen, Germany |
| Pipette tips PD sterile 2.5 ml | Brand, Wertheim, Germany |
| PP test tubes 15 ml | Greiner, Solingen, Germany |
| PP test tubes 50 ml | Greiner, Solingen, Germany |
| SafeSeal tips 1000 µl | Biozym Diagnostik, Olendorf, Germany |

| | |
|---|---|
| SafeSeal tips 100 µl | Biozym Diagnostik, Olendorf, Germany |
| Syringe driven filter units 0.22 µm | Millipore Corporation, Bedford, USA |
| Syringes 10 ml | Becton Dickinson S.A., Fraga, Spain |
| Syringes 2 ml | Becton Dickinson S.A., Fraga, Spain |
| Tissue culture plates, 24 well | BD Falcon, Heidelberg, Germany |

### 2.1.9 Appliances

| | |
|---|---|
| Biofuge pico | Heraeus Instruments, Hanau, Germany |
| BD FACSAria Cell Sorting System | BD Biosciences, Heidelberg, Germany |
| Casy 1 Cell Counter | Schärfe System, Reutlingen, Germany |
| Cell Culture Incubator $CO_2$-Auto-Zero | Heraeus, Hanau, Germany |
| Centrifuge J6M-E | Beckmann, München, Germany |
| Confocal Microscope LSM 510 META | Carl Zeiss AG, Hallbergmoos, Germany |
| E max Precision Microplate Reader | Molecular Devices Co.,Sunnyvale, USA |
| Eppendorf pipettes | Eppendorf, Hamburg, Germany |
| FACS-Calibur Flow Cytometer | BD Biosciences, Heidelberg, Germany |
| Gradient Cycler PTC 200, MJ Research | BioRad Laboratories, München, Germany |
| Invert Fluorescence Microscope Axiovert 200M | Carl Zeiss AG, Hallbergmoos, Germany |
| Invert Fluorescence Microscope Axiovert S100 | Carl Zeiss AG, Hallbergmoos, Germany |
| LaminAir HLB 2448 GS | Heraeus, Hanau, Germany |
| Light Cycler ROCHE | Roche Diagnostics, Manheim, Germany |
| Megafuge 1.0 | Heraeus Sepatech, Osterode, Germany |
| Milli Q Water System | Millipore S.A., Molsheim, France |
| Eppendorf Multipipette | Eppendorf, Hamburg, Germany |
| Multipipette Finn | Labsystems GmbH, Quickborn, Germany |
| NanoDrop Spectrophotometer ND-1000 | Peqlab Biotechnologie GmbH, Erlangen, Germany |
| Rotations Microtome HM350 | Microm, Heidelberg, Germany |
| Scale Sartorius R160P | Sartorius, Göttingen, Germany |
| Shandon Hypercenter XP | GMI, Ismaning, Germany |
| Varifuge 3.2 RS | Heraeus Sepatech, Osterode, Germany |
| Ventana NexES-System | Ventana Medical Systems, Frankfurt, Germany |
| Vortex REAX 2000 | Heidolph Instruments, Schwabach, Germany |
| Waterbath GFL 1083 | GFL mbH, Burgwedel, Germany |

### 2.1.10

### 2.1.11 Software

| | |
|---|---|
| Adobe Photoshop 6.0 | Adobe Systems GmbH, München, Germany |
| AxioVision v.4.6 | Carl Zeiss AG, Hallbergmoos, Germany |
| AxioVision Release v.4.5 | Carl Zeiss AG, Heilbergmoos, Germany |
| BD Cell Quest Pro v.4.0.2 | BD Bioscience, Heidelberg, Germany |
| GeneSpring GX 7.5.1 | Agilent Technologies Inc., CA, USA |
| Light Cycler Software ROCHE v.3.5 | Roche Diagnostics, Manheim, Germany |
| LSM Image Browser | Carl Zeiss AG, Hallbergmoos, Germany |
| LSM Release v.4.2 | Carl Zeiss AG, Hallbergmoos, Germany |
| Microsoft Office 2003 | Microsoft Deutschland GmbH, Unterschleißheim, Germany |
| Origin 5.0 | OriginLab Corp., Northampton, MA., USA |
| Reference Manager 11 | The Thomson Co., Carlsbad C.A., USA |
| SoftMax Pro v.5 | Molecular Devices Co.,Sunnyvale CA., USA |
| SPSS 15.0 | SPSS GmbH Software, München, Germany |
| Win MDI 2.9 | TSRI, Scripps, Fl., USA |

## 2.2 Methods

### 2.2.1 Cell preparation and culturing

#### 2.2.1.1 Primary fibroblasts culturing

Primary fibroblasts from invasive ductal breast carcinomas (PF27T, PF53T, PF37T) were derived from fresh resected tumor surgery specimen, kindly provided by the department of Pathology, University of Regensburg. Normal skin fibroblasts VF1 were resected from healthy tissue, kindly provided by department of Hematology, University of Regensburg. All types of tissue were cultured as described earlier (Kunz-Schughart *et al.*, 2001b). Briefly, biopsy material was incubated with penicillin (5000 U/ml) and streptomycin (5 ng/ml) after removal of adipose tissue for 30-60 min, then sliced into 1-4 $mm^3$ fragments and transferred into culture flasks that were kept in an incubator at 37°C for about 1-2 h in upright position. After attachment, tissue fragments were covered with special enriched growing medium (DMEM with 20% FCS and high glucose – 25 mM) and cultured in a humidified atmosphere (5% $CO_2$ in air, 37°C), see chapter 2.2.1.3. When sufficient outgrowth of cells was achieved, cells were enzymatically harvested (see chapter 2.2.1.3), tissue leftovers were removed via filters (cell strainer), and the cell suspension was transferred into T75 tissue

culture flasks in standard medium (DMEM with 10% FCS and 5 mM glucose). After reaching subconfluence, cells were dissociated and frozen stocks were prepared from passage 1-2 cells using 90% FCS and 10% DMSO for storage in liquid $N_2$ (see also chapter 2.2.1.4). Cultures of primary fibroblasts were morphologically and immunohistochemically characterized with: anti-CD90 (AS02) antibody - THYmocyte differentiation antigen 1 (directed against fibroblasts) – positive; anti-Cytokeratin 18 antibody (epithelial cell marker) – negative; anti-CD31 antibody called PECAM-1 – platelet endothelial cell adhesion molecule-1 (specific for endothelial cells) – negative, and α-SMA (α-Smooth Muscle Actin), which determines specificity for a donor myofibroblast fraction. For immunohistochemical staining, cells were cultured as monolayer on sterile microscope slides, and stained according to an established protocol (see chapter 2.2.1.8).

For experiments, fibroblasts were subsequently recultured from the frozen stocks in complete DMEM with 10% FCS plus ingredients (see chapter 2.2.1.3) as routine monolayer and passaged twice before spheroid initiation (see chapter 2.2.1.4).

#### 2.2.1.2 Monocyte isolation, freezing and reculturing

Leukocyte enriched blood concentrates were obtained from healthy donors using leukapheresis. Peripheral blood mononuclear cells (MNC) were isolated from the concentrate by density gradient centrifugation over Ficol/Hypaque and next washed with PBS (Spottl *et al.*, 2001). Subsequently, monocytes were isolated from MNC by counter current centrifugal elutriation in a J6M-E centrifuge using a large-volume chamber (50 ml), a JE-5 rotor at 2500 rpm, and a flow rate of 111 ml/min in Hanks' balanced salt solution supplemented with 8% autologous human serum (Sanderson *et al.*, 1977). Through adjustment of pump pressure against centrifugal force of cells, the cells were sorted according to their size and weight (the larger and heavier cells the more pressure power must be employed). Purity of elutriated MO taken for spheroid experiments was >90% as determined by morphological criteria and routine immunophenotyping (Krause *et al.*, 1998).

In most experimental series, freshly isolated MO were applied for co-culturing. However, for some settings, freshly isolated MO were centrifuged and resuspended at a concentration of $1x10^7$ per 1 ml of medium to prepare frozen stocks. 60% RPMI-1640 medium, 30% FCS and 10% DMSO on ice was used as freezing medium and monocytes were rapidly transferred into cooled CRYO.S tubes. Cells were freezed gradually at -20℃, -80℃ and finally stored in liquid $N_2$ (-196℃).

For recultivation, MO stocks were taken from the liquid $N_2$, thawed in a water bath (37ºC) and rapidly transferred into PP test tube previously filled with 30 ml of standard medium. The MO suspension was then centrifuged at 1500 rpm for 10 min, medium was removed

and 1 ml of fresh standard medium was added to the cell pellet for resuspension. The number of viable cells was determined using the CASY-1 cell analyzer system and MO were immediately used for experiments following preparation of appropriate cell concentration.

#### 2.2.1.3 Routine monolayer cultures

All breast tumor cell lines and fibroblasts were routinely cultured as adherent monolayers in tissue culture flasks (75 $cm^3$ or 175 $cm^3$). Standard conditions for incubation were 37ºC, 5% $CO_2$ in a humidified incubator. Cells were kept in Dulbecco's Modified Eagle Medium (DMEM) containing 0.2% phenol red with 5% fetal calf serum (FCS) and 100 U/ml penicillin plus 100 µg/ml streptomycin (standard medium). The cell number was chosen according to doubling time (see Tab. 2.5); so that the cultured cells can be transferred one time per week in a subconfluent state (fibroblasts) or in exponential growth state (breast tumor cell lines). Medium was renewed every second day.

**Tab. 2.5 Number of cells routine seeded for monolayer culturing and the corresponding culture doubling times of the different cell**

| Cells | Surface of tissue culture flask | | Mean doubling time (h) |
|---|---|---|---|
| | **75 $cm^3$** | **175 $cm^3$** | |
| Fibroblasts | 0.5 x $10^6$ | 1.0 x $10^6$ | 35 – 120***** |
| BT474 | 0.5 x $10^6$ | 1.0 x $10^6$ | 68 |
| T47D | 0.3 x$10^6$ | 0.6 x$10^6$ | 48 |
| MCF-7 | 0.2 x $10^6$ | 0.4 x $10^6$ | 29 |
| BT549 | 0.2 x $10^6$ | 0.4 x $10^6$ | 35 |
| Hs578 | 0.2 x $10^6$ | 0.4 x $10^6$ | 52 |

*** VF1 - 35 h; PF27T - 75 h; PF37T, PF53T - 120 h. Doubling times for fibroblasts may increase with number of passages.**

Exponentially growing breast tumor cell lines or subconfluent fibroblast were washed with phosphate buffered saline (PBS), and dissociated by enzymatic and mechanic means using a 0.05% trypsin-0.02% EDTA solution in PBS. The incubation time was 0.5 – 2.5 min, dependent on cell line, at 37ºC. Detachment of the cells was microscopically monitored and cell suspension was transferred into 50 ml tubes containing sufficient amounts of standard medium, to stop enzyme activity. The cell suspension was centrifuged (450 g, 5 min),

supernatant was removed and pelleted cells were resuspended in 10 ml or 20 ml of standard medium (depending on estimating cell concentration). 100 µl of the cell suspension was used for estimating cell numbers and concentrations, respectively. This aliquot of cells was added to 9.9 ml of CASYton (dilution liquid for cell cultures) and cell number was counted using the CASY1 cell analyzer. The rest of the cell suspension was centrifuged again and pelleted cells were resuspended to a concentration of $1x10^6$ cells/ml.

#### 2.2.1.4 Freezing and recultivation of adherent cells

Frozen stocks were prepared following dissociation, counting and centrifugation of early passage cells. Pelleted cells were resuspended in cold freezing medium cells with a concentration of $1x10^6$ cells/ml (90% FCS + 10% dimethyl sulfoxide, DMSO) and rapidly transferred into cooled CRYO.S tubes on ice. Cells were freezed gradually at -20 ºC, -80 ºC and finely stored in liquid $N_2$ (-196ºC). For subsequent recultivation, cell stocks were taken from the liquid $N_2$, rapidly thawn in a waterbath (37ºC), immediately transferred into a cell culture flask filled with double volume of growing medium (20 ml in T75 culture flask) and placed in 37ºC. After minimal time of 30 min and monitoring of cell attachment, medium was renewed, cells were passaged at least twice before usage. Breast tumor cells entering experiments were transferred for a maximum of 20 passages (100-120 cumulative population doublings) starting with the passage purchased. Fibroblasts were used only up to passage 7 (≤ 40 cumulative population doublings) to avoid effects due to cell senescence.

#### 2.2.1.5 3-D mono- and co-cultures

Multicellular spheroids (MCS) were generated according to the liquid overlay technique (Konur *et al.*, 1996; Kunz-Schughart *et al.*, 2001a, Friedrich *et al.*, 2009). using agarose-coated 96 well plates. To coat plates, 1.5% agarose was dissolved in DMEM, autoclaved for at least 20 min and transferred into the wells of a 96-well plate at a temperature of approximately 60ºC (50 µl/well). The coated plates were left for 10-20 min uncovered to cool down agarose and evaporate moisture. Agarose-coated plates were hermetically sealed and used up to one week. Storage of plates was at room temperature in the dark.
To initiate spheroid cultures, defined concentrations of single cell suspensions were prepared from exponentially growing tumor cells or subconfluent fibroblast monolayers (Tab. 2.6 and Tab. 2.7). 200 µl of the cell suspension was seeded per well with a multipipette. After four days of standard culturing (see chapter 2.2.1.5) cells created round-shaped aggregates (without central necrosis). The number of cells was optimized to obtain a desired spheroid diameter at day 4 in culture (>300 µm, <400 µm). In order to determine

the appropriate seeding density, experiments with different cell numbers used for their inoculation into agarose-coated wells were performed.

To determine the number of viable cells, spheroids were transferred with a Pasteur pipette into a 15 ml tube and washed with cold PBS. After removing the PBS, washed spheroids were dissociated by incubation with a 500 ml of 0.17% trypsin/0.07% EDTA in PBS, at 37ºC for 5 min (500 µl) and mechanic means (gentle pipetting). Enzyme activity was stopped by addition of 500 µl of supplemented DMEM. The whole volume of cell suspension (1 ml) was added to 9 ml of CASYton and cell number was counted using the CASY1 cell analyzer. Subsequently, the number of cells per spheroid was calculated.

**Tab. 2.6 Cell numbers inoculated to initiate 3-D cultures from breast carcinoma cell lines.**

| Cell line | Cell number per well (200 ml) |
|---|---|
| BT474 | 2000 |
| BT549 | 4500 |
| Hs578T | 7000 |
| MCF-7 | 750 |
| T47D | 3000 |

**Tab. 2.7 Cell numbers inoculated to initiate 3-D cultures from tumor-associated fibroblasts.**

| Cells | Cell number per well (200 ml) |
|---|---|
| PF27T | 4000 |
| PF37T | 4000 |
| PF53T | 4000 |
| VF1 | 4000 |

In order to co-culture spheroids with monocytes (MO), 3-D aggregates were generated as described for spheroid mono-culturing. At day 4 in culture, 100 µl of the supernatant was replaced with 100 µl of a freshly prepared monocytes suspension ($1x10^4$ MO per spheroid) in supplemented standard medium. Monocyte migration was monitored as a function of time in co-culture or after defined time intervals. e.g. 4 h, 20 h and/or 40 h following monocyte addition. In most experimental series, spheroid co-culture were dissociated and

flow cytometric analyses of single cell suspensions were performed to quantify the proportion of migrated monocytes.

### 2.2.2 Experimental designs to affect cells in co-culture

#### 2.2.2.1 Manipulation of the fibroblast milieu

##### 2.2.2.1.1 Wash-out experiments

To reduce the level of paracrine factors such as CCL2 in the milieu of fibroblast spheroids, 100 µl of conditioned medium (1/2 of total volume) was replaced with fresh medium. This process was repeated 6 times to obtain a 1:64 dilution of conditioned medium. In step 6, 100 µl supernatant was replaced by 100 µl the MO suspension ($1x10^4$ MO per spheroid). In parallel, supernatants were collected, frozen (-80°C) and used for CCL2 level determination by ELISA (see chapter 2.2.6). An aliquot of the spheroids (≥48) was collected and dissociated (see chapter 2.2.1.4) to estimate cell number per spheroid and calculate cellular CCL2 release rates. Flow cytometric analysis of cell distribution in spheroid co-cultures was performed after 2 h, 4 h, 6 h, 8 h and 20 h of incubation. Experiment were performed in triplicate.

##### 2.2.2.1.2 Addition of rhCCL2 to fibroblasts 3-D co-cultures

Two hours before the addition of MO, rhCCL2 was added to fibroblast spheroids by replacing 100 µl of the supernatant by 100 µl of fresh medium supplemented with rhCCL2 in the following concentrations: 0.04 µg/ml and 0.4 µg/ml for TAF, 0.004 µg/ml and 0.04 µg/ml for VF1 spheroids. The final concentrations of rhCCL after the addition of $1x10^4$ MO/spheroid (suspended in 100 µl of medium) were: 0.02 µg/ml and 0.2 µg/ml (TAF) or 0.002 µg/ml and 0.02 µg/ml (VF1). After 4 h of incubation in a humidified atmosphere (37°C), spheroids (≥48) were collected and dissociated (see chapter 2.2.1.5). Finally, flow cytometrical analysis of MO migration, as described in chapter 2.2.4.3 was carried out. Experiment were performed in triplicate.

#### 2.2.2.2 Modulation of the MO suspension

##### 2.2.2.2.1 Application of blocking toxins

To block the signaling pathways of various chemokines, MO were pretreated with two different toxins before co-culturing with fibroblast or tumor cell spheroids. Pertussis toxin (PTX) holoenzyme and PTX B-oligomer were applied at concentrations of 1 ng/ml, 10 ng/ml and 50 ng/ml. Cholera toxin (ChTX) holoenzyme or ChTX B-subunit were used at concentrations from 0.1 ng/ml up to 50 ng/ml. PTX B-oligomer and ChTX B-subunit were

used as negative controls. These subunits bind to the cell surface but they do not have the enzymatic activity of the toxin. MO ($0.2x10^6$/ml) were incubated for 30 min in 15 ml tubes, at room temperature with the toxins diluted in supplemented DMEM. The MO number and its viability were then estimated using the CASY-1 cell analyzer system and $1x10^4$ cells in 100 µl were added to each well containing fibroblast spheroids. After 4 h of incubation in a humidified atmosphere (37°C), the effect of to xins on MO migration into spheroids was recorded via flow cytometry following co-culture and dissociation (see chapters 2.2.1.5, 2.2.4.3). Experiment were performed in triplicate.

#### 2.2.2.2.2 Application of blocking antibodies

To exclusively block receptor CCR2A/B, the specific monoclonal antibody DOC-3 (kindly provided by Prof. Matthias Mack; University of Regensburg, Germany) was used and tested for TAF-MO and Hs578T-MO co-cultures. Control experiments were performed with blocking antibody CD11b (MAC-1) which should be irrelevant for MO migration. MO ($0.2x10^6$/ml) were incubated in 15 ml tubes for 30 min at room temperature with DOC-3 or CD11b or with corresponding isotype controls (IgG1 and IgG2a, respectively) and then added to spheroids. DOC-3 antibody was applied in concentration of 1 and 10 µg/ml. After incubation, the MO number and viability were estimated using the CASY-1 cell analyzer system. $1x10^4$ MO incubated with DOC-3 or CD11b in 100 µl were added per well each containing TAF or Hs578T (only MO incubated with DOC-3) spheroids. Spheroid co-culturing was carried out in presence of antibodies. After 20 h (fibroblasts spheroid + MO) or 40 h (Hs578T spheroid + MO) of incubation in a humidified atmosphere at 37°C, the effect of substance on MO migration was monitored via flow cytometry following spheroid dissociation according to chapters 2.2.1.5 and 2.2.4.3. Incubation was performed in the presence of antibodies. Cell viability was established with CASY-1 cell analyzer. Experiment were performed in triplicate.

### 2.2.3 Immunohistochemistry

#### 2.2.3.1 Immunohistochemical characterization of fibroblasts

For immunohistochemical staining, freshly isolated fibroblasts (see chapter 2.2.1.1) were seeded on sterile microscope slides ($2.5 \times 10^4$ per slide) and cultured in standard medium (see chapter 2.1.2.3). After 2-3 days of culturing, slides were fixed in cold acetone (10 min), air-dried and stained applying the ABC-method (or stored in -20°C). Primary and secondary antibodies used for staining and their working concentrations are listed in Tab. 2.8.

Biotinylated goat-anti-mouse antibody (1:100) was used as secondary antibody. Staining was performed according to the protocol given in Tab. 2.9.

**Tab. 2.8 Concentrations of antibodies used for immunohistochemical characterization of fibroblasts.**

| Antibody | Stock Concentration | Working Concentration | Dilution |
|---|---|---|---|
| AS02 | 0.2 mg/ml | 4 µg/ml | 1:50 |
| CK18 | 2 mg/ml | 200 µg/ml | 1:100 |
| CD31 | 345 mg/L | 4.3 µg/ml | 1:80 |
| α-SMA | 0.1 mg/ml | 1 µg/ml | 1:100 |

#### 2.2.3.2 Immunohistochemistry on paraffin section

Paraffin sections of spheroids were first rehydrated (2x 5 min Xylene; 2x propanol 100%; 2x ethanol 96%; 2x ethanol 70%; each time 5 min) and then stained via the ABC-method (described in chapter 2.2.3.1). A monoclonal mouse-anti-human CD45 antibody, 1:600 (stock concentration 450 mg/L) was used. The staining was performed automatically using the Ventana NexES System. After the staining procedure, microscope slides with spheroids sections were washed (10 min) in tap water with additive of rinsing agent and finally dehydrated according to the protocol given in Tab. 2.9 steps 14-17 before coverage with entellan.

**Tab. 2.9 Staining protocol for immunohistochemical antigen detection in cuvette system**

| Nr. | Substance | Conditions | Step |
|---|---|---|---|
| 1. | 2% $H_2O_2$ in methanol (fresh) | 15 min | blockade of tissue peroxides |
| 2. | PBS | 5 min | washing |
| 3. | 2.5% BSA in PBS | 90 min, 4ºC | blockade of unspecific protein bindings |
| 4. | Primary antibody in 1% BSA/PBS | 16 h, 4ºC | binding of specific antibody |
| 5. | PBS | 3 x 5 min | washing |

| | | | |
|---|---|---|---|
| 6. | Biotinylated goat-anti-mouse secondary antibody (1:100) | 45 min, 20ºC | binding of secondary antibody |
| 7. | PBS | 3 x 5 min | washing |
| 8. | Streptavidin-biotin-peroxidase (1:1:100) | 45 min, 20ºC | strengthening |
| 9. | PBS | 3 x 5 min | washing |
| 10. | DAB Chromogen in Substrate Buffer (1:50) | 5 min, 20ºC | color development |
| 11. | distilled $H_2O$ | 5 min | washing |
| 12. | Hematoxylin | 1 min | counter staining |
| 13. | Running tap water | 3 min | washing |
| 14. | Ethanol 70% | 5 min (1x) | dehydration |
| 15. | Ethanol 96% | 5 min (2x) | dehydration |
| 16. | Propanol 100% | 5 min (2x) | dehydration |
| 17. | Xylene | 5 min (2x) | dehydration |
| 18. | Entellan | | covering |

### 2.2.4 Flow cytometric (FC) analysis

#### 2.2.4.1 Technology

Flow cytometry is a method for analyzing particles and cells in suspension. Among others, expression of cell surface and intracellular molecules can be monitored in single or simultaneous multi-parameter analysis of single cells.

In a flow cytometer, cells in suspension are hydrodynamically focused in a sheath of fluid and then presented to a laser (a source of light excitation). The cells/particles passing through the beam scatter the light, which is detected as forward scatter (FSC) and side scatter (SSC) and analyzed by a series of filters and photomultiplier tubes that convert the light signal into electrical impulses. In normal cells, FSC correlates with the cell size and SSC relates to the cell density. Fluorochromes used for staining emit light when excited by a laser with corresponding excitation wavelength.

#### 2.2.4.2 Monocyte characterization

Monocytes ($5x10^6$ per test) were stained with antibodies in established dilution to avoid non-specific binding. Depending on available reagents, one step direct staining or two step indirect staining was performed. Cells were incubated with antibody in each staining step for 30 min at 4℃. To wash out excessive, non-bound antibody, PBS containing 1% FCS was added; the cells were spun down at 450 g and resuspended in PBS. If needed, secondary antibody was added and incubation and washing step was repeated. Stained cells were diluted in 100 µl of PBS and transferred into polypropylene tubes for flow cytometric measurement. The antibodies applied to characterize and also to sort MO are listed and detailed in Tab. 2.10.

**Tab. 2.10 Antibodies used for monocytes staining.**

| | Antigen | Primary Ab | Stock Concentration and Dilution of Ab | Secondary Ab | Volume and Dilution of Ab |
|---|---|---|---|---|---|
| **CCR2 expressio** | CCR2 | DOC-3 | 1.43 µg/µl; 3 µl, undiluted | goat-anti-mouse-FITC | 10 µl, 1:10 |
| | Isotype Control | IgG1 | 1 µg/µl; 4 µl undiluted | goat-anti-mouse-FITC | 10 µl, 1:10 |
| **CD14/CD 16** | CD14 | anti-CD14-PE/Cy5 | 5 µl undiluted | – | – |
| | CD16 | anti-CD16-PE | 5 µl undiluted | – | – |
| **CD14/CD49e/CD11a or CD11b expression** | CD11a | anti-CD11a | 1 µg/µl, 4 µl undiluted | goat-anti-mouse-PE | 10 µl, 1:100 |
| | CD11b | anti-CD11b | 1 µg/µl, 4 µl undiluted | goat-anti-mouse-PE | 10 µl, 1:100 |
| | CD49e | anti-CD49e-FITC | 5 µl undiluted | – | – |
| | CD14 | anti-CD14-PE/Cy5 | 5 µl undiluted | – | – |

The samples were measured on a FACS-Calibur flow cytometer. Samples labeled with FITC, PE, PE/Cy5-conjugated antibodies were measured in channel FL1, FL2, FL3, respectively (for excitation and emission spectra see table 2.10, chapter 2.2.4.4). For each sample $2x10^4$ events were collected and analyzed using the associated CellQuest Pro software. Data were visualized in dot plots or histogram plots.

### 2.2.4.3 Analysis of monocytes from co-cultures

Prior to flow cytometric analysis, spheroid co-cultures were dissociated and single cell suspensions were prepared as described in chapter 2.2.1.5 To determine fibroblast or tumor cell to MO ratio, a minimal number of 48 co-cultures was collected per sample and transferred into 15 ml tubes. Spheroids were washed 3x in cold PBS to remove monocytes loosely attached to the spheroid surfaces and the rest of medium, and were then dissociated as described in chapter 2.2.1.5. Finally, cells were washed with PBS containing 1% FCS. For fibroblast staining, cells were left 10 min in contact with 1% FCS in PBS in order to block unspecific binding. Cells ($1x10^4$ - $2x10^4$ cells per sample, depending on cell type) were incubated with antibodies for 30 min at 4° C, then washed with PBS (1% FCS) and pelleted at 450 g for 5 min. Stained cells were diluted in 100 µl of PBS and transferred into polypropylene tubes for flow cytometric measurement.

Tumor cell to MO ratio was estimated after staining with an APC-conjugated anti-CD45 antibody which is specific for monocytes. FSC, SSC and FL4 fluorescence signals were recorded. Regions/gates were defined in the SSC *vs*. FL4 dot plot diagrams for MO and tumor cells discrimination (Fig. 2.1.a). To distinguish monocytes from fibroblasts, cells were stained with a FITC-conjugated fibroblasts specific antibody AS02 (stock concentration 0.2 µg/µl; dilution 1:25). FSC, SSC and FL1 fluorescence signals were recorded. Regions/gates were defined in the SSC *vs*. FL1 dot plot diagrams for MO and fibroblasts discrimination (Fig. 2.1.b). All experiments were performed in triplicate. In Tab. 2.11 excitation and emission spectra for fluorophores are listed.

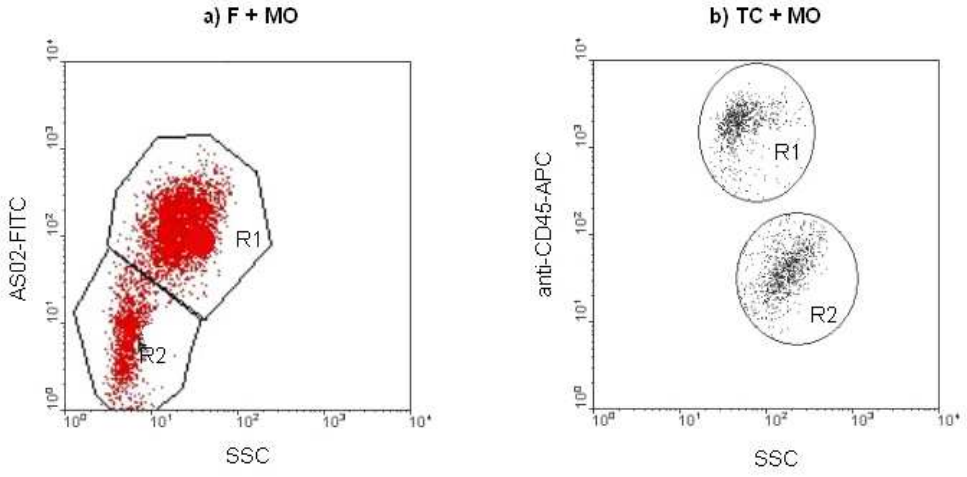


**Fig. 2.1 Representative flow cytometric dot plot diagram of dissociated spheroids co-cultures. (a) R1 – region/gate 1 of fibroblasts (F) stained with FITC-conjugated AS02-antibody, R2 – region/gate 2 of unstained monocytes (MO). (b) R1 – region/gate 1 of unstained tumor cells (TC) with FITC-conjugated AS02-antibody, R2 – region/gate 2 of MO stained with APC-conjugated CD45-antibody.**

**Tab.2.11 Excitation and emission spectra.**

| Fluorophore | Excitation (nm) | Emission (nm) |
|---|---|---|
| FITC | 495 | 519 |
| PE | 480;565 | 578 |
| PE/Cy5 | 480;565;650 | 670 |
| APC | 650 | 660 |

### 2.2.5 Fluorescence Activated Cell Sorting (FACS)

#### 2.2.5.1 Technology

FACS allows the isolation of cells (not only analysis) from heterogenous populations based on their spectral characteristics. The FACS device used for the present study is a high-speed sorter with a piezocristal vibration unit and a nozzle system leading to the formation of droplets from the stream as soon as the hydrodynamically focused cells have passed the laser beam. A positive or negative electrical charge is applied to the droplets containing cells of interest. The charged droplets then fall through an anode/cathode deflection system that diverts the droplets into containers as detailed in Fig. 2.2.

#### 2.2.5.2 Isolation of MO subpopulations for co-culturing

To isolate monocyte subpopulations, freshly isolated MO were double stained with PE-conjugated anti-CD14 and PE/Cy5-conjugated anti-CD16 antibodies (see Tab. 2.10, chapter 2.2.4.2). About $4x10^7$ MO were centrifuged and antibodies, each in volume of 100 µl were added to cell pellet. The cells were left at 4℃ for 30 min, followed by three washes with PBS. Next, 1 ml of PBS was added and cells were filtered and separated via Fluorescence-activated cell sorting. SSC, FSC, FL2 (for PE fluorescence), FL3 (for PE/Cy5 fluorescence) signals were recorded. Regions/gates were defined in the FL2 *vs*. FL3 dot plot diagrams for discriminating MO subpopulations. Four regions/gates were defined: R1 - $CD14^{++}CD16^{-}$, R2 - $CD14^{++}CD16^{+}$, R3 – $CD14^{++}CD16^{++}$, R4 – $CD14^{+}CD16^{++}$.
Sorted MO fractions were collected into PP tubes containing 1 ml of FCS. Cell concentration was measured using the CASY1 cell analyzer and adapted to obtain $1x10^4$ MO in 100 µl for addition to the prepared fibroblast spheroids ($1x10^4$/sphreoid, see chapter 2.2.1.5). The cells were co-cultured for 40 h to compare their migration capacity.

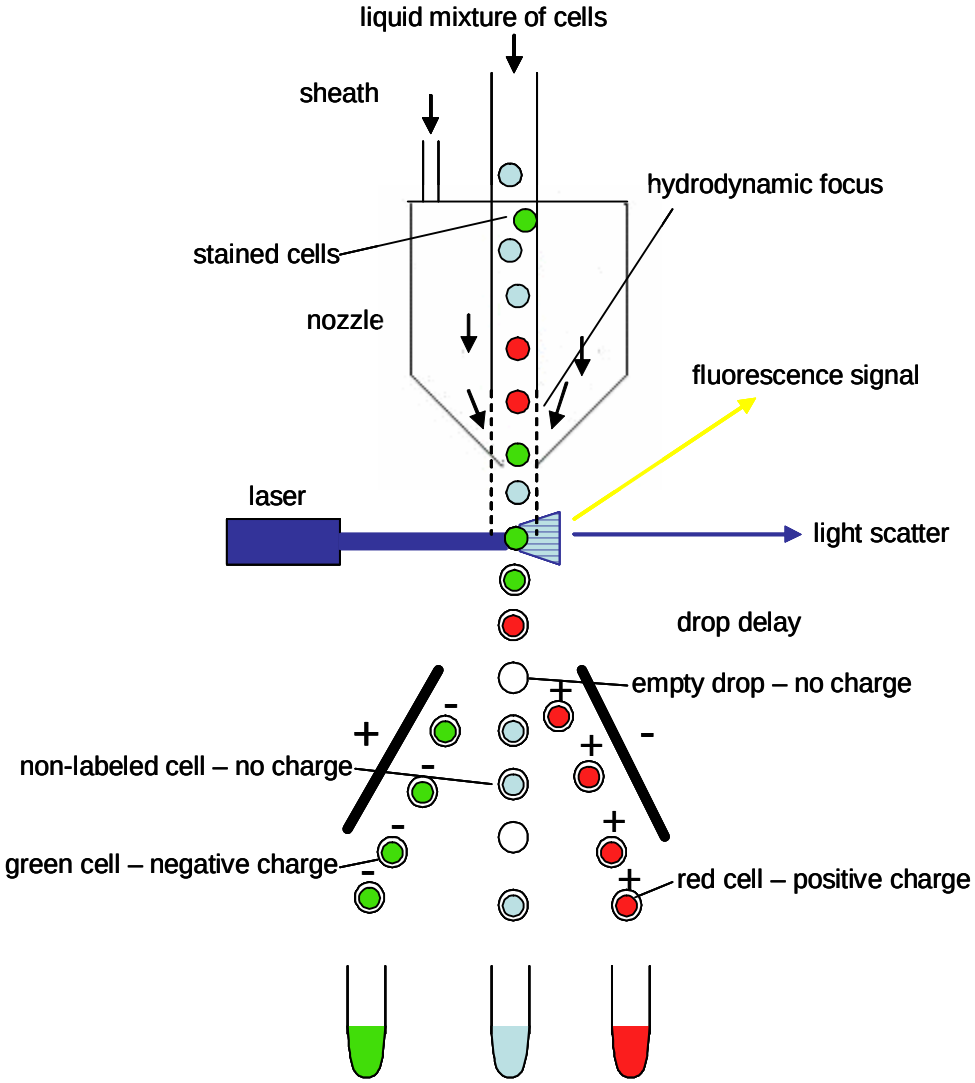


**Fig. 2.2 FACS system. FACS uses the principle of hydrodynamic focusing for presenting cells to a laser. A suspension of cells is forced at high pressure through a vibrating nozzle to create tiny charged droplets, each containing a single cell. Particles/cells passing through the beam will scatter the light, which is detected as forward scatter and side scatter. The combination of scattered and fluorescent light is detected and analyzed. Droplets with different cell types are deflected by a static electrical field and directed into separate collection vials.**

Each MO fraction was added to 48 fibroblast spheroids. To exclude artifacts, which could result from staining and/or sorting procedures, the following controls with whole blood monocytes were prepared: unsorted/unstained, unsorted/stained and sorted/stained. Experiment was performed in triplicate.

#### 2.2.5.3 Isolation of cells from co-cultures for further analysis

Sorting of cells (with FACSAria Cell Sorting System) was also used to separate co-cultured TAF and MO. Spheroids were trypsinized (chapter 2.2.1.5) and stained with fibroblasts specific antibody (AS02-FITC, see chapter 2.2.4.3). FSC, SSC and FL1 fluorescence signals were recorded. Regions/gates were defined in the SSC *vs*. FL1 dot plot diagrams for MO-fibroblast discrimination and cell population were sorted. Purity of population was 96-98% for MO and 98-99% for fibroblasts. To achieve cell numbers sufficient for microarrays experiments, 24 plates each with 96 spheroids were required. Experiment was performed in triplicate.

### 2.2.6 ELISA assay – determination of CCL2 concentration

Supernatants of fibroblasts and tumor cell lines were collected 4 days after initiation of spheroids or 24 h after last change of medium for monolayer cultures, aliquoted and stored at -80℃. Under these conditions of storage no loss of the cytokine immunoreactivity is described. However, levels of CCL2 were always determined after a maximum of 6 weeks of storage. CCL2 levels in the supernatants of various mono- and co-cultures were measured with a commercial ELISA kit (Human CCL2/MCP-1 Quantikine, R&D Systems) after subsequently thawing the samples. CCL2 concentration was determined in cell culture supernatant according to the manufacturer's manual. In brief, samples, standards and controls were pipetted into microplates pre-coated with monoclonal antibody specific for CCL2 and incubated 2 h at room temperature. After washing away unbound substances, HRP-labeled antibody (detection antibody) was added and incubated for 1 h. Unbound detection antibody was washed away. Then, a detection reagent (*e.g*. streptavidin/HRP) was added to the wells. The plate was washed again and substrate solution (TMB/hydrogen peroxide) was added. Color developed relative to the amount of CCL2 bound in the initial step. The color development was stopped after 20 min by the addition of sulphuric acid and the signal intensity was measured with an E max Precision Microplate Reader. The cytokine content was measured in pg/ml and referred to cell number per spheroid.

### 2.2.7 RNA expression analysis

#### 2.2.7.1 Total RNA isolation

Total RNA for real-time PCR was isolated by TRIzol Reagent following the manufacturer's instructions. After adding the proper volume of TRIzol Reagent and homogenization, samples were incubated for 5 min at room temperature. 0.2 ml of chloroform were added per 1 ml of TRIzol. Tubes were shaken vigorously by hand for 15 sec and incubated 3 min

at room temperature. Samples were then centrifuged at 12,000 x g for 15 min at 4º C. The upper colorless aqueous phase containing RNA was transferred to a fresh tube. Subsequently, 0.5 ml of isopropyl alcohol per 1 ml of TRIzol were added, samples were incubated at room temperature for 10 min and centrifuged at 12,000 g for 10 min at 4º C. After centrifugation, supernatant was removed and the RNA pellet was washed with 75% ethanol. The samples were mixed by vortexing and centrifuged at 7,500 x g for 5 min at 4º C. At the end of the procedure, the RNA pellet was briefly dried and dissolved in RNase free water. Concentration and purity of RNA was determined by spectrophotometry (NanoDrop) using 2 µl of undiluted RNA. Pure RNA has an $A_{260nm}/A_{280nm}$ absorbance ratio of 2.0.

#### 2.2.7.2 Reverse transcription

First-strand cDNA synthesis from RNA was performed using the reagents and reaction conditions specified in Tab. 2.12. Control samples to identify potential contamination (no reverse transcriptase control and no RNA control) were prepared. The final volume of the reaction was 20 µl.

**Tab. 2.12 Reagents and conditions for cDNA synthesis**

| | | | |
|---|---|---|---|
| | total RNA | 1 µg | |
| | random hexamers | 0.2 µg | |
| | $H_2O_{DEPC}$ | to 11 µl of vol. | 70ºC, 5 min; chill on ice |
| RT-Mix: | 5x M-MuLV RT buffer | 4 µl | |
| | 10x dNTPs Mix (10 mM) | 2 µl | |
| | DTT (0.1 M) | 2 µl | 25ºC, 5 min |
| | RevertAid M-MuLV RT (200 U/µl) | 1 µl | 25ºC, 10 min |
| | | | 37ºC, 60 min |
| | | | 70ºC, 10 min |
| | | | 4ºC |

### 2.2.7.3 Real-Time PCR

Real-Time PCR is a quantitive PCR method for the determination of copy number of PCR templates such as cDNA in a PCR reaction. In the present study an intercalator-based technology was applied, also known as SYBR Green method. This approach requires a double-stranded DNA dye in the PCR reaction which binds to newly synthesized double-stranded DNA and gives fluorescence. The Real-Time PCR was performed using the QuantiTect SYBR Green PCR Kit (Qiagen) following the manufacturer's instructions. The reaction condition and amount of reagents are given in Tables 2.13 and 2.14 The final volume of reaction was 20 µl. For amplification with CCL2 primers, 40 cycles were performed and for amplification with 18S primers (control, housekeeping gene) 35 cycles were performed.

**Tab. 2.13 Real-Time PCR: Reaction Mix**

| | |
|---|---|
| 2x QuantiTect SYBR Green PCR | 10 µl |
| Primer Mix (20 µM) | 1 µl |
| cDNA template | 2 µl |
| $H_2O_{DEPC}$ | 7 µl |

**Tab. 2.14 Real-Time PCR: Real-Time Cycler Conditions**

| Step | Time | Temperature |
|---|---|---|
| ***PCR initial activation*** | 15 min | 95ºC |
| ***3-step cycling*** | | |
| Denaturation | 15 sec | 95ºC |
| Annealing | 20 sec | 58ºC |
| Extension | 25 sec | 72ºC |
| ***Cycle nr.*** 35 (18S) or 40 (CCL2) | | |

#### 2.2.7.4 cDNA microarrays

##### 2.2.7.4.1 Technological basics

A microarray is defined as a collection of microscopic spots arranged in an array and attached to a solid surface. These spots, referred to as probes, are designed such that each probe binds a specific nucleic acid sequence corresponding to a particular gene through a process termed hybridization. The sequence bound to a probe, referred to as the target, is labeled with some kind of dye such as a fluorophore. The level of binding between a probe and its target is quantified by measuring the fluorescence emitted by the labeling dye when scanned. This signal provides a measure for the expression of a specific gene containing the target sequence.

##### 2.2.7.4.2 Analysis of migrated MO *versus* non-migrated

The experiment was designed to analyze the gene expression profile of migrated *versus* non-migrated MO and included: 1) co-culturing of MO with fibroblast spheroids and subsequent sorting of co-cultured cells; 2) gene expression analysis.

1) Co-culturing and separation of MO and fibroblast spheroids for cDNA microarrays

To compare migrating and non-migrating monocytes, 24 plates, each with 96 spheroids were prepared according to the protocol described in chapter 2.2.1.5. MO were co-cultured with fibroblasts spheroids for 4 h, to allow complete MO migration. To collect migrating monocytes, spheroids were placed in 15 ml tubes and washed 3 times with 10 ml of PBS and then dissociated by enzymatic means (see chapter 2.2.1.6). Non-migrated MO remaining in culture dishes were collected together with medium, centrifuged (450 g, 10 min) and washed with PBS. Both MO populations were stained with FITC conjugated AS02 antibody (1:25) and sorted as described in chapter 2.2.5.3. A set of controls was prepared to exclude artifacts which could occur as a result of incubation, staining or sorting (Tab. 2.15). Samples and controls were then lyzed and RNA was subsequently isolated (see 2.2.7.1).

**Tab. 2.15 Samples and controls for cDNA microarrays**

| | Incubation time/ environment | Stained | Run through sorter |
|---|---|---|---|
| **Control 0** untreated MO | - | no | no |
| **Control 1** MO kept on ice | 4 h, 4℃ | yes | yes |
| **Control 2** MO kept in Teflon bag* | 4 h, 37℃, Teflon bag | yes | yes |
| **MO outside** non-migrating MO** | 4 h, 37℃, culture dish | yes | yes |
| **MO inside** MO migrated into fibroblast spheroids | 4 h, 37℃, spheroids inside | yes | yes |

*** Teflon bag provide optimal culturing conditions**
**** Non-migrating MO during incubation time stayed in contact with agar-coated 96 well plate (culture dish)**

2) Gene expression analysis

Total RNA for cDNA microarrays was prepared from cell pellets using the “RNeasy Mini Kit” according to the manufacturer’s instructions. RNA concentration and purity was determined by spectrophotometry using a 1:30 diluted RNA sample. Pure RNA has an $A_{260nm}/A_{280nm}$ absorbance ratio of 2.0.

Preparing and labeling of cDNA hybridization, washing and scanning were performed according to the One-Color Microarray-Based Gene Expression Analysis Protocol (Agilent Technologies). Fig. 2.3 is a standard workflow for sample preparation and array hybridization design. Microarrays data clustering and comparative analysis was done with the GeneSpring GX 7.5.1 software.

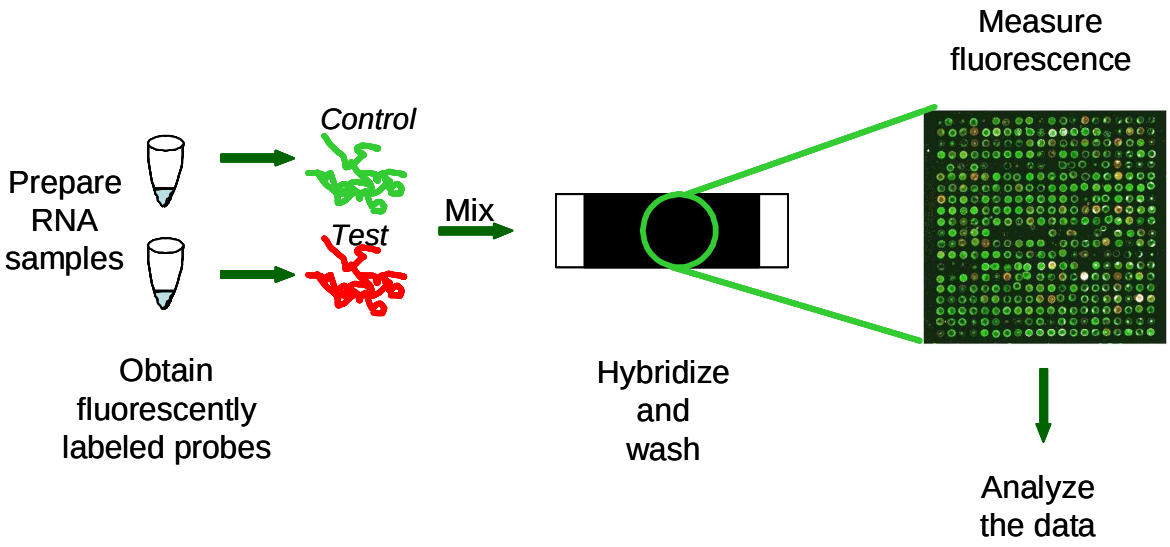


**Fig. 2.3 The major steps in a cDNA microarray experiment. Isolated RNAs from both control and test samples are converted into cDNAs (reverse transcription). cDNAs are labeled with fluorescent probes (Cy3 - green and Cy5 - red). After hybridization and washing procedures, cDNA microarrays are scanned at 540 nm (green) and 630 nm (red), respectively, for the experimental channel. Finally, a two-channel Red-Green image is obtained.**
**Black-colored spots signalize no hybridization; no detectable signal. Green-colored spots indicated less binding of the test samples than the control sample; down regulation. Yellow-colored spots indicate equal binding between samples; constant regulation. Red-colored spots indicate greater binding of the test sample than the control sample; up–regulation.**

### 2.2.7.5 RNAi approaches

#### 2.2.7.5.1 Technological basics

RNA interference (RNAi) is a phenomenon of post-transcriptional gene silencing (Fig.2.4) Introduction of double stranded RNAs (dsRNAs; typically >200 nt) into certain organisms and cell types causes degradation of the homologous mRNA. Because of potential antiviral response of mammalian cells, the dsRNA cannot be used for inhibiting gene expression. This response dsRNA degradation can be bypassed, however, by the introduction of short interfering RNAs (siRNAs; 20-25 nt) (Elbashir *et al.*, 2001).

In order to down regulate CCL2 expression in fibroblasts, different RNAi approaches were tested.

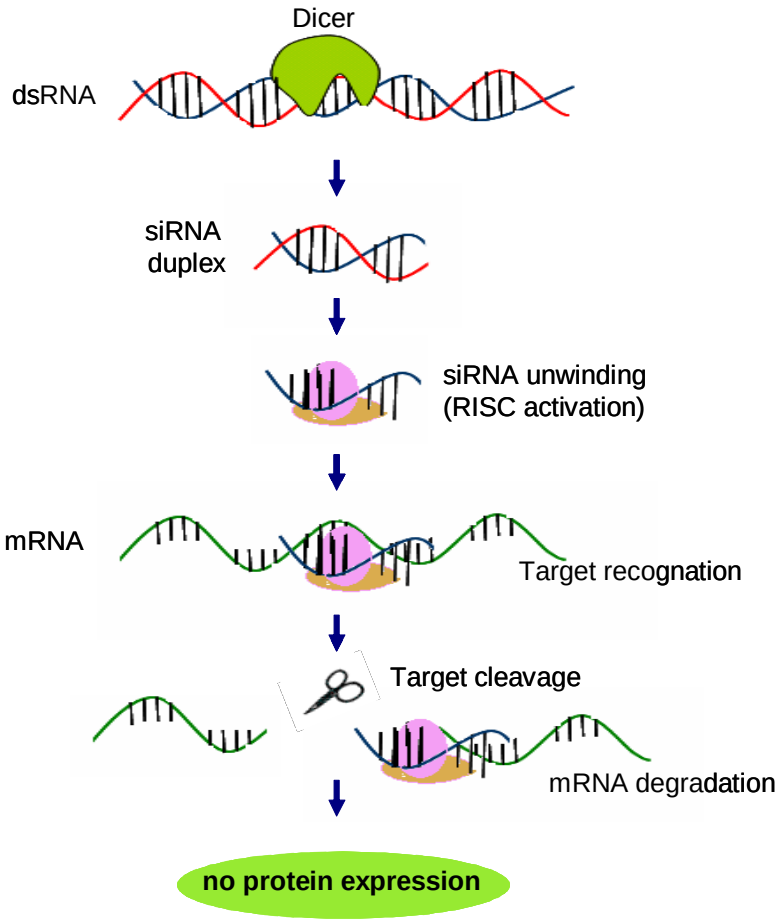


**Fig. 2.4 RNAi – mechanism. Double stranded RNA is introduced into a cell and gets chopped up by the enzyme dicer to form siRNA. siRNA then binds to the RISC complex and is unwound. The antisense RNA complexed with RISC binds to its corresponding mRNA which is then cleaved by the enzyme and degraded, so that protein expression is abrogated.**

#### 2.2.7.5.2 Experimental set-up to down-regulate CCL2 in fibroblasts

Fibroblasts were seeded as monolayers in 24 well plate ((3-3.5)x$10^4$ cell/well) and incubated 24 h under standard culture conditions to reach a confluence level of about 50% at the time of transfection. The transfection mix using serum-free medium Opti-MEM I, the transfection reagent Oligofectamine and the siRNAs were prepared according to the protocol given in Tab 2.16.

**Tab. 2.16 Transfection mix for siRNA transfection (amounts per well are given)**

| | | | |
|---|---|---|---|
| Tube 1 | Opti-MEM I | 5.5 µl | |
| | Oligofectamine | 2 µl | mix; 10 min, room temperature |
| Tube 2 | Opti-MEM I | 40 or 41.25 µl | |
| | siRNAs | 1.25 or 2.5 µl | mix |
| | | (end concentration 200 nM) | |
| | Tube 1 + Tube 2 | | mix; 15-20 min, room temperature |

The medium was changed one day and three days after transfection. At day four after transfection cells were dissociated according to a standard procedure (see 2.2.1.3) and seeded again as monolayers and as spheroid mono-cultures (see 2.2.1.3 and 2.2.1.5). Previous to the dissociation, supernatants were collected and frozen at (-80º) C to check CCL2 protein release from day 3 to 4 (24 h release rates) after transfection as described in chapter 2.2.6. The cells were cultured until day 7 after transfection. At day 7 supernatants were again collected and frozen both from monolayer and spheroid cultures for subsequent CCL2 protein analysis. Monolayer and spheroid cultures were then dissociated according to the routine procedures described in chapters 2.2.1.3 and 2.2.1.5, and the number of viable cells per well and per spheroid, respectively, was determined via the CASY1 cell analyzer system. Cell count analysis was performed at days 4 and 7 in culture to allow calculation of CCL2 protein release rates per cell. Parallel to samples transfected with siRNA potentially reducing target protein, control samples were run to identify artifacts due to down-regulation of gene expression through siRNA per se. As negative controls, short sense sequences of RNA corresponding to working dsRNAs were used.

The experiments performed in the present work to modulate CCL2 release from fibroblast monolayer and spheroid cultures included the following applications and modifications of the RNAi approach:

- ✓ Different fibroblast cultures were tested: PF27T, PF53T, PF37T
- ✓ Commercially available siRNA (siRNA Silencer from Ambion) were compared with self-designed siRNAs (1 ds siRNA, 2 ds siRNA)
- ✓ Different dissociations means (trypsin/EDTA, accutase, collagenase III) were applied
- ✓ Additional fluorescence siRNA control - Alexa Fluor488 was included
- ✓ CCL2 reduction on RNA level was verified by isolating and analyzing total RNA at day 4 and day 7. The RNA was isolated via TRIzol, transcribed into cDNA and amplified with the Real-Time PCR technique as detailed in chapters 2.2.7.1-3.

### 2.2.8 Statistical analyses

Statistical significance, e.g. to verify differences between data sets of control and treated groups, was routinely evaluated using the nonparametric Mann-Whitney *U* test in the SPSS 15.0 software. The relationship between CCL2 release and MO infiltration was assessed by linear regression analysis in the Origin 5.0 software program. Values of $p<0.05$ were considered to be statistically significant.

# 3. Results

The results chapter is divided into the three following sectors: 1) monitoring of MO migration into spheroids of breast tumor origin, 2) verifying influence of chemokines and specifically CCL2 on spheroidal MO migration and 3) trials of identifying migrated MO subpopulation.

## 3.1 Migration of monocytes into spheroids of breast tumor origin

### 3.1.1 Migration of monocytes into fibroblast spheroids

Studies performed by Silzle et al. (Silzle *et al.*, 2003), have shown that the proportion of MO migrating into spheroids of breast tumor-derived fibroblasts is significantly higher than in spheroids from normal skin and breast fibroblasts. To better understand this process, the migration kinetics of MO into spheroids of breast tumor-derived fibroblasts was monitored. At the time of MO addition spheroids were about 300-330 µm in diameter, consisted of (1.5-2)x$10^3$ cells and showed no central necroses. MO to fibroblasts ratios were estimated after 10, 20 and 40 h using flow cytometry (Fig. 3.1a). No significant difference in MO to fibroblast ratio was observed after 10, 20 and 40 h in three independent experiments indicating that MO migration is completed within 10 h. To determine the exact time required to complete MO migration, the MO to F ratio after 2, 4, 6, 8 and 20 h of co-culturing was determined. This experiment shows that MO migration is completed within only 4 h (Fig. 3.1b). Mean proportion of MO and fibroblasts in spheroid co-cultures after completing of MO migration is shown in Tab. 3.1.

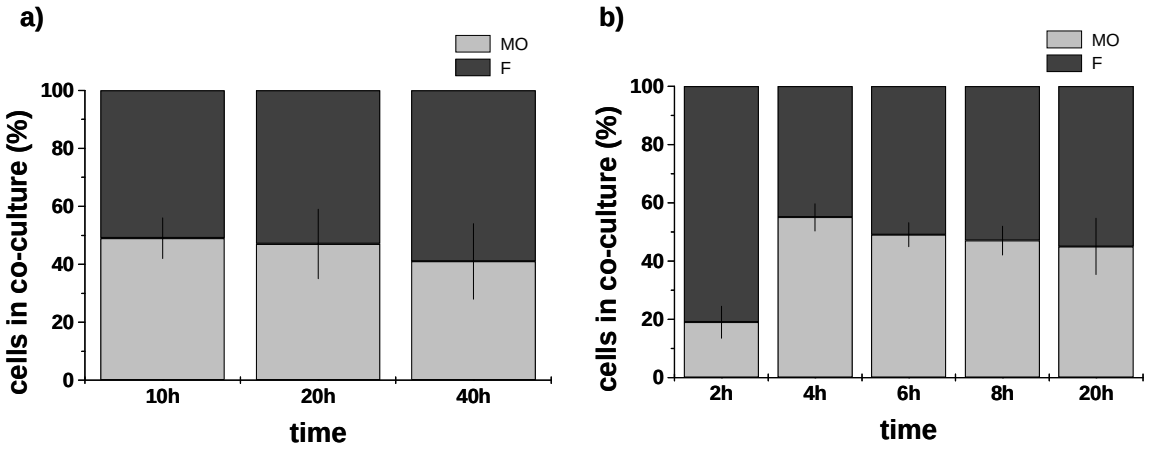


**Fig. 3.1 Monocyte migration into tumor-derived fibroblast spheroids. MO to fibroblasts proportion in PF27T spheroid co-culture was checked (a) 10, 20 and 40 h and (b) 2, 4, 6, 8 and 20 h after addition of 1x$10^4$ MO per spheroid. The cell ratio (± SD) was determined using flow**

**cytometric analysis following spheroid dissociation. Columns in graphs show mean values and SD of three independent experiments with MO from 3 different healthy donors.**

**Tab. 3.1 Mean proportion of cells (MO and fibroblasts) in spheroid co-cultures 4 h after addition of MO.**

| | Percentage of monocytes in co-culture (%) | | |
|---|---|---|---|
| **TAF** | **MO (%)** | **F (%)** | **SD** |
| PF27T | 54.5 | 45.5 | 4.7 |
| PF37T | 44.7 | 55.3 | 2.7 |
| PF53T | 60.6 | 39.4 | 2.6 |

### 3.1.2 Migration of monocytes into different breast tumor cell line spheroids

Five breast tumor cell lines of different invasiveness were chosen and MO migration was proved. The aim of this experiment was to find out if/how MO invade breast tumor cells spheroids and compare outcomes with MO migration into fibroblast 3-D cultures.

The chosen breast tumor cell lines were tested and adopted to produce spheroids with a mean diameter of about 350 µm and without central secondary necrosis at the day of MO addition. Depending on cell line, spheroids showed different packaging, from most round and compact BT474 spheroids to least compact spheroids created by MCF-7 cell line (see Fig. 3.2). In contrast to the tumor-derived fibroblast 3-D cultures, which are growth arrested, some of the tumor cell lines (BT474, MCF-7, T47D) still proliferate in spheroid culture and spheroid volume increases throughout culturing. Tab. 3.2 shows the average spheroid diameter for different cell lines at day 4 and day 6 after inoculation. Number of cells used for spheroid inoculation is given in Tab. 2.5, chapter 2.2.1.4. Mean proportion of MO and tumor cells in spheroid co-cultures after completing of MO migration is shown in Tab. 3.3.

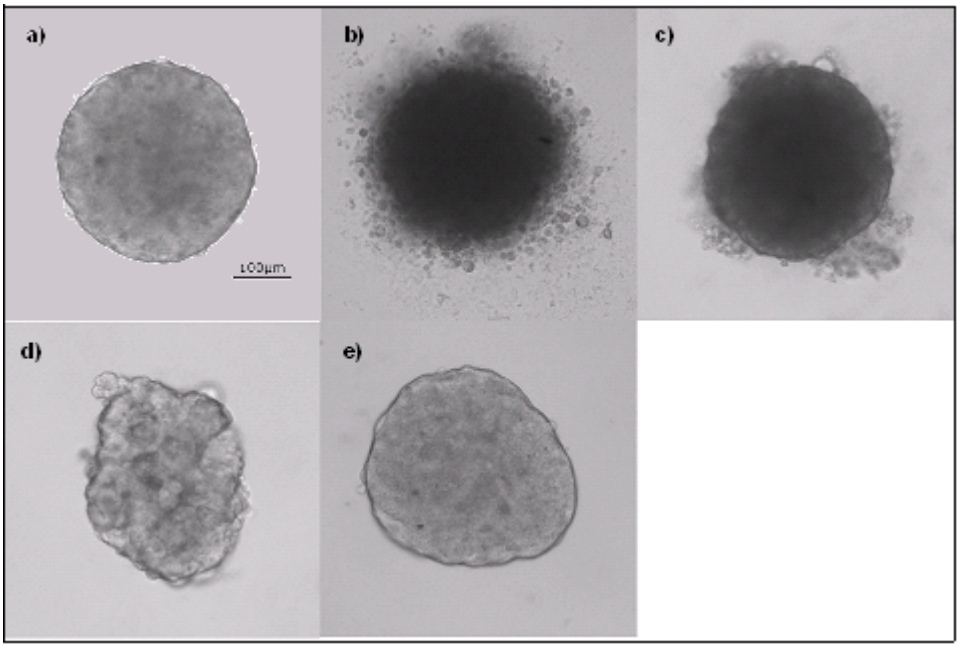


**Fig. 3.2 Representative spheroids derived from breast tumor cell lines. Phase contrast images were made 4 days after inoculation. Magnification of 10 x objective was used. (a) BT474; (b) BT549; (c) Hs578T; (d) MCF-7; (e) T47D. Bar = 100 µm applies to all images.**

**Tab. 3.2 Diameter of spheroids originated from breast tumor cell lines at day 4 and day 6 after inoculation**.

| Cell line | Diameter of spheroids and SD (µm) | | | |
|---|---|---|---|---|
| | day 4 | | day 6 | |
| | average | SD | average | SD |
| Hs578T | 373 | 15 | 369 | 14 |
| T47D | 371 | 6 | 402 | 3 |
| BT549 | 352 | 3 | 347 | 8 |
| MCF-7 | 300 | 14 | 367 | 7 |
| BT474 | 336 | 9 | 376 | 3 |

Flow cytometric analysis of cells from spheroid co-cultures and paraffin sections of spheroids derived from the five different breast tumor cell lines co-cultured for 40 h with peripheral blood MO showed, that MO to breast tumor cell ratios differ between individual cell lines (Tab. 3.3, Fig. 3.3 and Fig. 3.4). MO migrated most effectively into Hs578T breast cancer cell line spheroids, T47D spheroid infiltration by MO was intermediate and BT549, MCF-7 and BT474 were poorly infiltrated. Because of massive MO migration into Hs578T,

these co-culture were further studied in more detail, *e.g.* with respect to MO migration kinetics.

**Tab. 3.3 Mean proportion of cells (MO and tumor cells) in spheroid co-cultures 40 h after addition of MO.**

| | Percentage of monocytes in co-culture (%) | | |
|---|---|---|---|
| **Breast tumor cell line** | **MO (%)** | **T (%)** | **SD** |
| Hs578T | 48.3 | 51.7 | 5.1 |
| T47D | 18.6 | 81.4 | 1.3 |
| BT549 | 8.4 | 91.6 | 2.6 |
| MCF-7 | 3.8 | 96.2 | 3.8 |
| BT474 | 1.3 | 98.7 | 1.0 |

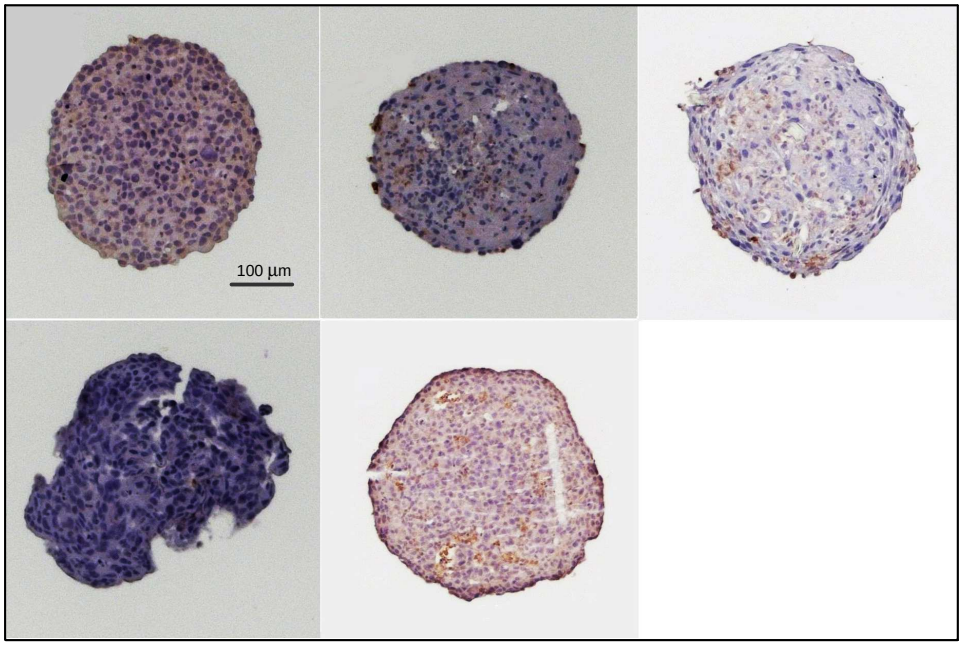


**Fig. 3.3 Representative stained paraffin section (4 µm) through the center of spheroids consisting of various tumor cells and MO co-cultured for 40 h. The sections were stained for monocytes marker CD45 using ABC/DAB method for detection; counterstained with hematoxilin. Cell lines: (a) BT474; (b) BT549; (c) Hs578; (d) MCF-7; (e) T47D. Bar = 100 µm applies to all parts a-e. MO are stained brown.**

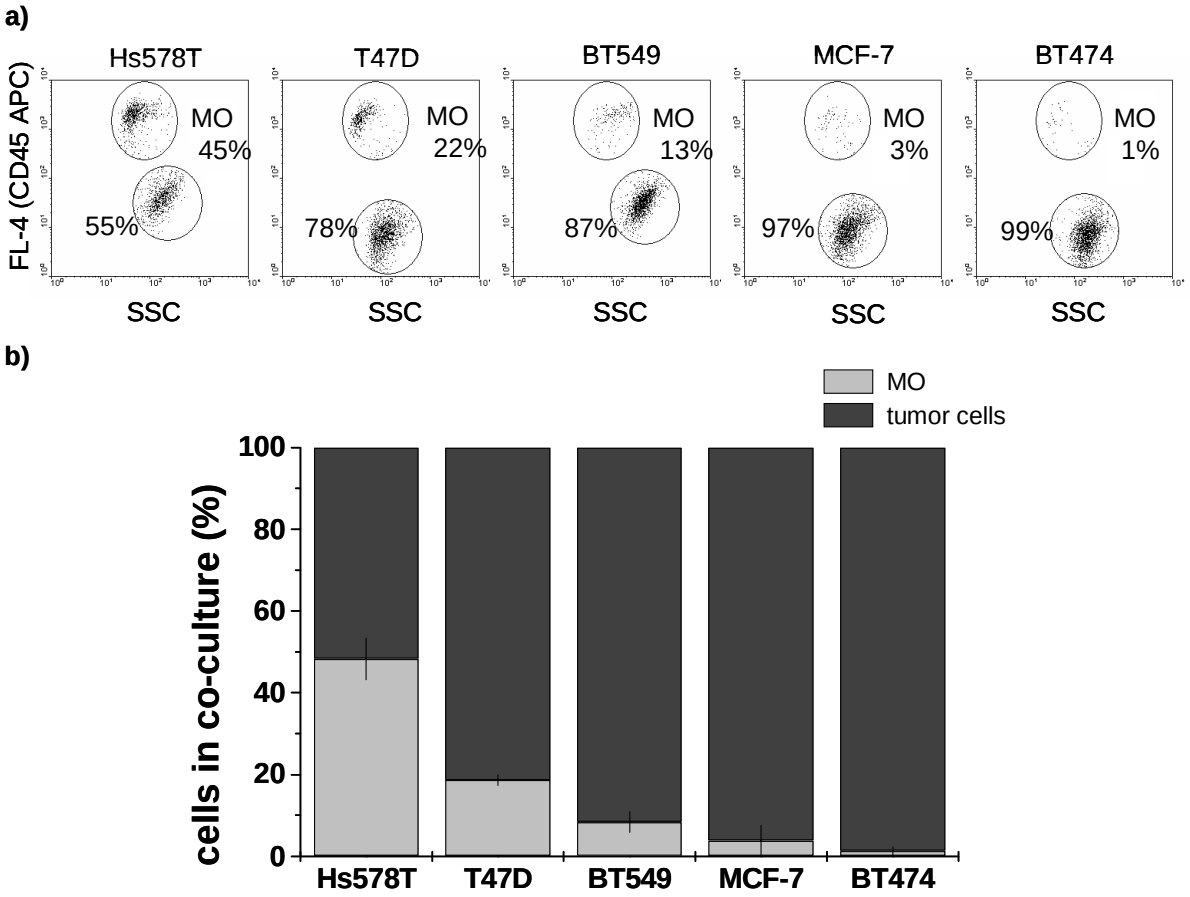


**Fig. 3.4 MO to breast tumor cell ratio in spheroid co-cultures with Hs578T, T47D, BT549, MCF-7, BT474 cell lines. The ratio of a mixed cell suspension isolated from tumor spheroids (40 h co-culturing, 1x10$^4$ MO/spheroid) was determined using flow cytometry. Cells were stained with APC-conjugated CD45 antibody. (a) Representative dot plot diagram showing FL-4 fluorescence versus 90° scatter signals, (b) Column s in graphs show averaged mean values and SD of three independent experiments with MO from 3 different healthy donors.**

To determine the minimal time for successful and reproducible MO and Hs578T co-culturing, the MO migration kinetics into Hs578T spheroids was analyzed by determining the tumor cell to MO ratios after 4, 10, 20 and 40 h in co-culture. Fig. 3.5 shows that the MO infiltration process is completed within 10 h, and slower than into fibroblast spheroids (4 h, Fig. 3.1). Hence, the 10 h co-culturing was chosen as optimal for all further experiments with Hs578T spheroids.

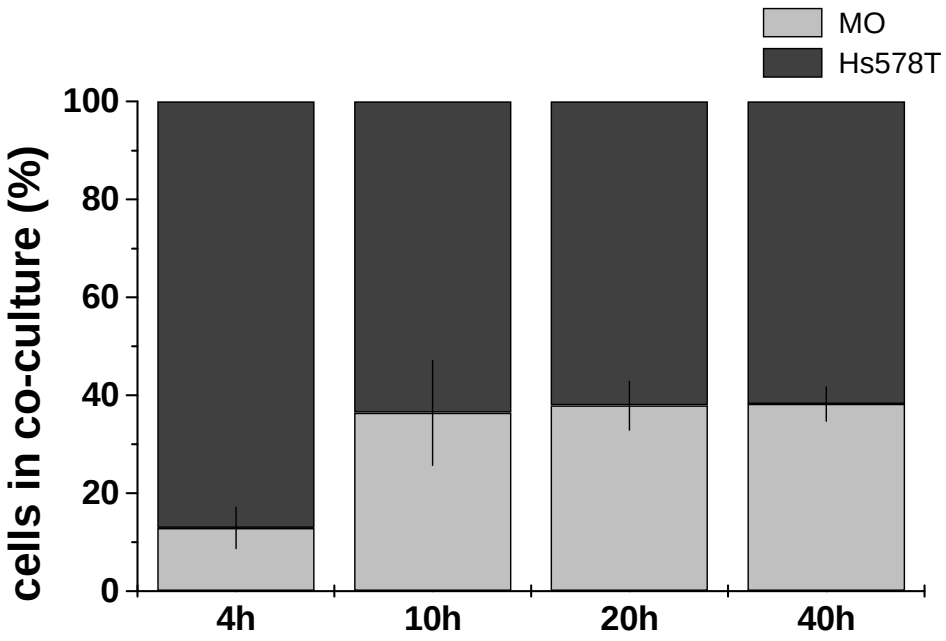


**Fig. 3.5 Monocyte migration into Hs578T breast tumor cell line spheroids is completed within 10 h. MO to breast tumor cell line proportion in Hs578T spheroid co-culture was checked 4, 10, 20 and 40 h after addition of $1x10^4$ MO per spheroid. The cell ratio (± SD) was determined using flow cytometry following spheroid dissociation and staining with monocyte specific APC-conjugated anti-CD45 antibody. Columns in graphs show mean values and SD of three independent experiments with MO from 3 different healthy donors.**

### 3.1.3 Migrating MO population

Flow cytometric analysis of co-cultures consisting of MO and fibroblasts or MO and tumor cells described in chapters 3.2.1 and 3.2.2 allowed to determine the cell ratio (F or tumor cell to MO) in spheroids. However, since the total cell number differed for each spheroid type at the day of analysis and depended on the growth characteristics of the individual cell type, the number of infiltrated MO was calculated from the data and the proportion of migrated blood MO relative to the number of MO applied per spheroid ($1x10^4$) was estimated. The results summarized in Tab. 3.3 and 3.4 show that migrating MO population is not equal with percentage of MO in spheroid. For Hs578T cells, for example, mean proportion of MO equals 48.3% of spheroid co-culture and size of migrating MO subpopulation equals 25.9%, PF27T-MO co-cultures consist in 54.5% from MO (Tab. 3.1), however migrating MO subpopulation is smaller than for Hs578T cells and equals 14.8%.

**Tab. 3.4 Proportion of blood MO that migrated into tumor cell line spheroids or spheroids of tumor-derived fibroblasts (co-culture time: 40 h for tumor cell line spheroids, 4 h for fibroblast spheroids).**

| | Migrating MO subpopulation (%) | |
|---|---|---|
| **Breast tumor cell line** | **average** | **SD** |
| Hs578T | 25.9 | 3.6 |
| T47D | 8.9 | 1.2 |
| BT549 | 2.7 | 0.8 |
| MCF-7 | 1.1 | 1.0 |
| BT474 | 0.6 | 0.5 |
| **TAF** | **average** | **SD** |
| PF27T | 14.8 | 2.2 |
| PF37T | 11.7 | 1.1 |
| PF53T | 17.9 | 0.8 |

## 3.2 Experiments to verify the role of chemokines (CCL2) in MO migration into spheroids

### 3.2.1 CCL2 release from spheroids of breast tumor origin

CCL2 release of breast tumor spheroids was measured and compared to that released from TAF spheroids. Supernatants were collected 96 h after cell inoculation in liquid overlay to reflect the CCL2 concentration at the onset of co-culturing. Also cell number at this time point was checked and is given in Tab. 3.5. Chemokine level was checked via ELISA and release rates were calculated per cell and are presented in Fig. 3.6 and Tab. 3.6.

**Tab. 3.5 Cell number calculated per spheroid 96 h after cell inoculation in liquid overlay.**

| | Cell number pro spheroid | |
|---|---|---|
| **Breast tumor cell line** | **average** | **SD** |
| Hs578T | 3211 | 455 |
| T47D | 3848 | 339 |
| BT549 | 3550 | 410 |
| MCF-7 | 2293 | 256 |
| BT474 | 3632 | 565 |

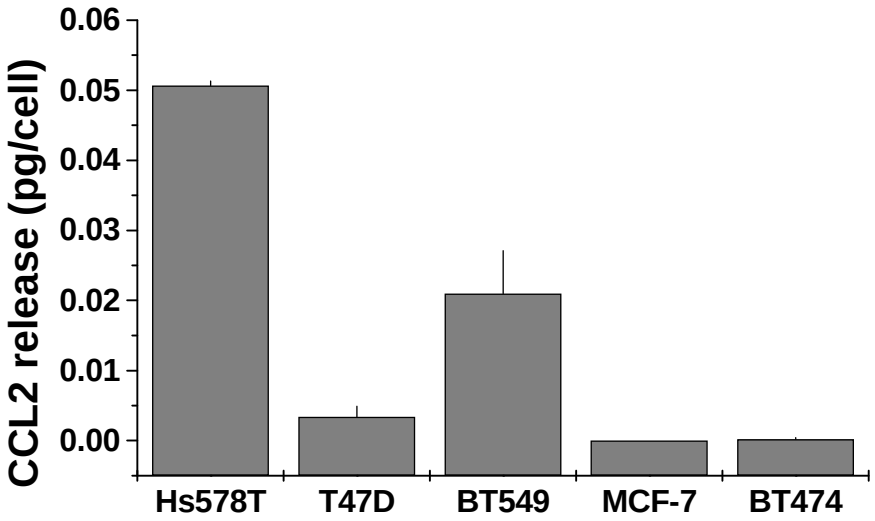


**Fig. 3.6 CCL2 level and cellular release rates differs between five breast tumor cell lines in spheroid culture. CCL2 release was determined by ELISA and calculated in pg/cell.**

The data summed up in Tab. 3.6 reveal that MO strongly infiltrate those cell lines which express relative high amounts of CCL2. Cell lines which do not produce CCL2 or at much lower levels were poorly infiltrated by MO. However, the mean proportion of MO to tumor cells does not simply increase with CCL2 level. In general, four of five tumor spheroid types, show a lower infiltration by MO than tumor-derived spheroids. MO infiltration rates reach about 50% which can be compared with that for TAF spheroids only in the Hs578T tumor spheroid type.

**Tab. 3.6 Release rate of CCL2 protein for breast tumor cell lines, calculated pro one cell and mean ratio of MO that migrated into tumor cell line spheroids.**

| | CCL2 release (pg/cell) | | Percentage of MO In c-culture (%) | |
|---|---|---|---|---|
| **Breast tumor cell line** | **average** | **SD** | **average** | **SD** |
| Hs578T | $50.7x10^{-3}$ | $0.6x10^{-3}$ | 48.3 | 5.1 |
| T47D | $3.4x10^{-3}$ | $1.5x10^{-3}$ | 18.6 | 1.3 |
| BT549 | $21x10^{-3}$ | $6.1x10^{-3}$ | 8.4 | 2.6 |
| MCF-7 | 0 | 0 | 3.8 | 3.8 |
| BT474 | $0.2x10^{-3}$ | $0.2x10^{-3}$ | 1.3 | 1.0 |

### 3.2.2 Exogenous modulation of the paracrine milieu (of fibroblast spheroids)

#### 3.2.2.1 Wash-out approaches

The paracrine factors released by fibroblasts can influence spheroid infiltration by MO. To evaluate their impact on MO migration, level of paracrine factors (including CCL2) was reduced by washing out of supernatant and replacing it with new, unconditioned medium. The conditioned medium from the milieu of spheroids seeded in 96 well plates, was removed (90%) just before addition of the MO suspension ($1x10^4$ MO per spheroid), as described in chapter 2.2.1.2. In parallel, control experiments without medium replacement was conducted. Both “wash out” and unchanged samples were checked for CCL2 release (ELISA) and MO infiltration (FC) after 2, 4, 6, 8 and 20 h of co-culturing (Fig. 3.7a and b, respectively).

As shown in Fig. 3.7.a, CCL2 level is high (5959±351 pg/ml) at the onset of co-culturing but does not significantly increase over a period of 20 h. CCL2 level in “wash out” samples is reduced to about 20% of the control spheroids but then accumulates slowly. After 20 h, CCL2 level has reached 80% of the control values.

Removing of paracrine factors in “wash out” samples, significantly delayed ($p<0.05$) migration kinetics of MO into “wash out” fibroblast spheroids relative to control spheroids which is reflected by a lower number of migrated MO after 4 h and 6 h of co-culturing as documented in Fig. 3.7b.

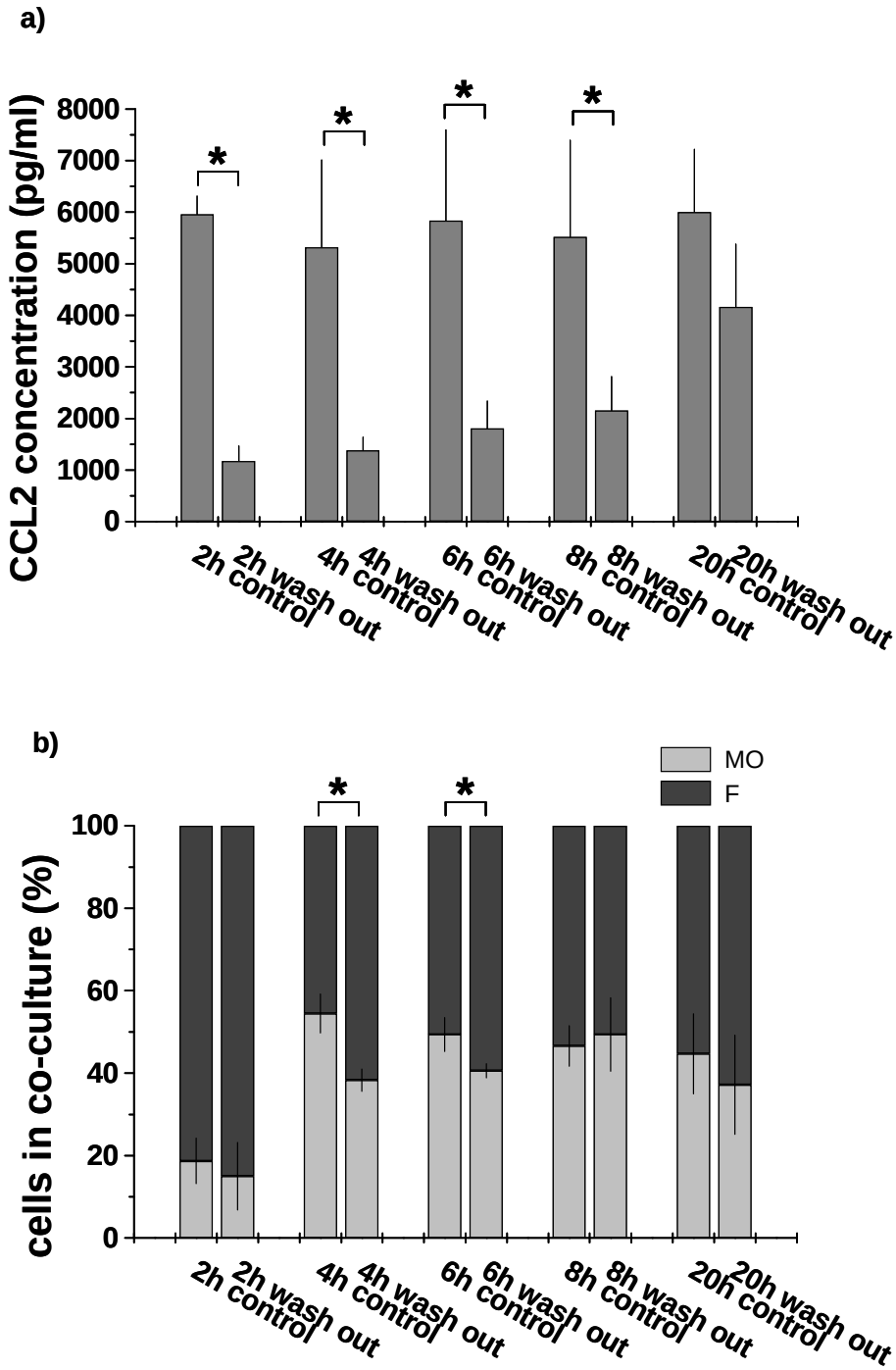


**Fig. 3.7 "Wash out" of paracrine factors from external milieu of TAF spheroids results in delayed MO migration. (a) CCL2 concentration was determined as a representative paracrine factor of interest by ELISA. In "wash out" samples after 2, 4, 6, 8 h CCL2 is reduced as compared to control supernatants, the difference is significant ($p<0.05$). CCL2 concentration increases as a function of time in culture to reach the level in control wells with fibroblast spheroids after 20 h of co-culturing. (b) Removing of paracrine factors through "wash out" delays migration kinetics of MO into fibroblast spheroids relative to control for 4 h and 6 h of co-culturing, the difference is significant ($p<0.05$). Columns in graphs show mean values and SD of three independent experiments with MO from 3 different healthy donors.**
*** Significance level: $p< 0.05$**

#### 3.2.2.2 Addition of CCL2

According to the hypothesis, that high release of CCL2 by TAF can be responsible for enhanced MO migration into tumor-derived fibroblast spheroids, experiments were performed to alter the gradient of CCL2. If there is a gradient within the fibroblast spheroids, supplementation of the exogenous milieu with high levels of rhCCL2 should invert the gradient of this protein with respect to intra- and extraspheroidal distribution as schematically shown in Fig. 3.8.

The addition of rhCCL2 at a concentration of 0.02 μg/ml (10x) reduced MO migration into TAF (PF53T) spheroids by about 50%. When the extraspheroidal CCL2 concentration was increased by addition of 100x the amount released by the tumor-derived fibroblast spheroids, MO migration decreased to 5% of the control level (Fig. 3.9). This observation was revealed in three independent experiments, i.e. with MO from three healthy donors.

Normal fibroblasts produce significantly less CCL2 than breast tumor-derived fibroblasts. MO migration to spheroids originated from normal tissue is also significantly lower (Silzle *et al.*, 2003). To find out if MO migration into normal fibroblast spheroids may also depends on CCL2 gradient an analogue experimental series as these explained in Fig. 3.8, was performed. In this set of experiments, normal foreskin fibroblasts VF1 that have low CCL2 release and MO infiltration rates were used. The concentration of added CCL2 was adopted in order to obtain an external milieu enriched in CCL2 by a factor of 10 (0.002 μg/ml) and 100 (0.02 μg/ml) relative to control. As shown at Figure 3.10, MO migration is unaltered by exogenous rhCCL2, indicating that CCL2 is not responsible for the basic, non-tumor-associated MO migration into normal fibroblast spheroids.

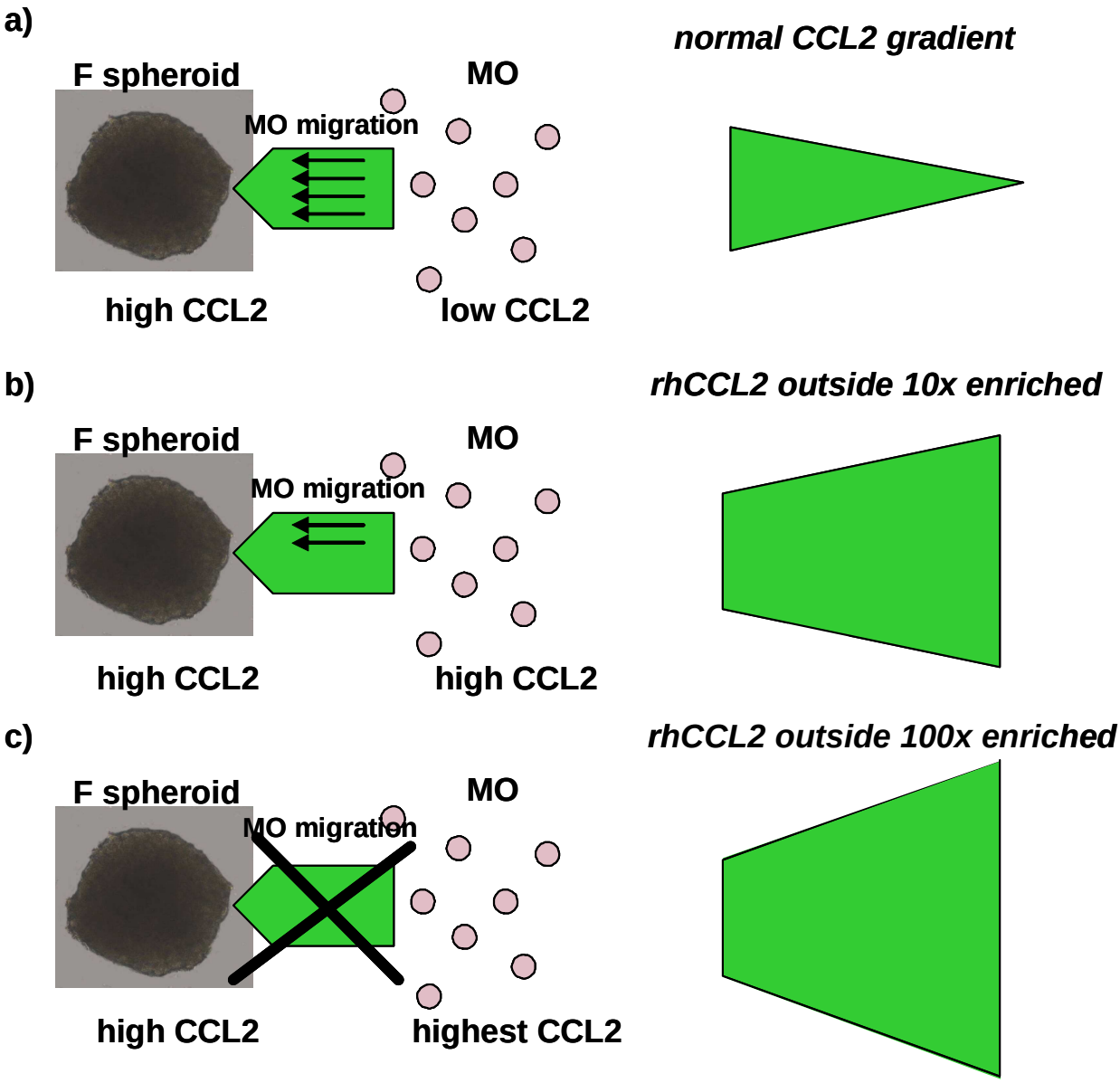


**Fig.3.8. Conditions to affect MO migration by the addition of exogenous rhCCL2. (a) control without supernatant supplementation, (b) supernatant supplemented with 10x higher concentration of CCL2 than released by tumor derived fibroblasts spheroids, (c) supernatant supplemented with 100x higher concentration of CCL2 than released by TAF spheroids.**

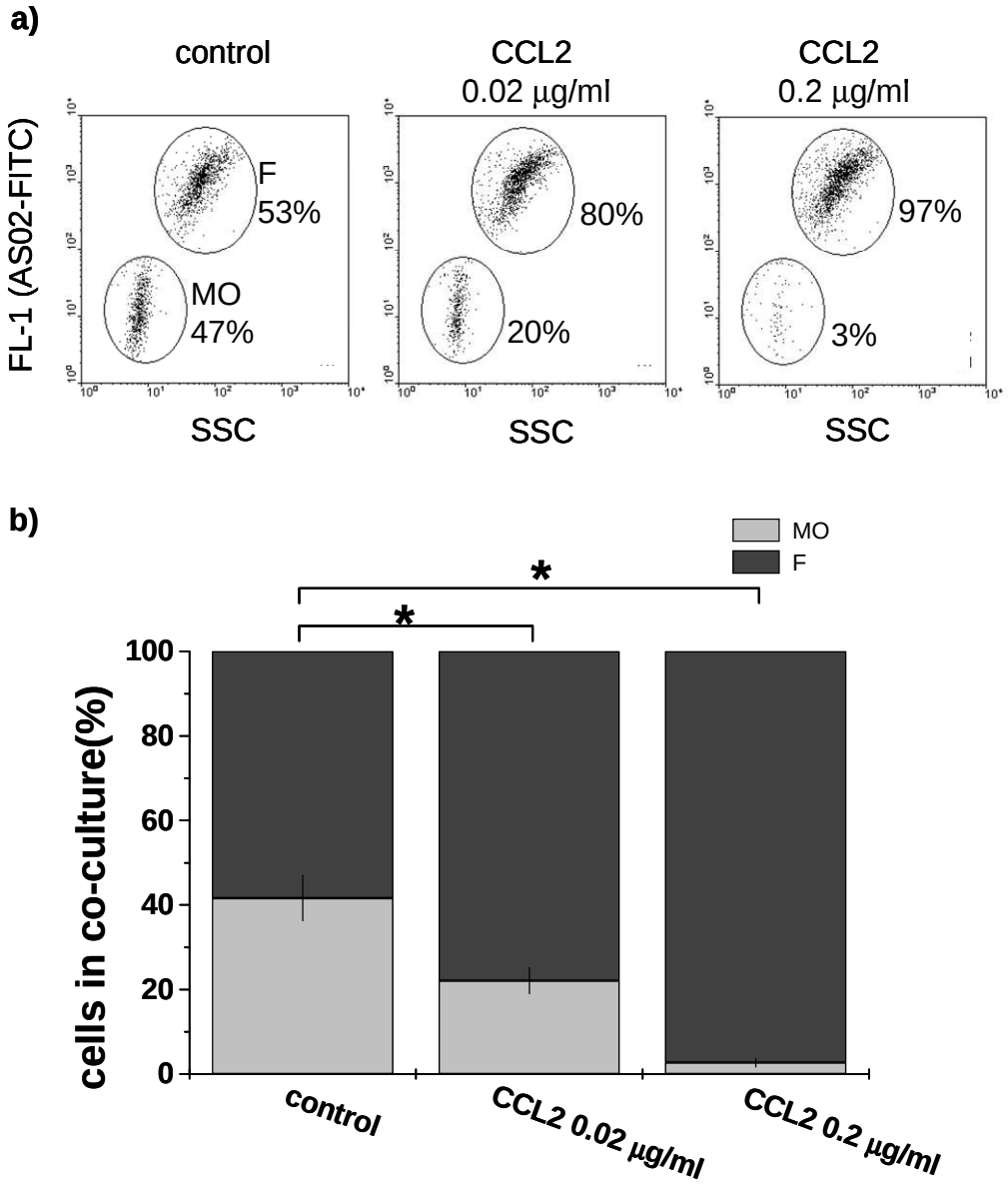


**Fig. 3.9 MO migration into tumor-derived fibroblast spheroids is reduced by the addition of rhCCL2 to the supernatant and loss of the CCL2 gradient under standard culture conditions. (a) Representative dot plot diagrams and proportion (± SD) of fibroblasts and MO in spheroid co-cultures 4 h after addition of 1x10$^4$ MO/well and per spheroid. Dot plot diagrams show FL-1 fluorescence versus 90° scatter signals of a mixed cell suspension isolated from PF53T spheroids. The cell suspension was stained with the FITC-conjugated 'fibroblasts specific' antibody AS02. (b) Columns in graphs show averaged mean values and SD of three independent experiments with MO from 3 different healthy donors.**
*** Significance level: p< 0.05**

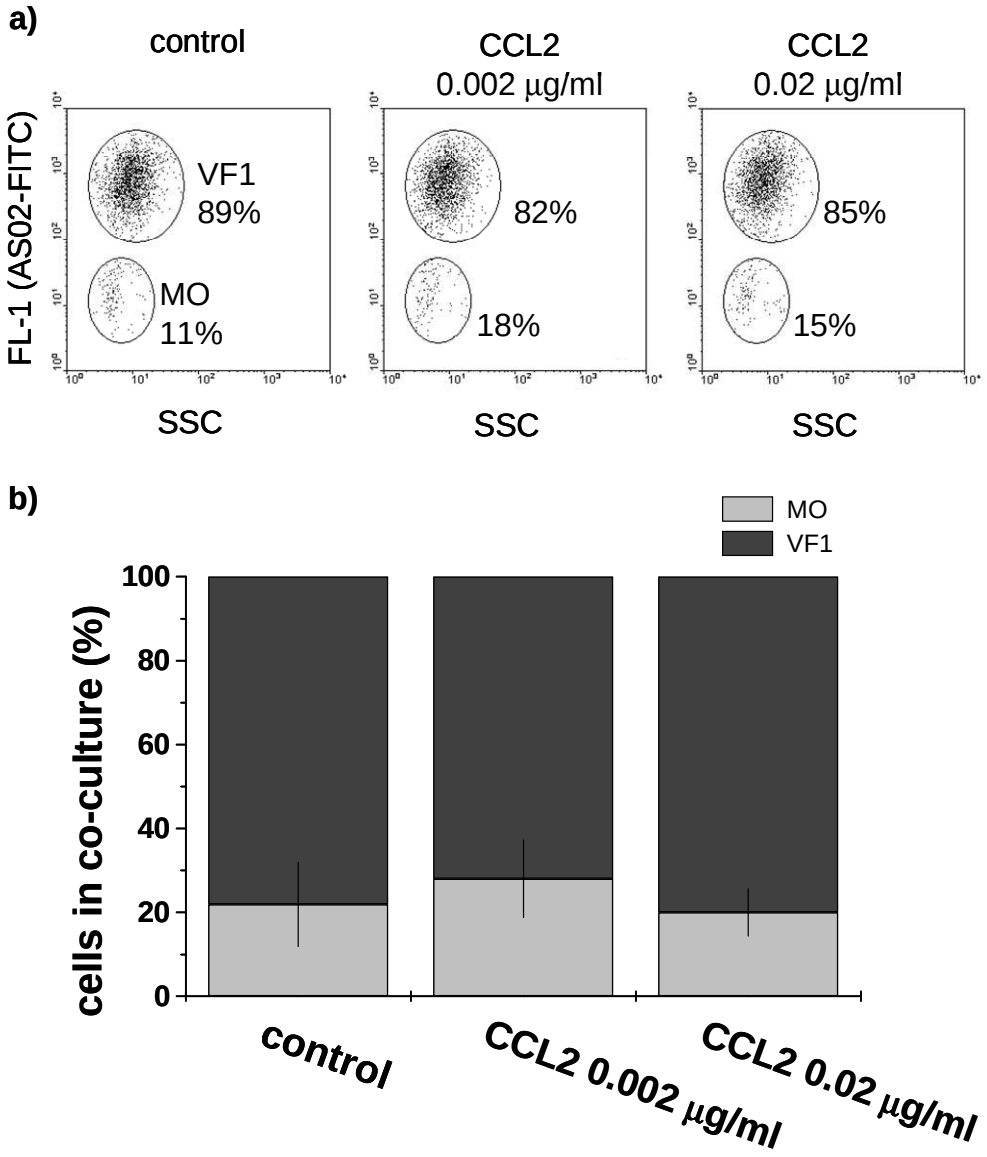


**Fig. 3.10 MO migration into normal foreskin fibroblast (VF1) spheroids is not influenced by the addition of rhCCL2 to the supernatant and loss of the CCL2 gradient under standard culture conditions. (a) Representative dot plot diagram and proportion (± SD) of fibroblasts and MO in spheroid co-cultures 4 h after addition of $1x10^4$ MO/well and per spheroid. Dot plot diagrams show FL-1 fluorescence versus 90° scatter signals of a mixed cell suspension isolated from VF1 spheroids. The cell suspension was stained with FITC-conjugated 'fibroblasts specific' antibody AS02. (b) Columns in graphs show averaged mean values and SD of three independent experiments with MO from 3 different healthy donors.**

### 3.2.3 Experimental approaches to modulate cellular CCL2 release from fibroblast spheroids by siRNA

The RNAi method was considered to down regulate CCL2 levels in breast-tumor-derived fibroblasts spheroids as an alternative to neutralization of endogenous CCL2 by a blocking antibody, which did not achieved the expected results. Application of siRNA, if successful, would allow further mechanistic studies on MO migration and the comparison of MO migration activity with endogenous CCL2 production when significantly reduced.

According to the standard procedure, at day 4 after transfection, cells grown in monolayer were harvested and seeded again in liquid overlay for spheroid initiation and as monolayer. Routinely for dissociation a trypsin/EDTA in PBS solution is used. To control the potential influence of dissociation means on CCL2 reduction, other enzymes were also tested: collagenase III and accutase. The collagenase III induced cell death, trypsin/EDTA and accutase neither influenced viability of cells nor the siRNA effect in monolayer relative to non-transferred cells. Trypsin/EDTA, as commonly used reagent, was chosen for all further experiments.

Breast-tumor-derived fibroblasts (PF27T) were transfected with use of self-designed siRNAs (ds1 + ds2) using oligofectamine. The amount of CCL2 was checked at protein level via ELISA. Protein level, both for 2-D and 3-D cultures was compared at day 7 after transfection and cellular release was monitored for a 24 h (monolayer) or 72 h (spheroid) time intervals. However, the desired effect of down-regulation (>80%) of CCL2 protein was achieved only for monolayer (2-D) cultures. The CCL2 release in spheroid cultures (3-D) as determined in the supernatant was unaltered (Fig. 3.11).

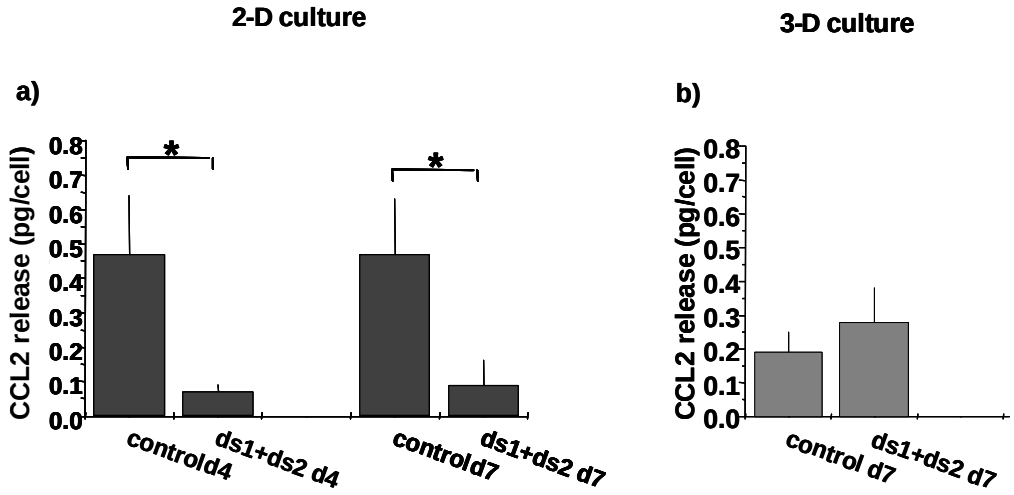


**Fig. 3.11 Transfection of fibroblasts with CCL2 specific siRNA results in reduced release of CCL2 protein from cells in 2-D but not 3-D culture. (a) Graph shows the 24 h cellular release rate of CCL2 measured in supernatants with ELISA (calculated in pg/cell) at days 4 and 7 (respectively: d4, d7) after transfection of PF27T fibroblasts. CCL2 protein expression is down regulated at days 4 and 7 after transfection. (b) In 3-D cultures, 7 days after transfection no reduction on protein level is observed; here, the 72 h CCL2 release was measured. PF27T fibroblasts were transfected with self-designed siRNAs (ds1+ds2) and transferred at day 4 after transfection using mild enzymatic means. Control cells were transfected with non-specific control siRNA. Columns in graphs show averaged mean values and SD of three independent experiments.**
*** Significance level: p< 0.05**

In order to verify that the discrepancy between monolayer (2-D) and spheroid (3-D) culture with respect to the siRNA efficiency is independent of the fibroblast type, a second batch of tumor-derived fibroblasts (PF53T) was applied in an identical experimental setting. Fig. 3.12 shows that the results are consistent with those obtained for PF27T. For monolayer (2-D culture) down-regulation of cellular CCL2 protein release of about 80% was obtained. The CCL2 release from spheroid cells (3-D culture) measured in the supernatant was unchanged by the siRNA approach.

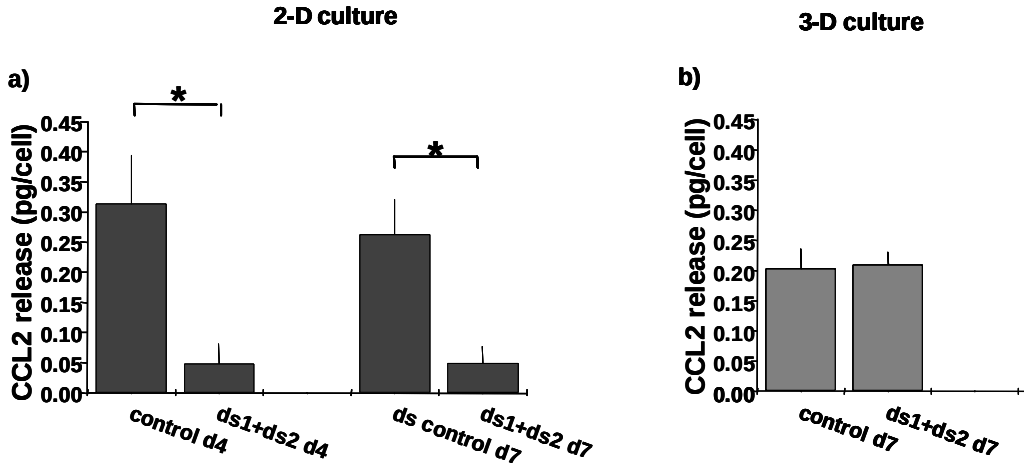


**Fig. 3.12 Transfection of fibroblasts with CCL2 specific siRNA results in reduced release of CCL2 protein from cells in 2-D but not 3-D culture. (a) Graph shows the 24 h cellular release rate of CCL2 measured in supernatants with ELISA (calculated in pg/cell) at days 4 and 7 (respectively: d4, d7) after transfection of PF53T fibroblasts. The 24 h release rate of CCL2 expression, measured with ELISA and calculated in pg/cell, is down regulated at days 4 and 7 after transfection. (b) In 3-D cultures, 7 days after transfection no reduction on protein level is observed; here, the 72 h of CCL2 release was measured. PF53T fibroblasts were transfected with self-designed siRNAs (ds1+ds2) and transferred at day 4 after transfection using mild enzymatic means. Control cells were transfected with non-specific control siRNA. Columns in graphs show averaged mean values and SD of three independent experiments.**
*** Significance level: p< 0.05**

While the experiments with self designed siRNA were in progress, a CCL2 specific siRNA became commercially available. Experiments with this siRNA from Ambion (Silencer siRNA) were performed according to the same scheme as for self designed siRNA, and the down regulating effects were compared. As shown in Fig. 3.13, the results were comparable to those achieved in experiments with self-designed siRNAs (ds1 + ds2). The data imply that CCL2 expression is on longer down-regulated after transfer of cells into a 3-D culture format. This cannot be due to extended culturing since CCL2 protein release was measured at day 7 after siRNA transfection in both culture settings (2-D and 3-D).

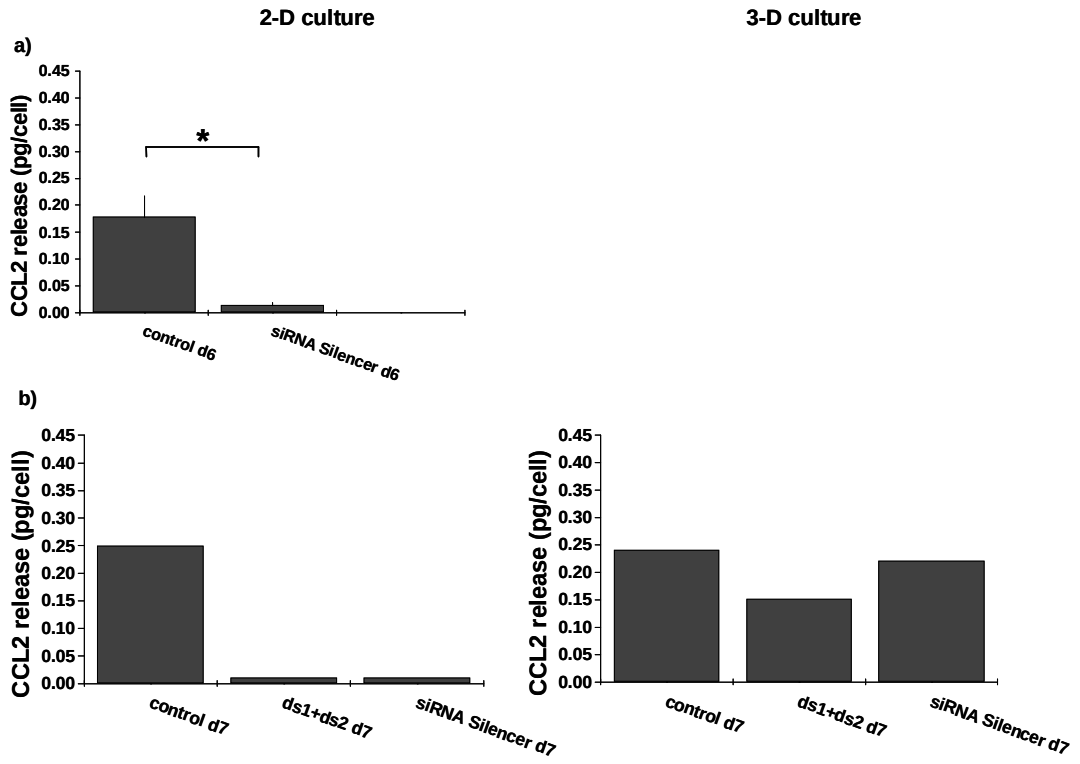


**Fig. 3.13 Transfection of PF27T fibroblasts with Silencer siRNA in 2-D culture reduces CCL2 on protein level. There is no difference in transfection efficiency between self designed siRNAs (ds1+ds2) and commercially available Silencer siRNA. (a) The 24 h CCL2 release rate was measured (ELISA) and calculated in pg/cell. Columns show mean values (± SD) of three independent experiments. The reduction is significant ($p<0.05$). (b) Columns show reduction of CCL2 in 2-D culture when transfected with either self-designed (ds1+ds2) or commercially available CCL2 specific siRNA as compared to control. At day 7 after transfection significant reduction in CCL2 release is observed. The 24 h release rate of CCL2 was measured in supernatant with ELISA and calculated relative to cell numbers in pg/cell. In 3-D cultures no or insufficient CCL2 protein reduction versus control is obtained. A single experiment was performed as it revealed in past the data presented in Fig. 3.12.**
*** Significance level: $p< 0.05$**

The aim of the next set of experiments was to clarify, if siRNA is still present in transfected cells when grown in a 3-D culture setting in spite of loss of down-regulation of CCL2 protein release. The experiments were performed according to the described scheme but included an additional fluorescently labeled negative control siRNA (Alexa Fluor488).

CCL2 level in monolayers was again successfully reduced. In 3-D cultures no reduction was observed (Fig. 3.15.a) as shown earlier. Invert fluorescence microscopy enabled the visualization of Alexa Fluor488-conjugated control siRNA in the cells (Fig.3.15.b). Additionally, confocal microscopy was used to verify that more than just the outer layer of spheroid cell is fluorescently labeled and thus contained siRNA at the onset of spheroid culturing. In summary, the technological tools applied, indicate that siRNA transfection in principle has been successful (Fig.3.15.c) and that siRNA was present at least when spheroids were initiated.

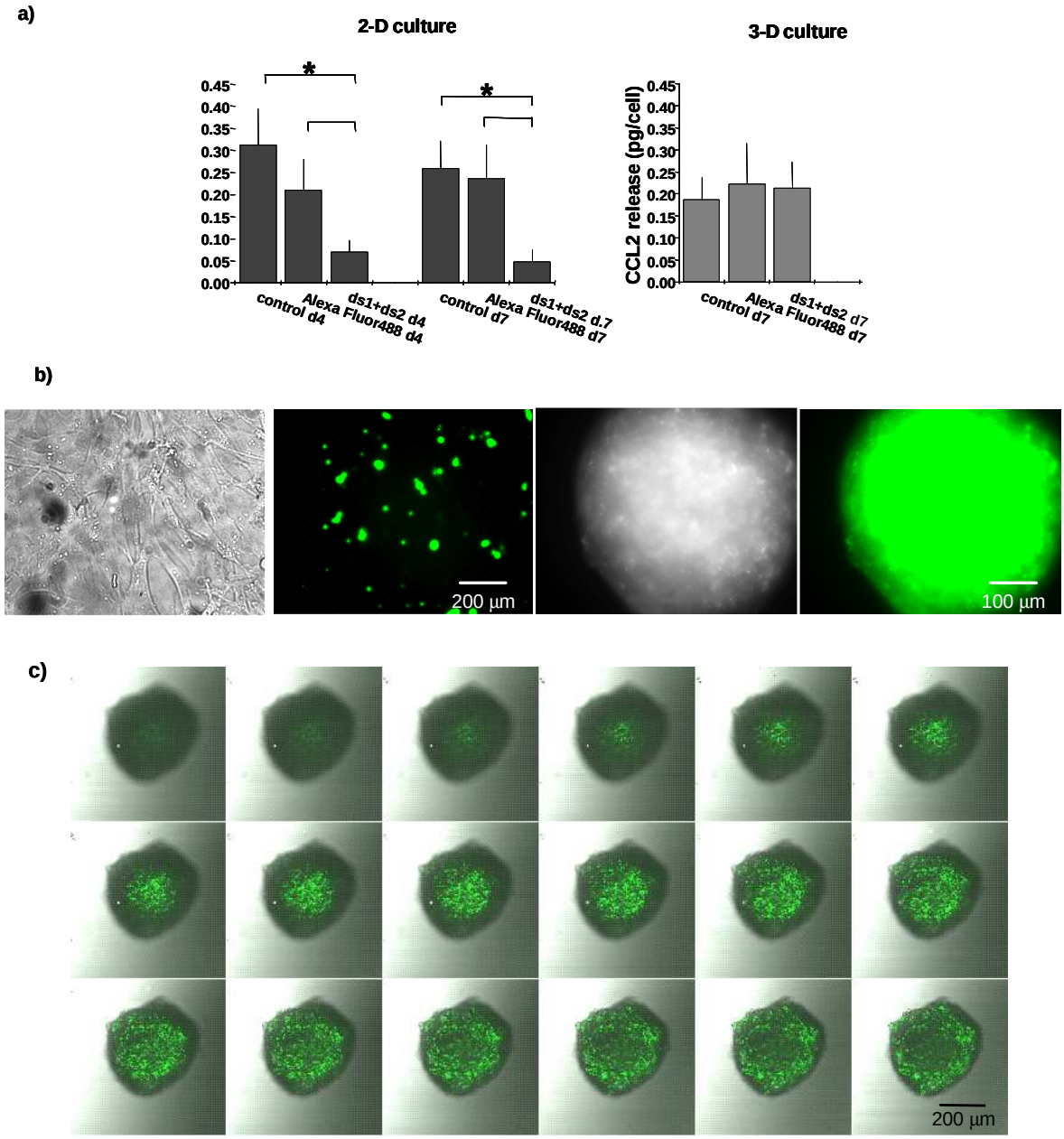


**Fig. 3.15 (a) PF53T fibroblasts were transfected with CCL2 specific siRNA ds1 + ds2 in parallel to a fluorescently labeled negative control siRNA. As shown earlier, reduction of CCL2 protein level in 2-D cultures after applying ds1+ds2 siRNA measured with ELISA was significant (p<005). In 3-D cultures no significant reduction was measured. Columns show mean values and SD of three independent experiments. (b) PF53T fibroblasts transfected with control siRNA Alexa Fluor488 are fluorescently labeled in 2-D and 3-D culture. Microscopic images: 1) phase contrast image of 2-D culture, 2) fluorescence image of 2-D culture, 3) phase contrast image of 3-D culture, 4) fluorescence image of 3-D culture. The fluorescent dye (bound to siRNA) is still visible at day 7 after transfection both in monolayer and in spheroid cultures. For images 1 and 2 magnification of 20 x objective was used, images 3 and 4 were taken with a 10 x objective. (c) PF53T fibroblasts transfected with Alexa Fluor488-conjugated control siRNA. 3-D culture was monitored by confocal microscope. A Z-stack of 5 µm sections was recorded with a magnification of 10 x objective.**
*** Significance level: p< 0.05**

The last set of experiments was performed to verify the differences in reduction of CCL2 protein release on the RNA level and thus to gain insight into the discrepancy between CCL2 regulation in 2-D *vs.* 3-D culture. Experiments were performed according to the standard protocol described in chapter 2.2.5.5. At day 7 after transfection RNA was isolated from cells cultured as monolayer and as spheroids. To verify quantity of isolated nucleic acid, RNA was converted into cDNA and Real-Time-PCR was performed. Supernatants used for the parallel analysis of CCL2 release rates confirmed previous outcomes. In 2-D cultures reduction of CCL2 RNA expression in cells transfected with ds1+ds2 siRNA as compared to control cells was observed. In 3-D cultures, however, RNA level was increased in samples transfected with ds1+ds2 siRNA (Fig. 3.16). Thus, the CCL2 protein levels corresponded to a reduced mRNA level in 2-D culture while in 3-D culture which lacked siRNA-related CCL2 protein reduction mRNA level was enhanced relative to control. It is unclear why the highly efficient silencing RNA in 2-D culture looses its efficacy in 3-D culture. Understanding this phenomenon was beyond the scope of the present work and the siRNA approach was therefore terminated at this point.

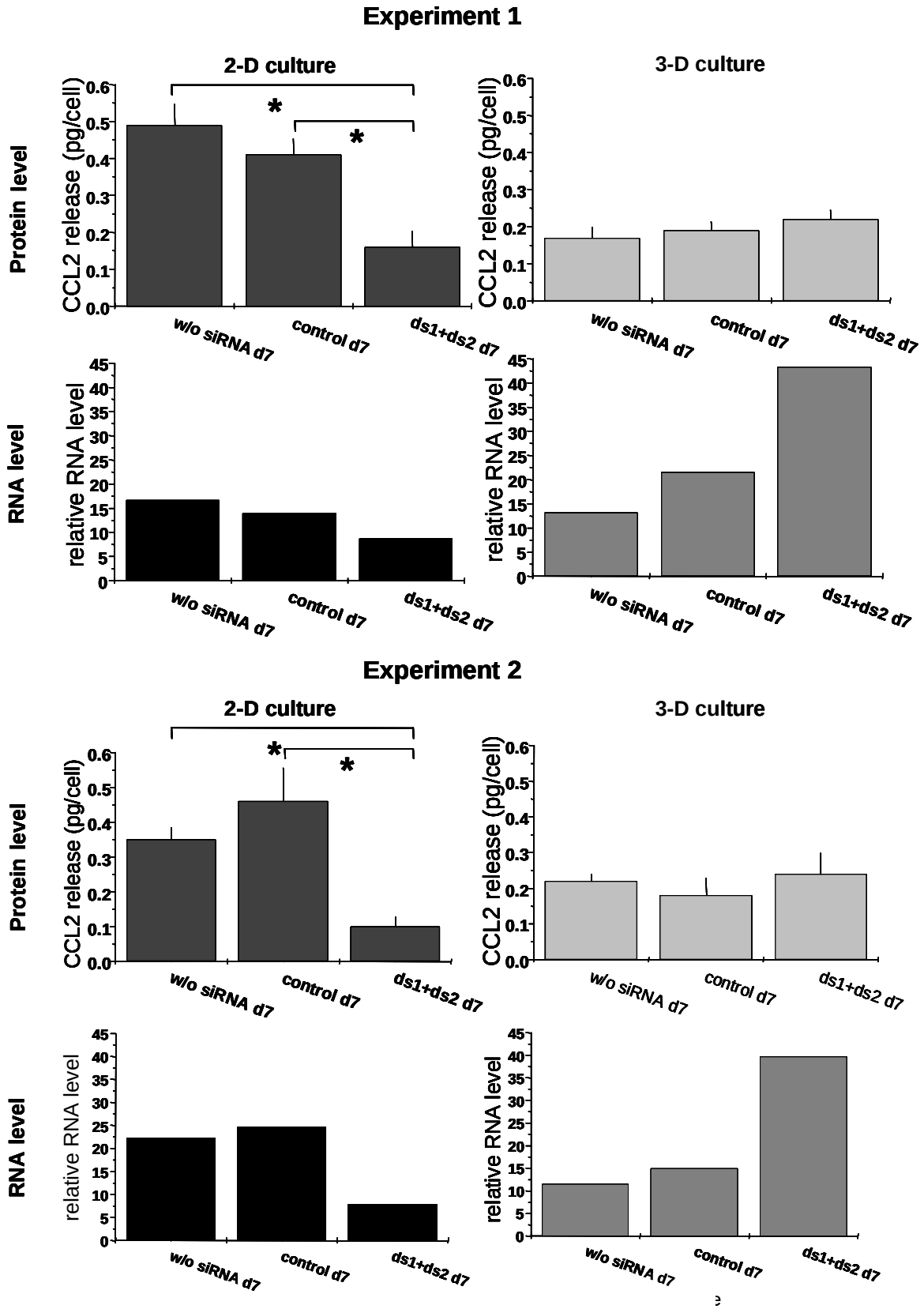


→ **Figure legend on pg 70**

**Fig. 3.16 Transfection of PF37T fibroblasts with self-designed siRNA (ds1+ds2), in two independent experiments significantly reduced CCL2 protein release and RNA expression at day 7 after transfection in 2-D (left panels) but not 3-D culture (right panels) (p<005). Protein level was measured with ELISA and calculated in pg/cell. CCL2 RNA expression was reproducibly up regulated in 3-D cultures after transfection of monolayer cells with CCL2specific siRNA.**
*** Significance level: p< 0.05**

### 3.2.4 Blockade of chemokine signaling pathways

#### 3.2.4.1 Application of toxins

All chemokines signal through interaction with 7-transmembrane spanning G protein coupled receptors. Pertussis toxin (PTX) is known to block signal pathways for some chemokines through its interaction with $G\alpha_{i/o}$ proteins. One of the receptors sensitive to PTX is the receptor for CCL2 – CCR2A/B (Combadiere *et al.*, 1998). PTX B-oligomer was used as negative control as it binds toxin to the target but has no ADP-ribosyltransferase activity to efficiently block signaling (Tamura *et al.*, 1982; Katada *et al.*, 1983).

MO were incubated with PTX or with PTX B-oligomer in concentrations of 1, 10 and 50 ng/ml for 30 min prior to addition to breast tumor-derived fibroblast spheroids and during co-culturing time. Their migration activity was monitored and compared with control MO (untreated). Flow cytometric analyses were performed after 4 h.

Incubation of MO with PTX blocked the migration of MO into spheroids for all applied concentrations of toxin. MO migration was critically reduced already with the lowest toxin concentration where the B-oligomer showed no effect (see Fig. 3.17). At high concentrations B-oligomer also affected MO migratory activity but the effect never reached a grade similar to PTX holoenzyme. The observed effect may be explained by the presence of holotoxin (≤1%) in the B-oligomer preparation as discussed later. The data clearly demonstrate that blockade of $G\alpha_{i/o}$ dependent signaling abrogates MO migratory activity in the 3-D culture model.

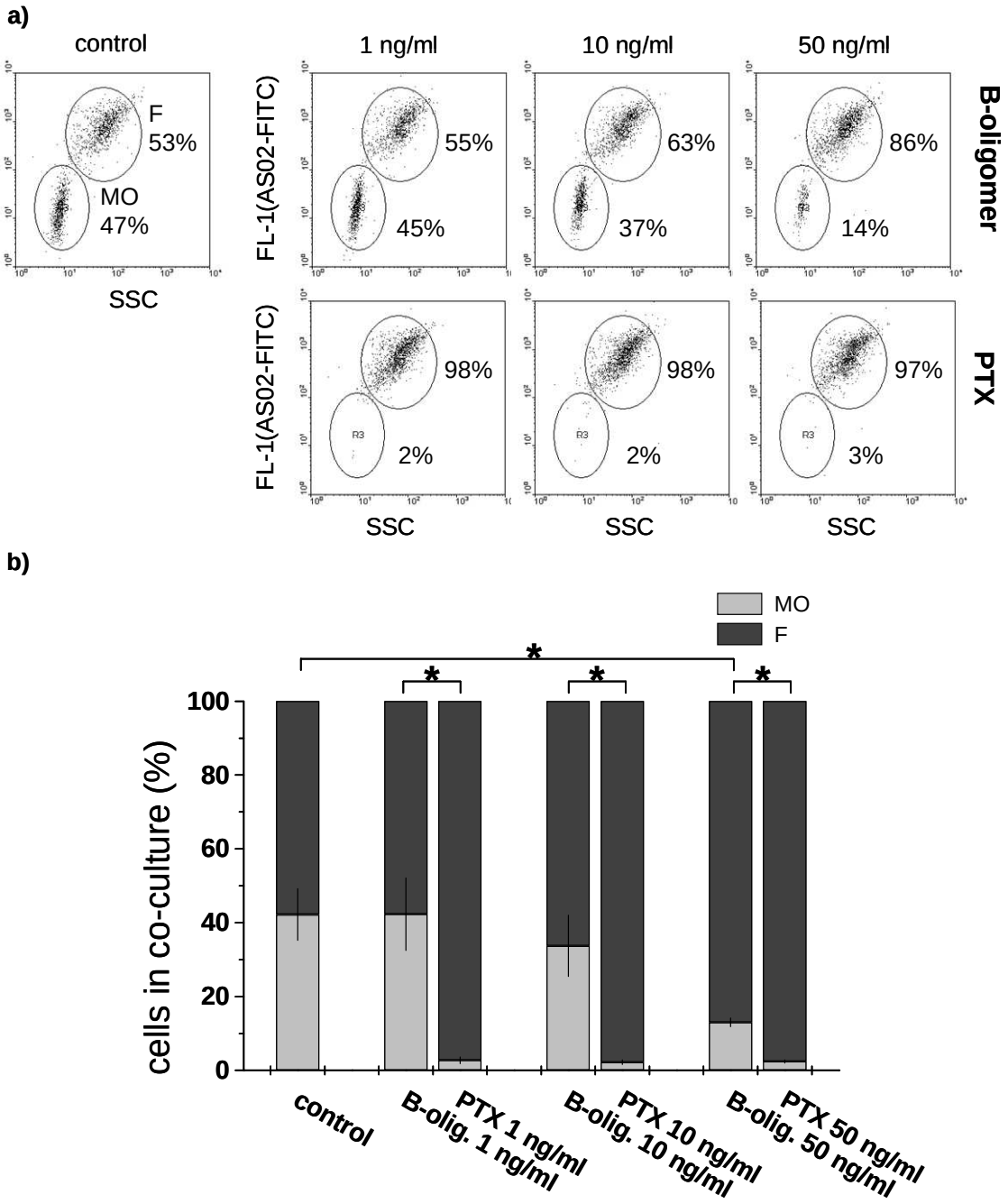


**Fig. 3.17 PTX blocks MO migration (p<005). PTX B-oligomer shows weak blocking effect on MO migratory activity only at the highest concentration (50 ng/ml). (a) Representative dot plot diagrams and proportion (± SD) of fibroblasts (F) and MO in spheroid co-cultures 4 h after addition of $1x10^4$ pretreated MO/well and per spheroid, respectively. Diagrams show FL-1 fluorescence versus 90° scatter signals in a dissoc iated cell suspension from PF37T - MO co-cultures. The cell suspension was stained with the FITC-conjugated 'fibroblasts specific' antibody AS02. MO pre-treatment was performed with 1, 10 or 50 ng/ml B-oligomer or PTX for 30 min at 37℃. (b) Columns in graph show averaged mean values and SD of three independent experiments according to (a) with MO from 3 different healthy donors.**
*** Significance level: p< 0.05**

To find out if the inhibition of MO migration is specific for PTX and $G\alpha_{i/o}$ dependent pathways, a set of experiments was performed using cholera toxin (ChTX). This toxin can block $G\alpha_s$ proteins in their active form but does not interfere with $G\alpha i/o$ (Chang and Bourne, 1989). Similar to the previous experimental series, MO were incubated with ChTX holoenzyme or with ChTX B-subunit which only possesses binding property but should not block $G\alpha_s$ (Fishman, 1982).

Both ChTX holoenzyme and B-subunit were applied in the following concentrations: 1 ng/ml, 10 ng/ml and 50 ng/ml. MO were exposed to toxins 30 min prior to addition to F spheroids and during co-culturing time. MO migration activity was monitored and compared with control MO (untreated). Flow cytometric analyses were performed after 4 h. The 1 ng/ml to 50 ng/ml concentrations were applied in three independent experiments with MO from three healthy donors and these results are shown in Fig. 3.18. The B-subunit did not affect MO migration activity at any concentration. However, the ChTX holoenzyme led to a significant and reproducible reduction in MO migration at concentrations of 10 ng/ml and 50 ng/ml. The concentration of ChTX required for significantly affecting MO infiltrative activity was thus by a factor of ≥10 higher than for PTX.

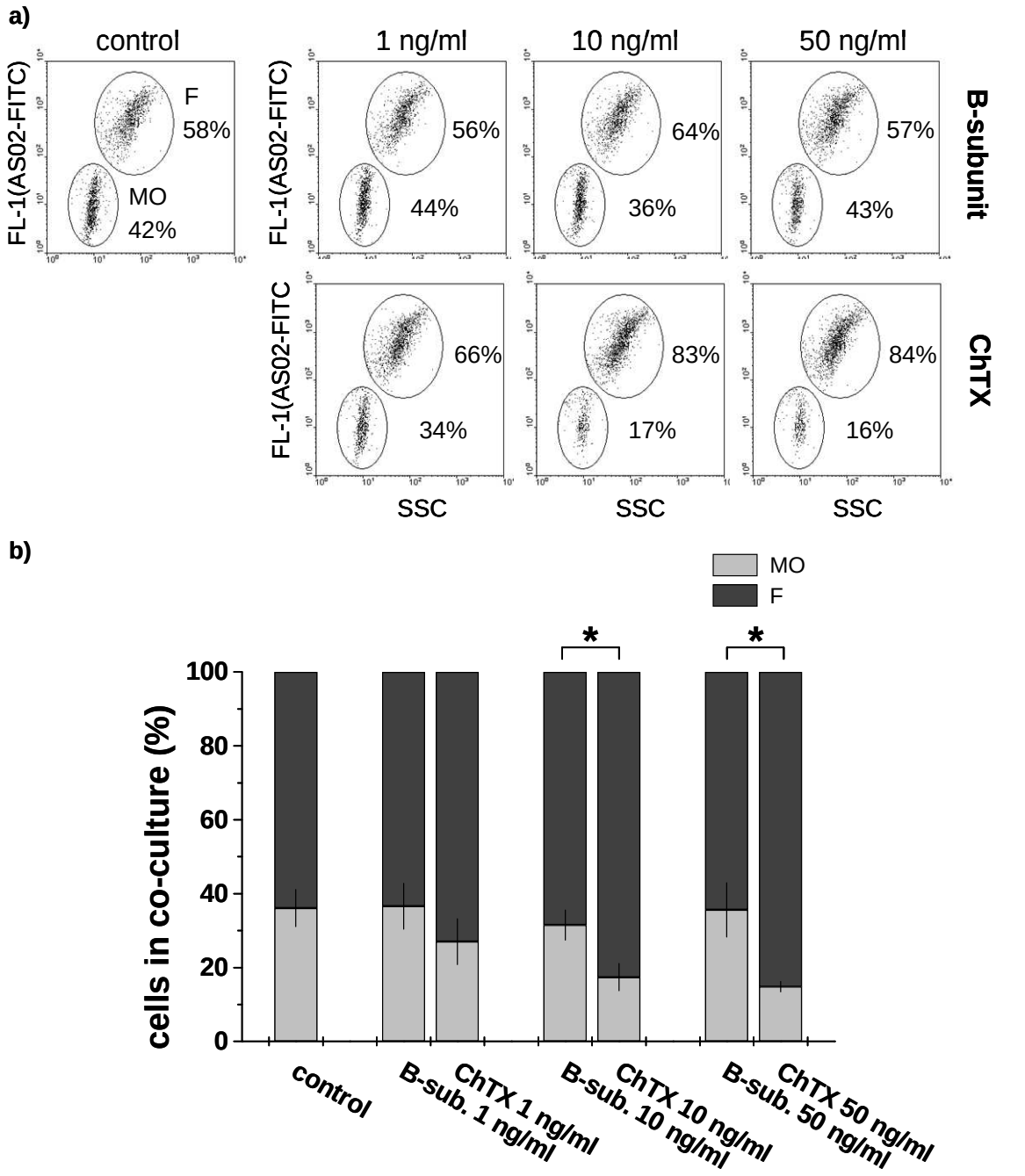


**Fig. 3.18 ChTX at concentrations of 10 and 50 ng/ml lead to a significant reduction of MO migration (p<005) . ChTX B-subunit shows no blocking effect on MO migratory activity. (a) Representative dot plot diagrams and proportion (± SD) of fibroblast (F) and MO in spheroid co-cultures 4 h after addition of 1x10$^4$ pretreated MO/well and per spheroid, respectively. Diagrams show FL-1 fluorescence versus 90° scatter signals in a dissociated cell suspension from PF37T-MO co-cultures. The cell suspension was stained with FITC-conjugated 'fibroblasts specific' antibody AS02. MO pre-treatment was performed with 1, 10 or 50 ng/ml B-subunit or ChTX for 30 min at 37℃. (b) Columns in graph show averaged mean values and SD of three independent experiments according to (a) with MO from 3 different healthy donors.**

*** Significance level: p< 0.05**

### 3.2.4.2 Application of blocking antibodies

#### 3.2.4.2.1 Studies with fibroblast spheroids

Experiment with PTX revealed a high relevance of $G\alpha_{i/o}$ protein mediated pathways for MO migration into spheroids of breast tumor-derived fibroblasts. From all previous data it was again hypothesized that the CCL2/CCR2A/B pathway is the critical determinant for MO migration in the present experimental 3-D culture system. DOC-3 blocks supposedly CCR2A/B receptor on MO (M. Mack - personal communication). To answer the question, if exclusive blockade of CCR2A/B is sufficient to reduce MO infiltration to levels described for normal fibroblast spheroids, DOC-3 was applied in this set of experiments.

DOC-3 (kindly provided by Prof. Matthias Mack; University of Regensburg, Germany) were applied in two concentrations: 1µg/ml and 10 µg/ml. The concentration of 1 µg/ml blocked MO migration only to some degree, thus finally concentration of antibody 10 µg/ml was chosen for experiments. Thus, MO were incubated with DOC-3 or with corresponding isotype (IgG1) 30 min prior to TAF spheroids and during co-culturing. Co-cultures were collected after 20 h and dissociated for flow cytometric analyses. The results clearly show that migration of MO after incubation with blocking Ab at the given concentrations significantly decreased the mean proportion of MO in fibroblast co-cultures from 53± 14% to 13±8% (Fig. 3.19).

To show that the inhibitory effect of DOC-3 antibody is not artificially caused by the MO exposure to a specific antibody, experiments with blocking Ab against CD11b were performed. According to the experimental series with DOC-3, MO were pre-incubated either 30 min with anti-CD11b Ab at a concentration of 10 µg/ml or with a corresponding isotype control (IgG2a) and then added to TAF spheroids. Co-cultures were also exposed to the Ab and were collected after 20 h for dissociation and flow cytometric analysis of fibroblast to MO ratio. No blocking effect of anti-CD11b Ab was observed (Fig. 3.20).

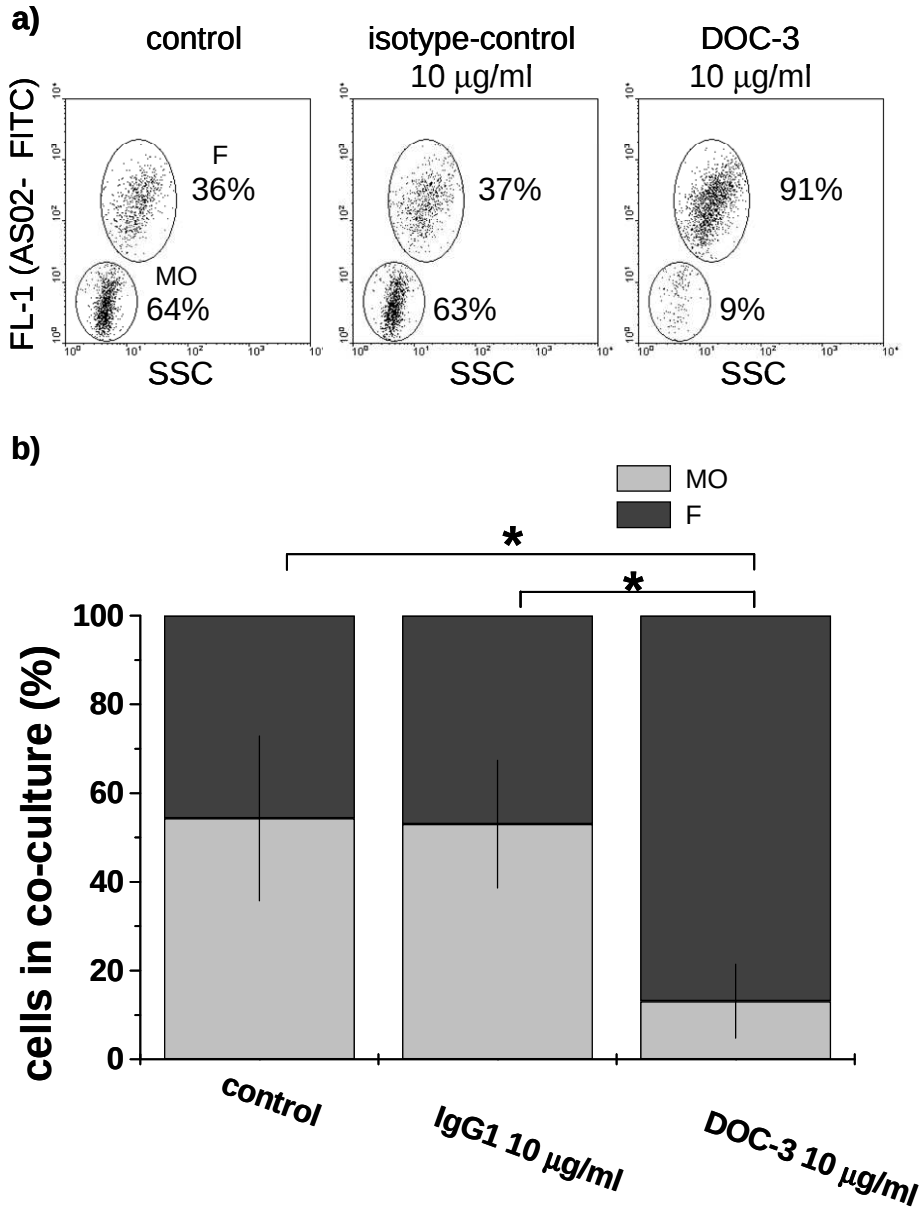


**Fig. 3.19 CCR2A/B blockade on MO by DOC-3 antibody significantly reduced MO migration into tumor-derived fibroblast spheroids (p<005). Isotype control IgG1 had no effect on MO migration. (a) Representative dot plot diagrams and proportion (± SD) of fibroblasts (F) and MO in spheroid co-cultures 20 h after addition of $1x10^4$ pre-treated MO/well and per spheroid, respectively. Diagrams show FL-1 fluorescence versus 90° scatter signals in a dissociated cell suspensions from PF37T-MO co-cultures. The cell suspension was stained with FITC-conjugated 'fibroblasts specific' antibody AS02; MO pre-treatment was performed with 10 µg/ml DOC-3 or isotype IgG1 for 30 min at 37℃. (b) Columns in graphs show averaged mean values and SD of three independent experiments according to (a) with MO from 3 different healthy donors.**

*** Significance level: p< 0.05**

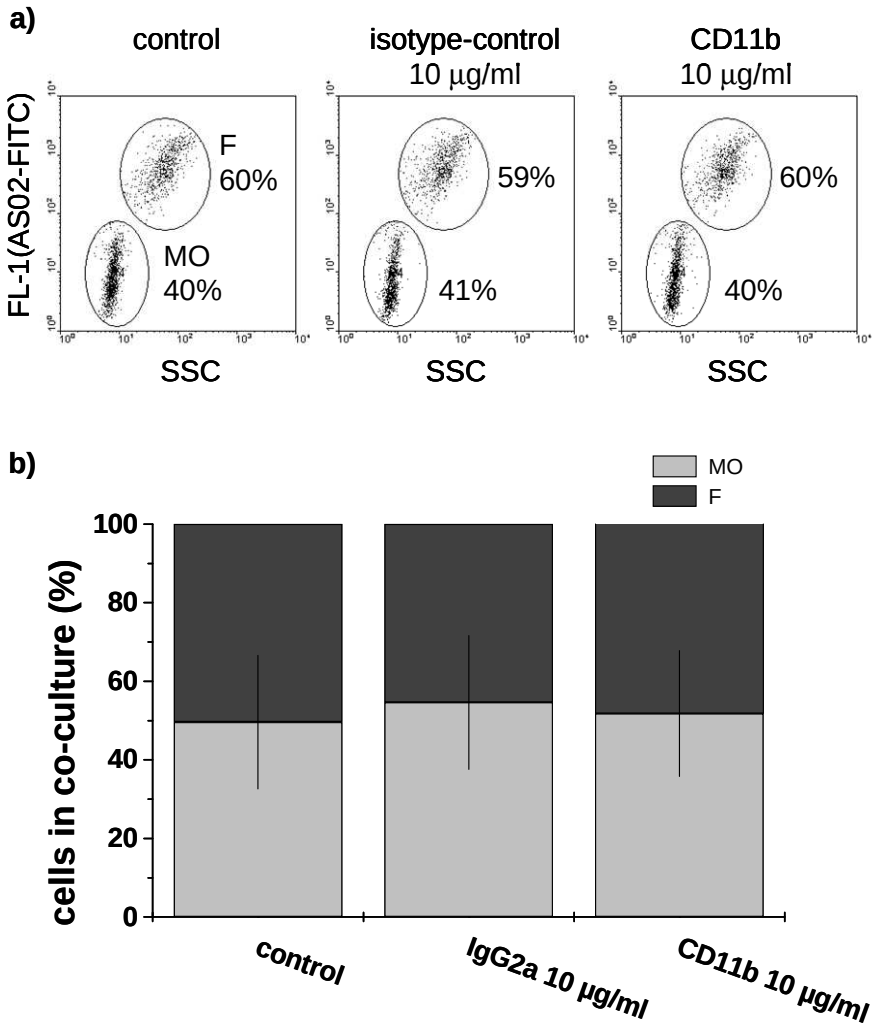


**Fig. 3.20 Anti-CD11b antibody does not influence MO migration. (a) Representative dot plot diagrams and proportion (± SD) of fibroblasts (F) and MO in spheroid co-cultures 20 h after addition of 1x10$^4$ pretreated MO/well and per spheroid, respectively. Diagrams show FL-1 fluorescence versus 90° scatter signals in a dissoc iated cell suspension from PF53T-MO co-cultures. The cell suspension was stained with FITC-conjugated 'fibroblasts specific' antibody AS02; MO pre-treatment was performed with 10 µg/ml CD11b or isotype IgG2a for 30 min at 37°C. (b) Columns in graph show averaged mea n values and SD of three independent experiments according to (a) with MO from 3 different healthy donors.**

#### 3.2.4.2.2 Studies with breast tumor cell line spheroids

Hs578T spheroids were characterized by high release of CCL2 and pronounced infiltration by MO. Since CCR2A/B blockade efficiently inhibited MO migration into tumor-derived fibroblast spheroids, it was hypothesized that the same approach blocks Hs578T infiltration by MO.

MO were pre-incubated with DOC-3 or with corresponding isotype (IgG1) for 30 min and than added to Hs578T 3-D cultures. Co-cultures were also exposed to the Ab and were collected after 40 h and dissociated for flow cytometric analyses. The data documented

in Fig. 3.21 clearly show that MO migration into Hs578T was unaffected by CCR2A/B blockade. According to previous studies this observation was reproduced in 3 independent experiments, i. e. with MO from 3 different donors.

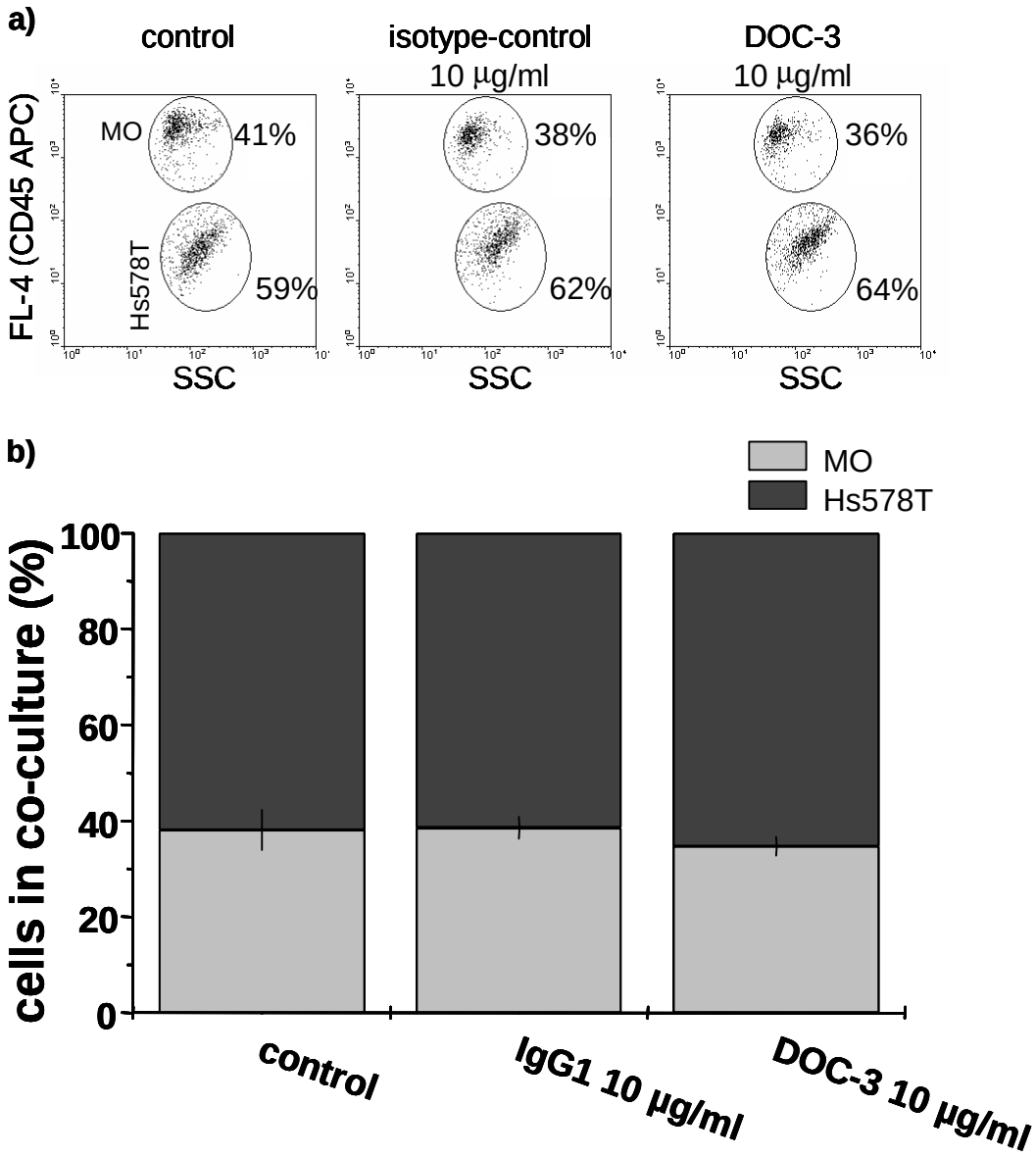


**Fig. 3.21 DOC-3 exposure and CCR2A/B blockade had no effect on MO migration into Hs578T spheroids. (a) Representative dot plot diagram and proportion (±SD) of Hs578T tumor cells and MO in spheroids co-cultures 40 h after addition of 1x10$^4$ pretreated MO/well and per spheroid, respectively. Diagrams show FL-4 fluorescence versus 90° scatter signals in a dissociated cell suspension from Hs578T-MO co-cultures. The cell suspension was stained with APC-conjugated monocytes specific CD45 antibody; MO pre-treatment was performed with 10 µg/ml DOC-3 or isotype IgG1 for 30 min at 37°C. (b) Columns in graph show averaged mean values and SD of three independent experiments according to (a) with MO from 3 different healthy donors.**

## 3.3 Experiments to identify the migrating blood MO subpopulation

The results obtained by Silzle et al. (Silzle *et al.*, 2003) imply a relatively constant subpopulation of blood MO capable of infiltrating tumor-derived/associated fibroblasts (TAF) spheroids. This was verified in the present study. The TAF spheroids used in presented thesis (PF27T, PF53T, PF37T) were reproducibly infiltrated by a blood MO population between 10% and 20% (see Tab. 3.4, chapter 3.1.3). Several experiments were designed to identify the potential migrating blood MO population

### 3.3.1 Flow cytometric analysis of monocyte subpopulations

#### 3.3.1.1 Expression of CCR2A/B

The experiments with the CCR2A/B blocking antibody DOC-3 implies a role of CCL2 in the MO migrating process into TAF but not tumor cell spheroids. The receptor for CCL2, CCR2A/B, on MO surface was stained with the DOC-3 antibody and a FITC-conjugated secondary antibody labeled in order to find out if there is a MO subpopulation with distinct expression of CCR2A/B receptor. The staining showed that roughly all MO express the receptor (Fig. 3.22) indicating that there is no difference in CCR2A/2B expression between migrating and non-migrating MO.

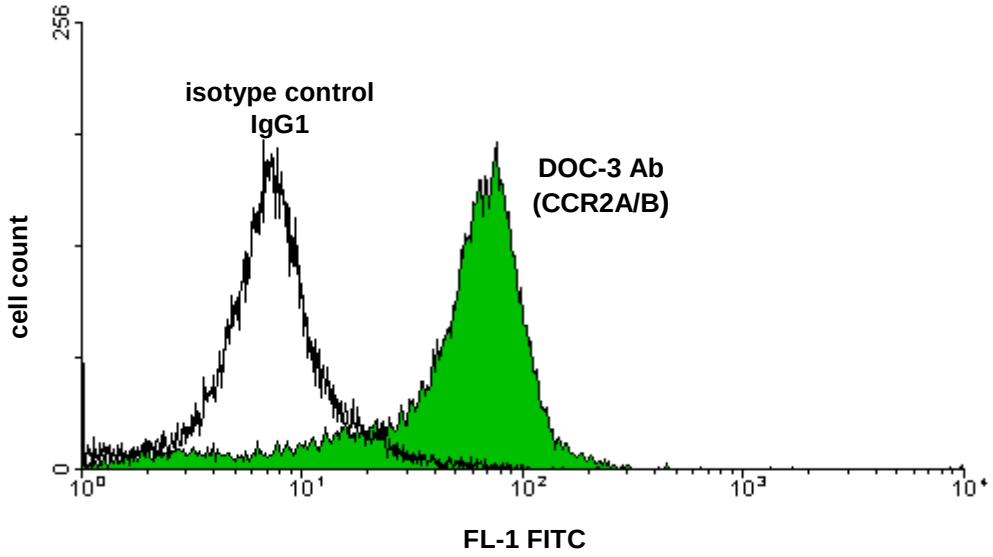


**Fig. 3.22 No 10%-20% MO subpopulation was identified by the CCR2A/B expression profile. Figure show representative overlay histogram of the blood MO isolated from a healthy donor by counter-current centrifugal elutriation, stained with DOC-3 primary antibody (green) or isotype control (white) and a FITC-conjugated secondary antibody.**

### 3.3.1.2 CD14/CD49e/CD11a or CD11b expression

According to MO surface expression profiles described in the literature, the following multicolor stainings were established for flow cytometric analysis of surface antigen expression: CD14/CD49e/CD11a and CD14/CD49e/CD11b. CD11a and CD11b are α subunits of two β integrins LFA-1 (Lymphocyte Function Associated Antigen-1) and MAC-1 (Macrophage Antigen-1), respectively. CD49e form with CD29 α-integrin called VLA-5 (Very Late Antigen-5). CD14 is LPS receptor, expressed on MO in different level.
Flow cytometric analyses of freshly isolated MO do not indicate a MO subpopulation of about 10-20% with a selective expression profile for the markers of interest as documented in Fig. 3.23.

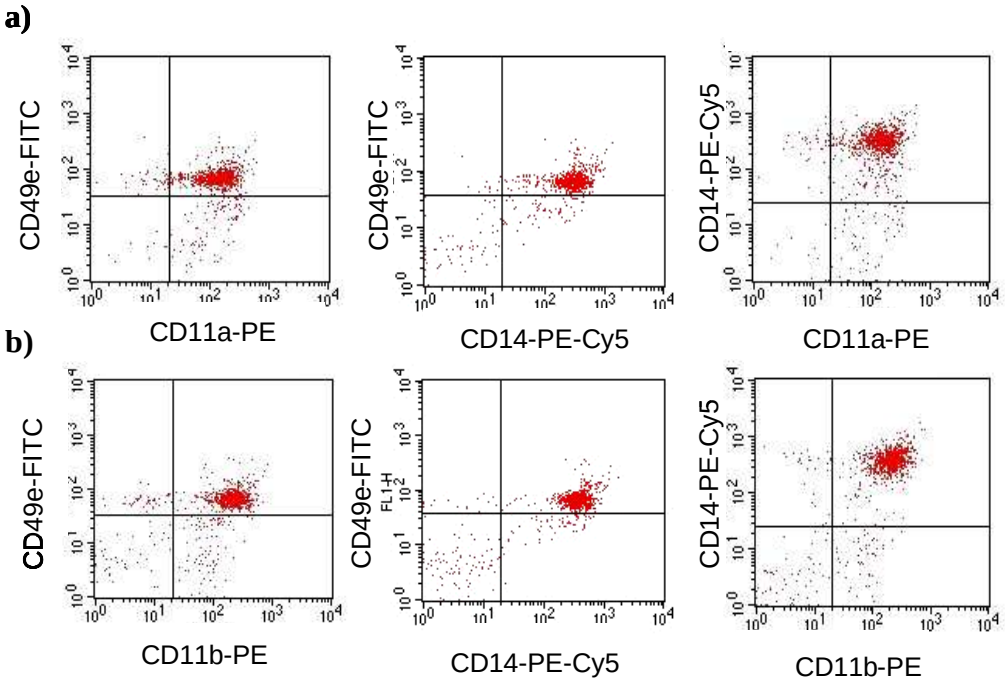


**Fig. 3.23 No 10%-20% subpopulation can be identified by the expression of the surface antigens CD14,CD49e, CD11a and CD11b which could relate to or reflect a high infiltrative MO population. Representative dot plot diagrams shows expression of: (a) CD14, CD49e, CD11a, (b) CD14, CD49e, CD11b antigens on the surface of blood MO isolated by counter current centrifugal elutriation.**

### 3.3.2 Migration of isolated MO subpopulations into fibroblast spheroids

It was reported in the literature that blood MO subpopulation can be differentiated by the antigens CD14 and CD16 and that particular CD14/CD16 subpopulations are characterized by enhanced migratory activity (Weber *et al.*, 2000). These subpopulations could indeed be identified by flow cytometric analyses. Gates (regions of interest) were defined to sort different fractions of MO for subsequent co-culturing experiments as shown in Fig. 3.24. In three independent experiments i.e. MO from three different donors were isolated

according to their expression profile via fluorescence-activated cell sorting and added to TAF spheroids with a concentration of $1x10^4$ MO per spheroid according to previous experiments. Migration potential of isolated MO subpopulations was analyzed by determining the F to MO ratio after 4 h of co-culturing. The results summarized in Tab. 3.7 show that all of these subpopulations infiltrate TAF spheroids with a similar potential.

**Tab. 3.7 Migration of MO into spheroids of tumor-derived fibroblast spheroids. MO fractions were sorted according to their CD14/CD16 expression as representatively shown in Fig. 3.24 and added with a concentration of $1x10^4$/spheroid.**

| **MO added to fibroblast spheroids** | | **Percentage of cells in co-culture and SD (%)** | | |
|---|---|---|---|---|
| | | **MO** | **F** | **SD** |
| **Control MO** | unstained* | 57.35 | 42.65 | 15.07 |
| | stained ($CD14^+CD16^-$)** | 57.98 | 42.02 | 16.83 |
| | stained + run through sorter*** | 58.41 | 41.59 | 3.7 |
| **Stained and run through sorter MO fractions** | $CD14^{++}CD16^-$ | 60.08 | 39.92 | 3.69 |
| | $CD14^+CD16^{++}$ | 53.83 | 46.17 | 5.59 |
| | $CD14^{++}CD16^{++}$ | 54.12 | 45.88 | 9.03 |
| | $CD14^{++}CD16^+$ | 50.44 | 49.56 | 15.22 |

*** Unstained control – untreated MO, whole blood MO population was added to F spheroids.**
**** Stained control – MO were stained with CD14 and CD16 antibody, stained whole blood MO population were added to F spheroids.**
***** Stained + run through sorter control - MO were stained with CD14 and CD16 antibody and run through sorter, after this treatment whole blood MO population were added to fibroblast spheroids.**

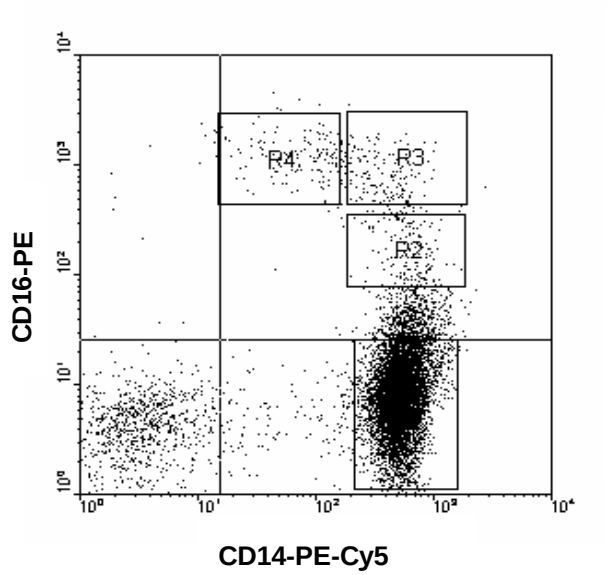


**Fig. 3.24. Representative dot plot diagram shows expression of CD14 and CD16 antigens on monocyte surfaces. Several fractions were gated for sorting:**
**R1 – $CD14^{++}CD16^{-}$**
**R2 – $CD14^{+}CD16^{++}$**
**R3 – $CD14^{++}CD16^{++}$**
**R4 – $CD14^{++}CD16^{+}$**

### 3.3.3 Isolation and expression profiling of migrated *versus* non-migrated MO

Since the search for surface antigens which could specify particular migrating blood MO did not result in the identification of characteristic subpopulation, a new approach was designed. The goal of the initial experimental series was to compare gene expression profiles in migrating and non-migrating MO using cDNA arrays. MO were co-cultured with TAF spheroids for 4 h (the minimal time required to complete MO migration) and then separated as described in chapter 2.2.5.2. The experiment was performed in triplicate. cDNA arrays were performed using RNA from fallowing samples: MO which migrated into spheroids and were subsequently separated from fibroblasts (MO inside); MO which during incubation time stayed outside spheroids and did not migrated (MO outside) and controls: MO kept 4 h at 4℃ (C1) and MO kept 4 h in Teflon bags at 37℃ (C2) (see Tab. 2.15, chapter 2.2.7.4.2). Gene expression profiles differed significantly between migrated MO (MO inside) and non-migrated MO (MO outside) as shown at Fig. 3.25. No difference is seen between control samples (C1 and C2) and non-migrated MO.

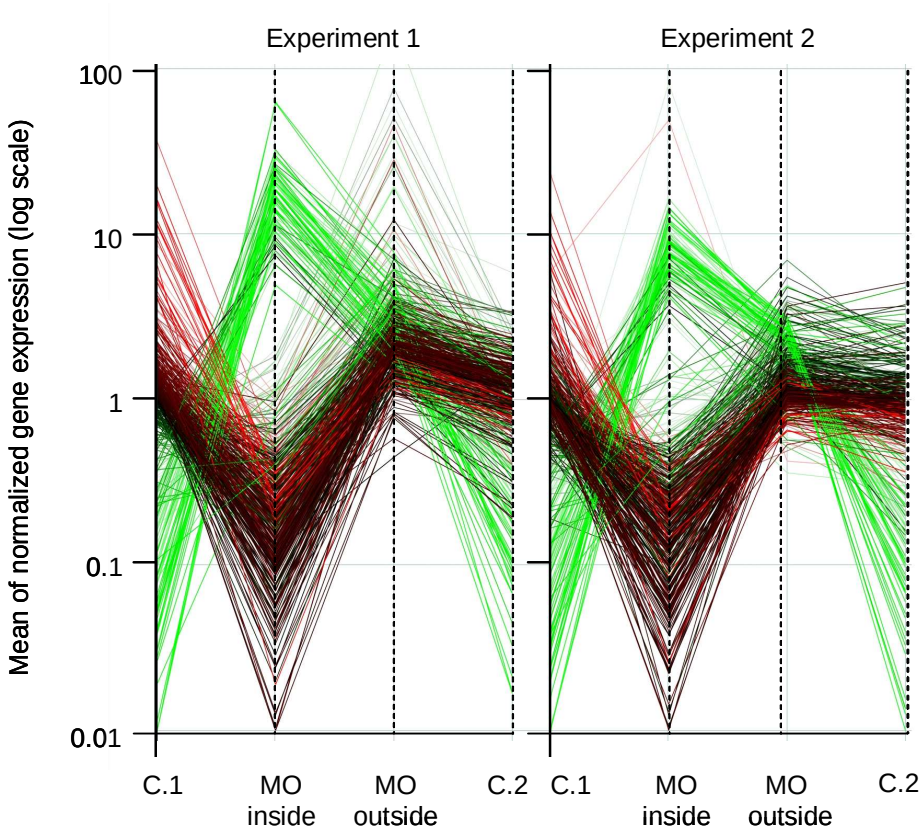


**Fig. 3.25 Gene expression profiles of migrated monocytes (MO inside) *versus* non-migrated monocytes (MO outside) and corresponding controls (whole blood monocytes). GeneSpring representation of two individual experiments showed no significant difference in gene expression between MO outside and controls. Gene expression of migrated MO (=MO inside) significantly differs from remaining samples. Colors represent relative expression (red – genes higher expressed comparing to controls, green – genes lower expressed comparing to controls).**

Tab. 3.8 presents 16 chosen genes from 23000 analyzed by assay which should be considered for future studies to identify the migrating MO subpopulation. Genes of interest were chosen according to their biological function which can influence their migration abilities. Products of listed genes are responsible for such a biological processes as cell adhesion, cell motility or proteolysis and peptidolysis what indicate that migrated MO in deed create specific and not random subpopulation of cells. Expression of showed genes in migrated MO is at least 4 time higher than in non-migrated one and control samples. The down regulated genes were excluded from further analysis because this result, with high probability, is due to fibroblasts contamination. Gene expression has not been verified by an independent technique so far.

**Tab. 3.8 List of up regulated genes analyzed by microarrays in migrated MO *versus* non-migrated MO chosen according to their biological function.**

| Gene Symbol | Gene Name | Biological Function | Array Fold Change |
|---|---|---|---|
| Up regulated | | | |
| *C1R* | complement component 1, r subcomponent | proteolysis and peptidolysis | 5.3 |
| *COL16A1* | collagen, type XVI, alpha 1 | cell adhesion | 4.5 |
| *C1S* | complement component 1, s subcomponent | proteolysis and peptidolysis | 5.0 |
| *CPE* | carboxypeptidase E | proteolysis and peptidolysis | 4,9 |
| *HAS1* | hyaluronan synthase 1 | cell adhesion | 4.6 |
| *ISLR* | immunoglobulin superfamily containing leucine-rich repeat | cell adhesion | 4.4 |
| *DDR2* | discoidin domain receptor family, member 2 | cell adhesion, proteolysis and peptidolysis | 6.0 |
| *FAP* | fibroblast activation protein, alpha | proteolysis and peptidolysis | 4.6 |
| *CPZ* | carboxypeptidase Z | proteolysis and peptidolysis | 4.3 |
| *DCBLD2* | discoidin, CUB and LCCL domain containing 2 | cell adhesion | 4.0 |
| *LAMB1* | laminin, beta 1 | cell adhesion | 4.2 |
| *SRPX* | sushi-repeat-containing protein, X-linked | cell adhesion | 4.1 |
| *PARVA* | parvin, alpha | cell adhesion | 4.7 |
| *POSTN* | osteoblast specific factor | cell adhesion | 4.3 |
| *SPOCK* | sparc/osteonectin, cwcv and kazal-like domains proteoglycan | cell motility, cell adhesion | 4.3 |
| *COL6A1* | collagen, type VI, alpha 1 | cell adhesion | 5.0 |

# 4. Discussion

## 4.1 Discussion of materials and methods

### 4.1.1 Cell lines and primary cells

A number of established human breast cancer cell lines derived from tumors or metastases of individual patients is commercially available. These cell lines show various characteristics that may serve as a tool to classify them into highly and poorly differentiated or infiltrative breast tumor cells. In the current work, two tumor cell lines were first chosen: T47D and BT474. Both cell lines derived from invasive ductal breast cancers, but T47D were isolated from pleural effusion while BT474 originated from a solid breast tumor. They are similar in terms of differentiation marker expression as E-cadherin, desmoplakin, vimetin and others and belong to a group of well-differentiated epithelial cell lines (Sommers *et al.*, 1994) known to form quite regular spheroid cultures (Seidl, 2001; Friedrich *et al.*, 2007; Friedrich *et al.*, 2009). However, in spite of these common features they differ for example in cellular CCL2 secretion and MO infiltration into the respective 3-D cultures was also different (see chapter 3.1.2). This observation encouraged to broaden the spectrum breast cancer cell lines to be examined in the present study. One more well-differentiated, epithelial cell line (MCF-7) and two poorly-differentiated cell lines (Hs578T, BT549) were chosen because they were shown earlier to express different levels of CCL2 (Mestdagt *et al.*, 2006). The choice of cell lines allowed to correlate the features of interest in this thesis (i) CCL2 expression and (ii) MO migration in 3-D cultures to draw a more general conclusions (see chapters 4.2.3). All cell lines investigated in the present study were able to create spheroids. However, the respective spheroid cultures differed in their density and shapes ranging from the compact, perfectly round BT474 spheroids to less dense, irregular MCF-7 spheroid cultures (see Fig. 3.2).

In addition, primary fibroblasts were used: tumor-derived fibroblasts (called also tumor-associated fibroblasts – TAF) were of major interest, healthy skin fibroblasts were chosen as a control in some experiments. TAF were grown from breast tumor sections. However, not all sections were able to initiate fibroblasts culture. Difficulties in using primary fibroblast were primarily caused by cell senescence and relative small number of fibroblasts in culture. In practice, fibroblasts were frozen with a routine protocol at low passage (1-2) and subsequently recultured for experimental set-up. Fibroblasts were then used only for 3-4 passages to avoid senescence-related artifacts. Accordingly, the available material was used up quite quickly. Preparing immortalized fibroblasts could be an approach

to overcome this problem in future studies. However, due to transformation process associated and required for immortalization, genomic alterations occur that clearly would have to be considered. Immortalization can be induced in human diploid fibroblasts by transfection with human telomerase reverse transcriptase (*hTERT*) that catalyze the addition of TTAGGG repeats to the telomeres of chromosomes (Bodnar *et al.*, 1998). The created immortalized cultures maintain a normal or almost normal phenotype with respect to growth regulation, morphology, genome stability (Jiang *et al.*, 1999; Morales *et al.*, 1999). Immortalization can also be induced by exposure to biological or physical agents as X-rays (Namba *et al.*, 1988) or infection with the simian virus 40 SV40 or its large T antigen (SV40 LT), but at much lower efficacy. Moreover, immortalization via infection with the SV40 or SV40 LT was shown earlier to result in an altered morphologic appearance and growth regulation of cells (Shay *et al.*, 1993). According to some reports, applying of hTERT or mutant SV40 LT alone was not sufficient for immortalization of freshly isolated normal adult human mammary fibroblasts. The combination of both genes sufficiently immortalized cells. However it also affected genomic stability (O'Hare *et al.*, 2001). Numerous studies would thus be required to verify that primary fibroblasts isolated from tumor tissues restore their TAF phenotype when immortalized. A systematic study has not been documented earlier and it was thus decided to not alter the existing model of TAF spheroids, using primary/secondary tumor-derived fibroblasts at low passage, in spite of the technical and logistic limitations.

MO were usually freshly isolated from whole blood and immediately used in migration experiments since freezing affected their viability and migration capacity. Because of these constraints, the experimental design and reproduction of results in the present thesis was extremely challenging.

### 4.1.2 Multicellular spheroids as a model for migration studies

Multicellular spheroids are an appropriate i*n vitro* system for a broad spectrum of systematic studies in cancer biology requiring a 3-D structure and pathophysiological gradients. Holtfreder and Moscona are considered pioneers in the field of 3-D cell culturing as they developed the initial methodology for 3-D culture formation. In the 1970s, Sutherland and his group inaugurated multicellular tumor spheroids (MCTS) as an *in vitro* model for systematic studies in the field of radiobiology. Since then, spheroids were used in a number of studies on biological mechanisms such as differentiation, regulation of proliferation, cell death, invasion, angiogenesis and immune response (Mueller-Klieser, 2000; Gottfried *et al.*, 2006; Friedrich *et al.*, 2007; Jakobsson *et al.*, 2007). The broad application of this culture model is related to its specific features which allow to consider

MCTS as intermediates between monolayer culture and i*n vivo* tumor. It has been demonstrated that cells in MCTS cultures more closely resemble the *in vivo* situation regarding cell shape and cellular environment than conventional culture systems. Monolayer cultures (2-D) of tumor cell lines, in spite of their widespread use for studying various molecular processes including cell death and cell proliferation, are not able to reflect 3-D organization of mammalian tissue with its 3-D cell-cell and cell-matrix interactions. Such interactions may critically affect cell physiology since cells form a complex communication network including biochemical and mechanical signals (Santini *et al.*, 1999; Santini *et al.*, 2000). This leads to loss of tissue-specific properties in 2-D cultures (Griffith and Swartz, 2006; Pampaloni *et al.*, 2007). Cell culturing on plastic surfaces (as in monolayers) changes cell morphology, which may affect on cell proliferation (Chen *et al.*, 1997), differentiation (Lelievre *et al.*, 1998), migration (Jiang *et al.*, 2005) and gene expression (Thomas *et al.*, 2002). Cukierman and his group observed that fibroblasts cultured as spheroids moved and divided more quickly compared to these cultured as monolayers. Also their shape and interactions with ECM were resembling in more details those occurring *in vivo* (Cukierman *et al.*, 2001).

Tumorall spheroids, in contrast to conventional suspension or monolayer cultures, reflect cellular heterogeneity of solid tumors and were found to be similar to avascular tumor nodules or microregions of solid *in situ* tumors. They posses a well-defined geometry with a reproducible concentric arrangements of different cell populations: proliferating, quiescent and secondary necrotic cells (Fig.4.1) (Mueller-Klieser, 1997;Kunz-Schughart, 1998; Kunz-Schughart, 1999, Kunz-Schughart, 2004; Friedrich *et al.*, 2007).

Spheroids are more or less densely packed reaggregates, since single cell suspensions obtained from tissue must again create “aggregates”. In order to create 3-D spheres, a culture condition must be provided which guarantees that adhesive forces between cells are greater than those for the substrate on which they are plated. There is a number of methods for achieving this effect: hanging drop cultures, culture plastic ware with non-adhesive surfaces, microfabricated microstructures, rotatory bioreactors, surface-modified substrates or scaffolds, centrifuge compression of cells or formation of MCS by clonal growth, as for example reviewed by (Lin and Chang, 2008). In the current work agarose was used to coat tissue culture surfaces and create a non-adhesive surface for culturing spheroids in 96-well plates in liquid overlay.

Despite the superiority to monolayer cultures, 3-D cell cultures, also have some limitations, since not all cells can form 3-D spheres under *in vitro* conditions. Some cell types do not aggregate at all or create only odd-shaped aggregates. Spheroid formation is determined both by properties of cells and by the cellular microenvironment (Mueller-Klieser, 2000).

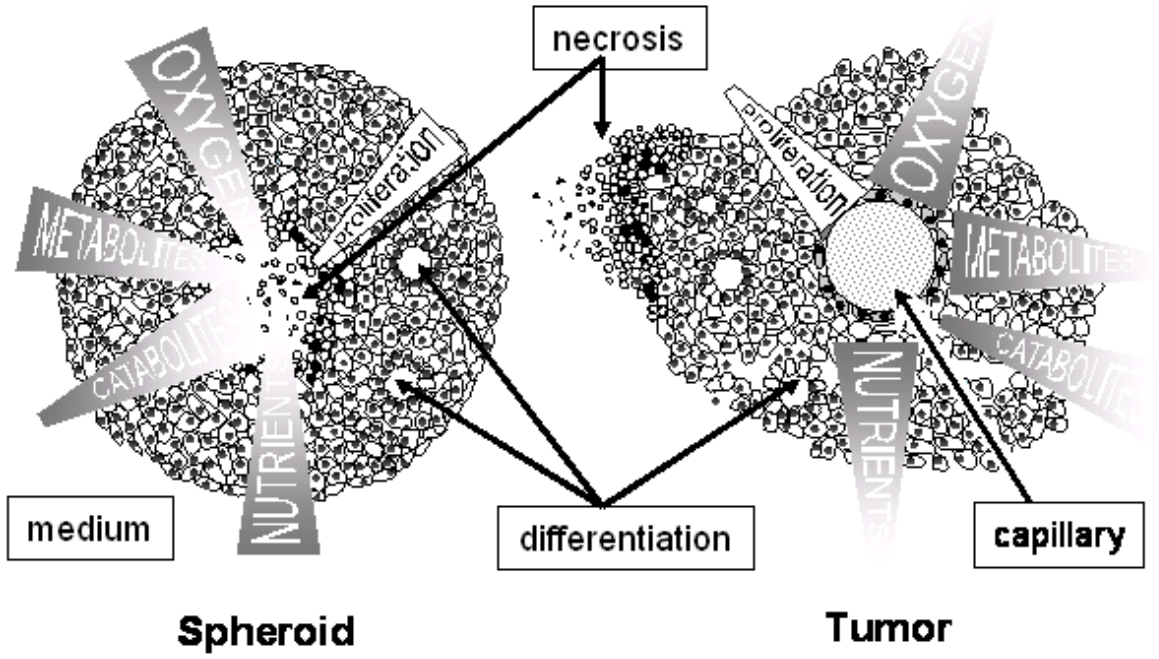


**Fig. 4.1 Schematic illustration of the analogy between multicellular tumor spheroids and tumor micromilieu (from Kunz-Schughart, Cell Biol Int,1999, 23: 157-161)**

Breast tumor cell lines differ in their ability to create spheroids. Some of these cell lines used in the present study, i.e. T47D, MCF-7 and BT474, create reproducible spheroids, with BT474 cells producing the morphological most compact ones but others such as MDA-MB231 do not aggregate on non-adherent surfaces (Seidl, 2001). Recently, Ivascu and Kubbies identified that spontaneous formation of spheroids in MCF-7, BT474 and T47D is mediated by E-catherin. Blocking of this adhesion molecule by inhibitory antibody led to the disintegration of the spontaneously formed spheroids. They also showed, that the addition of specific ECM compounds at defined concentrations are useful to obtain spheroid cultures from tumor cells that do not sufficiently attach to each other to form spheroids per se (Ivascu and Kubbies, 2007). Non-tumorigenic fibroblasts, regardless of their, origin created compact, ECM rich but non-proliferating spherical aggregates (Seidl, 2001).

Extending the 3-D culturing model to heterologous cell systems opened new perspectives. It enabled co-cultivation of: 1) different therapy-responsive tumor cells (Frenzel *et al.*, 1995); 2) growing tumor cells with stromal cell types such as endothelial cells (EC), fibroblasts or immunocompetent cells (Kunz-Schughart *et al.*, 1998); 3) different non-tumorigenic host cells e.g. fibroblasts with MO (Kunz-Schughart, 1999) or fibroblasts with EC (Kunz-Schughart *et al.*, 2006). Fibroblasts and MO may be initiated together with tumor cells and eventually form mixed aggregates. However, a disadvantage of this technique is that migration phenomena cannot be monitored. In order to monitor MO migration, as

in the present study, spheroids were created and subsequently co-cultured with MO suspensions according to (Hauptmann *et al.*, 1993;Konur *et al.*, 1996; Gottfried *et al.*, 2003; Silzle *et al.*, 2003). This technique allows to analyze immune cell infiltration of tumor and fibroblast spheroids.

3-D tumor spheroids-MAC co-cultures were first applied by Hauptmann et al (Hauptmann *et al.*, 1993) who showed different MAC populations to support tumor proliferation and migration. Later on, MO migration and MO-to-MAC maturation processes were studied in bladder cancer spheroids (Konur *et al.*, 1996; Konur *et al.*, 1998). Immune modulators may, however, be released by both tumor and by tumor stromal cells including fibroblasts. According to the urothelial cell line model mentioned, Silzle et al. (Silzle *et al.*, 2003) designed an experimental set-up to investigate the interactions between fibroblasts and MO. The size of spheroids is important in migration studies, since spheroids exceeding 500 µm diameter may develop central secondary necrosis due to pathophysiological gradients including hypoxia-related processes (Fig.4.1). It was shown, that hypoxia inhibits MO/MAC migration and downregulates CCL2 expression, although no causal relation was documented (Negus *et al.*, 1998; Grimshaw and Balkwill, 2001).

In the current work the 3-D fibroblast-MO and breast tumor cell-MO model of co-culturing was applied to investigate the role of fibroblast-derived chemokine signaling on the MO migration process in a three-dimensional cellular context.

### 4.1.3 Employment of siRNA approach in 3-D cell cultures

The mechanism of RNAi is described in the Methods Section, chapter 2.2.7.5.1 and schematically shown in Fig. 2.4. RNAi is an interesting biological tool for knocking down gene expression. Functional intermediates in the RNAi pathway, siRNAs, may be introduced into cells and cause gene silencing. Diagram 4.2 shows the most frequently used methods for siRNA delivery and evaluation of its effect.


**Fig. 4.2 Methods of siRNA delivery and methods suitable for gene silencing detection.**

siRNA used for gene silencing is increasingly used for gene function analysis. The silencing effect of siRNA is relatively stable and can persist even up to 10 days (Matuliene and Kuriyama, 2002). However, the reducing effect can be influenced by the target transcript, its expression level, turnover rate and regulation. siRNA method was proved to be useful in understanding the roles of individual genes in various cellular processes such as: cell cycle (Harborth *et al.*, 2001) apoptosis (Futami *et al.*, 2002), cell differentiation (Kawasaki *et al.*, 2002) or insulin signaling (Usui *et al.*, 2003). There is growing interest in RNAi utilization for the treatment of various human diseases since it can be applied for targeting disease-related genes or human pathogens (Miller *et al.*, 2003;). The experiments described by Banerjea et.al. demonstrate the utility of siRNAs delivered into hematopoietic stem cells via lentiviral vectors for future *in vivo* applications (Banerjea *et al.*, 2003).

The design and application of siRNA does not require dedicated technical training or special equipment as it is the case for gene knockouts performed in mice. Moreover, knockout of important genes in mice often generates embryonic lethality. The combination

of RNAi methodology with 3-D cultures by employing siRNAs in spheroids seemed to be far-reaching because of its supposed simplicity and diversity of potential applications. RNAi application in 3-D cultures, however, is not widespread. Only few researcher used this tool in the context of cancer research. Ivascu and Kubbies applied siRNA molecules to study proteins involved in spheroids formation of different breast cancer cell lines (Ivascu and Kubbies, 2007). Similarly, Ditttmer et al. silenced PTHrP (Parathyroid hormone-related protein) expressed also in breast tumors and proved its influence on spheroids aggregation in the MDA-MB-231 cell line (Dittmer *et al.*, 2008).

In the present work, siRNAs for CCL2 silencing in TAF were applied. The lipid-mediated transfection method was chosen to transfer siRNA either into monolayer cultures (subsequently cultured as spheroids) or into cell suspensions directly creating spheroids (data not shown). Both approaches failed to work in 3-D TAF cultures, as proved at protein level. Although several variants of experimental protocols were tested, the desired effect was not achieved. Experimental variations included: different dissociation means, siRNAs molecules, transfection means, other fibroblast batches. The effect was unexpected because satisfactory transfection results in monolayers were reproducibly obtained (~80% down-regulation as compared to control). The use of fluorescently labeled siRNA indicated that the transfer of transfected cells from 2-D into spheroid culture did not lead to loss of siRNA molecules. The green fluorescent light was still visible 7 days after transfection (Fig. 3.15). This shows that siRNA molecules were still in transfected cells. It was, however, reported, that siRNAs lacking stabilizing modifications may be degradeted and fluorescent tag may still remain intact leading to false positive effects (Dharmacon, 2004). A phenomenon that would have to be validated for the present study.

RNAi acts at the mRNA level and it was thus decided to verify whether loss of regulated CCL2 protein expression by siRNA relates to mRNA expression profile. In 2-D cultures CCL2 mRNA level was significantly decreased as expected and consistent with down-regulation at protein level. In 3-D cultures transfected with functional siRNA, relative CCL2 mRNA level was twice as high as in controls. At protein level no change in CCL2 expression was observed in 3-D cultures. This unexpected result is hard to explain. Since outcomes from two independent experiments were comparable, the occurrence of artifact is unlikely. Perhaps a systematic study of posttranscriptional regulation of *CCL2* would bring the answer. It was proven already herein, that fibroblasts cultured as spheroids differ in their properties from cultured monolayer (Cukierman *et al.*, 2001). Hence, the presumption that production of CCL2 in 2-D and 3-D cultures differs in terms of molecular regulation, cannot be rejected. The discussion is difficult because of lack of comparable research in this field. Authors may use other, probably more convenient ways of siRNA delivery that

were not tested herein (see schema 4.2). Moreover the technique of 3-D culturing in other studies using RNAi technologies differ from the one used in the current thesis (Oishi *et al.*, 2007; Dittmer *et al.*, 2008; Knight *et al.*, 2008) and finally there are no reports on RNAi silencing in fibroblasts. It would thus be interesting to determine if CCL2 can be down-regulated by siRNA in other 3-D cultures e.g. different tumor cell lines, to evaluate whether the phenomenon is cell type or culture dependent. Also it should be tested in extended studies if other genes despite CCL2 can be silenced by siRNA in fibroblasts, to verify if the lack of silencing effect is gene-specific. This, however, was beyond the scope of the present study.

## 4.2 Discussion of results

### 4.2.1 MO migration into spheroids of different origin

Experiments performed by Silzle et al. revealed that MO proportion in spheroids of breast tumor derived fibroblasts after 40 h of co-culture is significantly higher than in spheroids derived from normal skin and breast fibroblasts (Silzle *et al.*, 2003). Based on this report, MO migration into TAF 3-D cultures was analyzed and compared with MO migration in spheroids of a set of breast tumor cell lines and will be discussed in this chapter.

A relatively constant subpopulation of whole blood MO, roughly 12-15%, is able to infiltrate TAF spheroids as documented by Silzle et al. (Silzle *et al.*, 2003) and verified in the present study. However, 40 h co-culture time was the standard procedure established for MO migration experiments, according to a 3-D co-culture model of urothelial tumor cell lines and MO (Konur *et al.*, 1996). During this time interval, MO were capable of completing their migration into TAF or normal fibroblasts spheroids. The exact migration kinetics had not been monitored. In present study it could be shown that MO need only 4 h to entirely infiltrate TAF spheroids. In contrast, in the established urothelial tumor model (Konur *et al.*, 1996) 4 h after adding MO, migrating cells were detected only at the periphery of the tumor spheroids and the infiltration process was regarded as completed only after 24 h of co-culture. However, it should be considered that in the referenced study not the ratio of MO to tumor cell in spheroids was determined as analytical endpoint, but the time point when MO reached the spheroid center. Indeed, the maximum MO-tumor cell ratio could have been reached earlier. In the present study completion of MO migration was defined by the highest MO-tumor cell ratio using flow cytometric analysis of dissociated spheroid co-cultures. This method allows to more accurately estimate the proportion of MO in spheroid co-cultures as opposed to immunohistochemistry.

The study of MO migration into breast tumor tissue was performed using five different cell lines: Hs578T, T47D, MCF-7, BT549 and BT474, all derived from ductal carcinomas but possessing a different invasive potential *in vitro*. BT549 and Hs578T cell lines are described as poorly differentiated and highly invasive *in vitro*, (>80% determined by chemoinvasion assay), while MCF-7, T47D, BT474 cell lines are more differentiated and their invasiveness was graded from 0 to 40% (Sommers *et al.*, 1994). It was shown that MO infiltration depends on the tumor cell line applied in spheroid co-culture with MO. MO infiltration was most pronounced in Hs578T spheroids, T47D and BT549 were intermediate while MCF-7 and BT474 showed very poor infiltration. The 50% MO fraction in Hs578T co-cultures accounted to about 25% of the applied blood MO (see chapter 3.1.2 and Tab. 4.1). The increased MO infiltration correlated in most cases (excluding T47D) with the invasiveness. The results are consistent with the observation that high MO/MAC content in solid tumors is a unfavourable prognostic marker A high MAC index in human ductal breast carcinomas, for example, has been shown to correlate with poor prognosis and reduced survival of patients (Leek *et al.*, 1996;Goede *et al.*, 1999;Bingle *et al.*, 2002). Moreover, TAM infiltration was found to positively correlate with breast tumor cell proliferation as determined via Ki67 (MIB-1) immunoreactivity (Tsutsui *et al.*, 2005). However, as already mentioned, the outcomes achieved for T47D cell line does not match this hypothesis. T47D spheroids are intermediate infiltrated by MO although *in vitro* invasiveness of this cell line is week. MO infiltration is a complex process driven by chemokines and possibly other attractants that induces cell adhesion and locomotion (Luster, 1998), hence cell line invasiveness can only be one of cell feature important for MO infiltration.

Since Hs578T tumor cells were the only to show a high rate of infiltration by blood MO in spheroid co-culture, even higher than TAF (see Tab. 4.1), this breast tumor cell line was chosen for extended mechanistic studies. The subpopulation of infiltrated MO cannot be considered as identical to the one infiltrating TAF spheroids. They differ for example in time required to complete infiltration of Hs578T spheroids. MO clearly need longer then 4 h (which is a sufficient period of time in TAF spheroids) to complete the migration process in this tumor spheroid type. An additional discrepancy was shown when blocking the MO migration associated chemokine receptor CCR2A/B which will be discussed to some detail in chapter 4.2.2.3.

### 4.2.2 CCL2 and cancer

#### 4.2.2.1 Multifaced role of CCL2 in cancer

The role of CCL2 in cancer is controversial. It is likely that its effect on cancer is multifaceted depending on the particular setting in which it is expressed. CCL2 has been shown to display an antitumoral effect in several different models. In at least a few models, CCL2 stimulated host anti-tumor responses in a T-lymphocyte-independent manner (Rollins and Sunday, 1991). Another consequence of CCL2 activity can be enhancement of mononuclear cells to tumor antigen uptake or presentation (T-lymphocyte-dependent response) (Manome *et al.*, 1995). However, it is also likely that CCL2 primarily contributes to tumor growth and progression considering the fact that CCL2 is expressed by a variety of tumor types. Indeed, many tumor entities, including breast cancer are characterized by massive mononuclear cell infiltration (Yu and Rak, 2003; Daly and Rollins, 2003). A high macrophage content in ovarian, gastric esophageal and ductal breast carcinomas correlated with poor prognosis and clinical outcome (Visscher *et al.*, 1995; Leek *et al.*, 1996; Goede *et al.*, 1999; Bingle *et al.*, 2002; Hagemann *et al.*, 2006) and CCL2, which is known as a stimulator of mononuclear cell migration, was demonstrated as a factor that facilitates tumor growth and dissemination (Nakashima *et al.*, 1995; Ueno *et al.*, 2000; Salcedo *et al.*, 2000; Saji *et al.*, 2001). Furthermore, a study performed by M. Mestdagt *et al*. demonstrated a few years ago a transactivation of the CCL2 promoter following activation of the ß-catenin/TCF pathway in breast cancer cell lines and showed that CCL2 is selectively expressed in breast tumor cell lines known as highly invasive *in vitro* (Mestdagt *et al*., 2006). However, CCL2 can be produced by many cell types and meanwhile has also been detected in TAM, indicating the presence of an amplification loop (Balkwill, 2004). In general, tumor-derived CCL2 may contribute to carcinoma progression directly or indirectly. CCL2 may act directly on tumor cells, by stimulating themselves or neighboring cells (stroma or endothelium) to secrete CCL2. Indirect action may involve recruitment of leukocytes that provide growth and antiapoptotic signals, or that provide angiogenic signals to tumor cells (reviewed in: (Conti and Rollins, 2004).

#### 4.2.2.2 The role of CCL2 in MO migration into fibroblasts spheroids

In many solid tumors, including invasive ductal breast cancer, the MO infiltrate correlates with high expression of CCL2 (Mantovani, 1994; Amann *et al.*, 1998; Saji *et al.*, 2001; Silzle *et al.*, 2003). High spontaneous secretion of CCL2 in breast tumor derived fibroblasts *in vitro*, indicates some relevance of this chemokine for MO migration into fibroblastic areas

in tumors. Data from our laboratory published by Silzle et al. showed that CCL2 neutralization with specific antibodies was effective in a Boyden chamber assay as it decreased the migration of MO towards fibroblast conditioned media (Fig. 4.3.a). However, the addition of the same CCL2 neutralizing antibody to the external milieu of TAF spheroids, even at a higher concentration, had no effect on MO migration (Fig. 4.3.b).

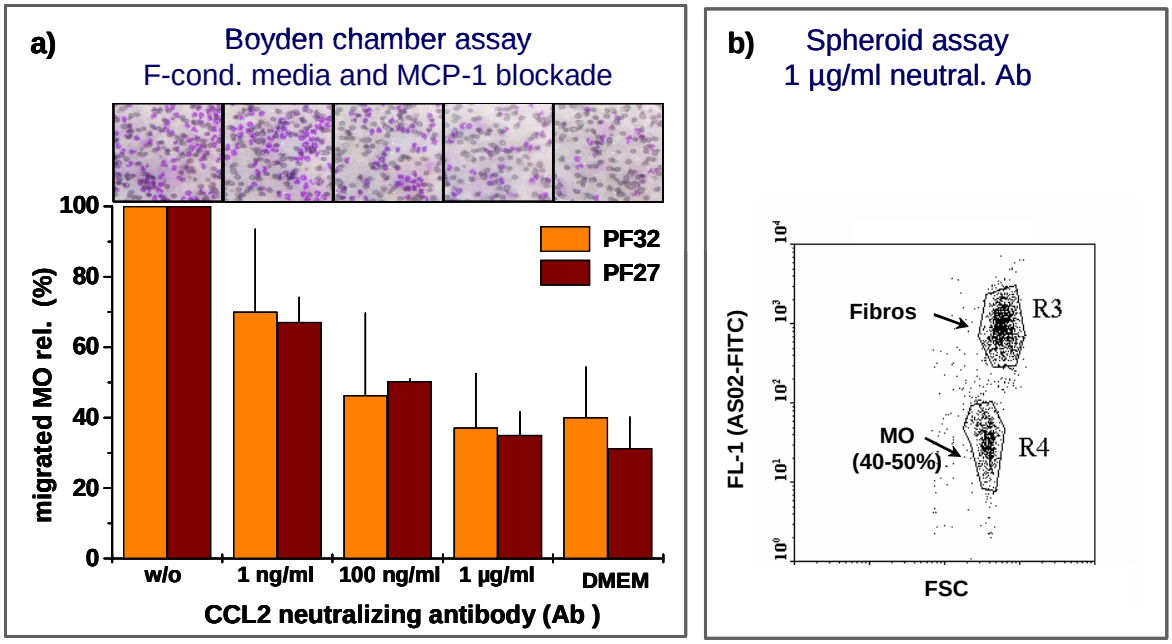


**Fig. 4.3 (a) Neutralization of CCL2 in conditioned medium of TAF spheroids PF27 and PF32 reduced the migratory activity of MO in the Boyden chamber assay. (b) Incubation of fibroblast spheroids with CCL2 neutralizing antibody did not reduce MO infiltration. The proportion of MO in fibroblast spheroid co-cultures was 40-50% as verified by flow cytometry after dissociation and staining independent of the absence or presence (see dot plot diagram) of CCL2 blocking Ab. (Silzle et al., Eur. J. Immunol. 2003, 33: 1311-1320)**

Reasons for lack of antibody efficacy in TAF spheroids may be that (i) CCL2 is accumulated inside TAF spheroids and in reality its level is much higher than measured in conditioned medium, (ii) antibodies cannot sufficiently penetrate the compact spheroid, or (iii) CCL2 is not a relevant factor for MO migration into spheroid. It is worth to mention that in the meantime another group used an antibody approach to neutralize CCL2 in 3-D cell culture. Here, neutralization of CCL2 resulted in an almost complete absence of MO migration into MCTS (Spoettl *et al.*, 2006). However, not only the Ab was applied three times, starting at the point of cell inoculation in liquid overlay but also the spheroid culturing strategy differed from the approach used herein. Spoettl et al. initiated mixed spheroids, i.e. they seeded tumor cells together with MO in the presence or absence of CCL2 neutralizing Ab. It is, however, claimed that the preculture of spheroids and addition of immune cells as suspension to an existing 3-D culture should better reflect the *in vivo* situation of immune

cell migration. An approach according to Spoettl et al. was thus not considered for the present thesis.

To answer the questions raised for the spheroid model used herein, several experiments were designed. First it was investigated if decreasing the levels of para/autocrine factors including CCL2 by replacing supernatant affects MO migration into TAF spheroids. Along the experiment, the CCL2 levels in extracellular milieu were monitored. The supernatant replacement led to time-delay in MO migration into TAF spheroids. The most prominent difference, compared to controls, was observed after 4 and 6 h of co-culturing. At these time points CCL2 levels were lower by about 70% and 82% respectively, compared to control levels. After 20 h incubation the CCL2 level had almost reached the control level. The results indicate that paracrine factors may indeed be responsible for the increased migration of MO into TAF as compared with normal fibroblasts. In spite of the observations by Silzle et al., who could not block MO migration into TAF spheroids by exposure to a CCL2 blocking antibody (Fig. 4.3). CCL2 as one of the paracrine factors reduced by wash-out experiments cannot be excluded as a factor responsible for MO migration. This hypothesis is supported by literature data. Nakagawa et al. studied metastatic colon cancers which are also characterized by high MO infiltration rates. They performed microarray expression analyses of cancer-associated stromal fibroblast and showed their expression profile differed from skin fibroblasts. One of the genes that were significantly up regulated was CCL2, another one was IL-6 (Nakagawa *et al.*, 2004). Interestingly, both IL-6 and CCL2 proteins had been described in our laboratory to be released with a high rate from breast tumor-derived as compared with normal fibroblasts (Silzle *et al.*, 2003). Here, it was also shown that IL-6 induces CCL2 production in an autocrine loop.

From experiments performed by Youngs et al. with using a Boyden chamber assay it is known that cell migration increases with increasing chemokine levels only up to certain concentrations. After exceeding this border-concentration, the migration is reduced. Moreover, this study showed that chemokine migratory responses rely at least in part on the presence of concentration gradients (Youngs *et al.*, 1997).

In the current study, only the level of CCL2 measured in supernatant is known, the concentration of chemokine inside the spheroid and a potential chemokine gradient are unknown and cannot be determined by any simple method. It is, however, expected that MO should migrate towards a rising CCL2 concentration. Therefore, we hypothesized that, if CCL2 gradient occurs and is important for MO migration, changing or abolishing the gradient may decrease MO infiltration into spheroids. Addition of recombinant CCL2 to TAF supernatant at 0.02 μg/ml and 0.2 μg/ml (to abolish or change CCL2 gradient) decreased to 50% or completely abolished MO infiltration into TAF, respectively. An analogical

experiment was performed with normal skin fibroblasts (VF1) spheroids, but here the change in CCL2 gradient had no effect on the basic MO migration (see chapter 3.2.2.2). Those results strongly support our hypothesis that CCL2 is important for MO migration into TAF spheroids and is not relevant for the basic process of MO migration into normal fibroblast spheroids. The relevance of stromal-cell derived CCL2 is also supported by a recent study performed by Fujimoto et al. They used five different breast cancer cell lines as xenograft model in SCID mice. Macrophage infiltration, angiogenic activity and tumor growth were recorded in parallel to the determination of various chemoattractants on the RNA level in human tumor cells versus mouse stromal cells. Stromal but not tumor cell CCL2 mRNA expression was shown to positively correlate with macrophage index. The authors also compared CCL2 immunohistochemical staining and macrophage infiltration with the clinicopathological data in 128 specimen of human breast cancer and found stromal CCL2 as an independent prognostic factor after tumor size and nodal status (Fujimoto *et al.*, 2009).

Based on literature data, other factors modulating MO migration into TAF spheroids and fibroblastic stromal areas in tumor, respectively, may include: BRAK (Kurth *et al.*, 2001), RANTES (Azenshtein *et al.*, 2002) or VEGF (Valkovic *et al.*, 2005) which will be further discussed in chapter 4.2.2.3. Previous studies also indicate that the interaction between tumor cells, MO/MAC, fibroblasts and CCL2 is reciprocal. CCL2 might be involved in the fibrotic process by inducing fibroblasts to produce collagen *via* a TGF-β (Ernst *et al.*, 1994). The study of Sakai et al. confirms this hypothesis and suggests that peripheral CD14-positive MO are directly involved in fibrogenesis through the production of collagen type I via autocrine/paracrine production of CCL2 and TGF-β1 through a CCL2/CCR2-dependent amplification loop (Sakai *et al.*, 2006).

From the observations in the present thesis, it can be concluded that (i) CCL2 is likely to play a critical role in MO migration into TAF spheroids and CCL2 may thus be a central factor in MO migration into fibroblastic areas and their local persistence; (ii) Neutralizing Ab probably was not able to penetrate created spheroids or to sufficiently block CCL2 within the TAF spheroids; (iii) Presumably CCL2 concentration inside the TAF spheroids is higher than in the external environment and abrogation of the CCL2 gradient diminished MO infiltration. The results provided by the performed experiments on the role of CCL2 in MO migration were thus incentive to get deeper insight into the phenomenon of MO migration in breast tumor tissue.

#### 4.2.2.3 The relevance of chemokine receptors for MO migration into fibroblastic tumor areas

As mentioned earlier, chemokines other than CCL2 and their receptors can be involved in MO migration (e.g. BRAK, RANTES. All chemokins activate their pathways by binding to 7-transmembrane spanning G-protein-coupled receptors which are generally, but not exclusively, coupled to pertussis toxin-sensitive $G\alpha_i$ proteins (Amatruda, III *et al.*, 1993; Bokoch, 1995). The application of PTX should block $G\alpha_i$ protein-mediated signaling. Reduced or abrogated migration of MO into TAF spheroids following PTX exposure would thus indicate chemokine receptor signaling to be relevant for increased MO migration as compare to normal fibroblasts. The predicted effect was achieved. A range of PTX concentrations was used, but all blocked MO migration completely suggesting that MO migration into TAF spheroids require chemokine/chemokine-receptor binding and signaling. The proportion of MO in TAF-MO co-cultures after exposure to PTX as detected by flow cytometry after dissociation is 2-3% which is in a range found in normal (non-tumor-derived) fibroblast spheroids. It is unclear whether an imperfect wash-out procedure and MO adhered to the spheroid surface may artificially contribute to this basic value of 3% MO in co-cultures. PTX B-oligomer which does not posses ADP-ribosyltransferase activity (negative control) influenced MO infiltration to some extend at the highest concentration. Blocking effect noticed for high concentration of PTX B-oligomer have been shown and is explained by other authors, through its contamination with holotoxin (<1%), as reported by the supplier (Whitman *et al.*, 2000). However, this contamination should not inhibit migration to the degree observed in experiment (about 60% smaller MO ratio for PTX B-oligimer-treated sample in compare to untreated control sample). Another explanation could be, as described by Alfano et al., an inhibitory effect of B-oligomer on CCR5-dependent signaling. CCR5 is a receptor for example for MIP-1$\alpha$ (CCL3), RANTES (CCL5) and MCP-2 (CCL8) and one of main function of this receptor is related to MO migration. Incubation with B-oligomer resulted in desensitization of CCR5 and loss of signaling activity associated with binding of the natural CCR5 ligands (Alfano *et al.*, 1999). Blocking of this signaling pathway can also result in altered MO migration.

The ligand for CCR5 - CCL5 is increasingly recognized in the literature in the context of inflammation and promalignancy. Similar to CCL2, CCL5 is minimally expressed by normal breast epithelial duct cells but may be highly expressed by breast tumor cells. Moreover, it is also produced by stromal cells in the tumor microenvironment, including immune cells, and may affect MO migration via paracrine and autocrine pathways (Azenshtein *et al.*, 2002; Soria and Ben-Baruch, 2008). O'Boyle et al. performed

chemotactic experiments for members of the MCPs family. They showed that ChTX could selectively inhibit MCP-2 (CCL8)-mediated chemotaxis, whereas it did not affect MCP-1 (CCL2), MCP-3 (CCL7) and MCP-4 (CCL13)-mediated migrations. PTX pre-treatment, however, abolished the migration mediated by each of the four MCPs (O'Boyle *et al.*, 2007). Analogical experiment was performed using ChTX. Cholera toxin is a specific activator of $G\alpha_s$ protein and its application can answer the question if signaling pathways independent from $G\alpha_{i/o}$ take part in the process of MO migration into TAF spheroids (Stryer and Bourne, 1986; Neer and Clapham, 1988) The ChTX at a concentration of 1 ng/ml had no effect but concentrations of 10 and 50 ng/ml decreased MO migration into TAF to about 30 to 50%. Since ChTX affected MO migration into TAF spheroids an impact of CCL8 may be considered. However, some experiments documented in the literature where PTX and ChTX toxins were used, suggested that different signaling pathways mediated by CCL2 may be under the control of different G-proteins and the response to PTX and ChTX may thus both relate to CCL2 signaling (Cambien *et al.*, 2001). CCR2 exists in the plasma membrane as a monomer and upon activation by ligand binding it homodimerized. Homodimerization in turn leads to G-protein coupling to receptor implicating the possible involvement of various signal transduction pathways (Bokoch, 1995). Thus, amongst others, CCL2 induces a PTX sensitive rise of intracellular calcium (Sozzani *et al.*, 1993) but it also triggers signaling through tyrosine phosphorylation of the receptor and activation of the JAK2/STAT3 pathway in a PTX-independent manner. However, the toxin blocks JAK2 kinase dissociation from the receptor (Mellado *et al.*, 1998). The understanding of signaling pathways triggered by chemokines, however, is even more complex due to the revealing possibility of chemokine receptor heterodimerization. Rodriguez-Frade et al. observed the formation of CCR2-CCR5 heterodimers induced by simultaneous presence of CCL2 and CCL5. The heterodimeric receptor complex showed unique features and seems to activate biochemical pathways different from those triggered by homodimers (Rodriguez-Frade *et al.*, 2001).

Two variants for CCR2 receptor exist but their biological significance is not clear. The isoforms are alternatively spliced variants of a single receptor gene that differ only in the sequence of the cytosolic carboxyl-terminal tail. Due to a shorter amino acid sequence in the carboxyl tail, CCR2A does not well traffic to cell surfaces and cannot be detected on the MO cell surface at greater than 10% of the level of CCR2B. Outcomes from this study also indicate that the CCR2A receptor variant binds CCL2 with high affinity, when expressed on the cell surface and is a functional receptor (Wong *et al.*, 1997). The experiments with transfected Jurkat T cells revealed differences between the two isoforms in terms of $Ca^{2+}$ flux induction. In CCR2B transfectants, CCL2 induced transient $Ca^{2+}$ flux

was partially sensitive to PTX. In CCR2A transfectants CCL2 did not induce $Ca^{2+}$ flux (Sanders *et al.*, 2000). These observations indicate functional differences between the two receptors. It would be interesting to determine the role of different CCR2 isoform in MO migration. Since there are no specific blocking agents available that distinguish between CCR2A and B isoforms, other experimental approaches e.g. knock-out experiments have to be design to study their function.

Applying of the toxins in the 3-D co-culture model used in the present study, suggests that MO migration into TAF spheroids is chemokine dependent. To selectively investigate the involvement of CCR2A/B signaling, a CCR2A/B specific antibody was applied. This antibody (DOC-3) specifically binds both CCR2 isoforms and block CCL2 signaling (Biber *et al.*, 2003; Mahad *et al.*, 2006). CCR2 blockade decreased MO migration into TAF spheroids to basal levels according to normal fibroblasts spheroids. Analogue experiments with CD11b antibody did not affect MO migratory activity. CD11b together with CD18 is called Macrophage-1-integrin (MAC-1) or complement receptor 3 (CR3). It binds to C3b and C4b, is present on leukocytes including MO, but is irrelevant for MO migration. This results provide clear evidence that CCL2/CCR2 signaling is required for enhanced MO migration into TAF spheroids. These finding is consistent with literature, where CCR2 deletion or down-regulation on MO/MAC resulted in absence of cell migration towards CCL2 (Sica *et al.*, 2000).

In summary, CCL2/CCR2 signaling is mandatory for the massive infiltration of spheroids from tumor-derived fibroblast, but an impact of other cytokines cannot be excluded so far. Chemokines to be considered for extended future studies include for example CCL2, CCL8 and CCL3 with their receptors.

### 4.2.3 CCL2 level and MO infiltration in breast tumor cell line spheroids

MO migration and its correlation with CCL2 expression was also evaluated for the breast cancer cell lines chosen for the present work (Hs578T, BT549, T47D, BT474, MCF-7). Since the amount of tumor cells used for inoculation of spheroids and after co-culture with MO differed between the cell lines, the number of migrated MO was also calculated as percent of total blood MO applied. The Hs578T cell line showed both highest levels of cellular CCL2 production and MO infiltration, while lines which expressed very little or no CCL2 (MCF-7, BT474) were poorly infiltrated. A correlation between cellular CCL2 release and MO migration was thus hypothesized and lines regression analysis was thus performed a basis for discussion (see Fig. 4.4). The significance level of 0.05 is just not reached probably because of poor number of values. Poor correlation was primarily due to the fact that BT549 cells expressed relatively high level of CCL2 but were infiltrated by MO to

a lesser extent than T47D spheroids with showed a lower cellular release of CCL2 into the supernatant (see Tab. 4.1 and Fig. 4.4).This indicates that MO migration into tumor cell areas is more complex and does not exclusively depend on cellular CCL2 production, in spite of the fact that cellular release rates calculated from the CCL2 level in supernatant may not reflect a potential discrepancy in intraspheroidal CCL2 accumulation and development of a gradient.

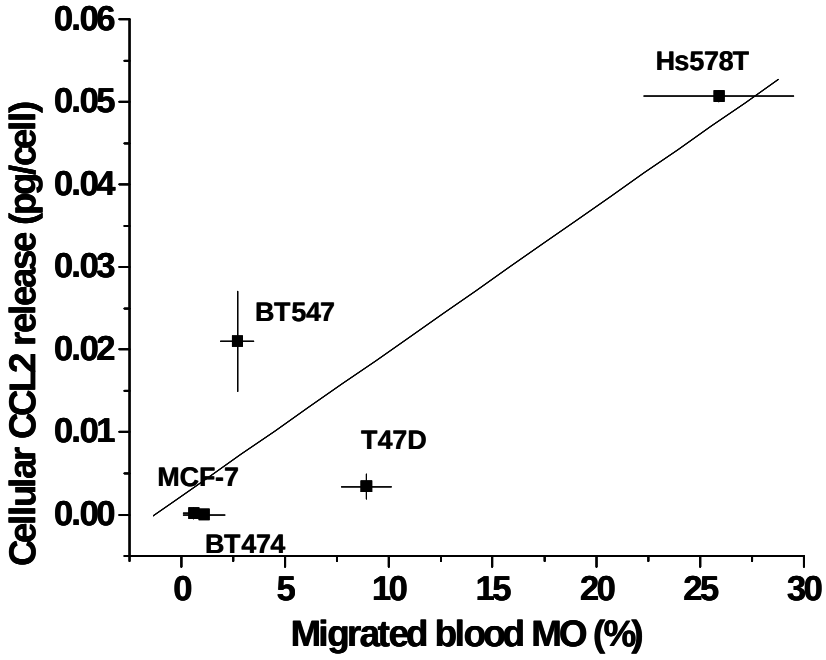


**Fig. 4.4 Correlation of cellular CCL2 release (pg/cell in 96 h) of various breast tumor cell types in spheroid culture with the infiltration of blood monocytes. y= ax+b.**
**Correlation coefficient: r=0.88**
**Significance level: p=0.0509**

A study performed by Lu et al. for prostate cancer cell lines showed that CCL2 expression positively correlated with cell lines invasiveness. The malignant prostate cell lines expressed significantly more CCL2 as compared to non-neoplastic prostate epithelia. Moreover, the high expression correlated positively with an advanced pathological state (Lu *et al.*, 2006).

**Tab.4.1 Comparison of cell line characteristics of breast tumor cell lines related to MO migration and CCL2 secretion**

| Breast tumor cell line | Invasiveness* | Amount of MO in spheroid (%) | Migrating blood MO subpopulation (%) | CCL2 secretion (pg/cell) | CCL2 secretion (pg/ml) |
|---|---|---|---|---|---|
| Hs578T | +++ | 48.3 | 25.9 | 0.0507 | 716 |
| BT549 | +++ | 8.4 | 2.7 | 0.0210 | 337 |
| T47D | + | 18.6 | 8.9 | 0.0034 | 57 |
| MCF-7 | + | 3.8 | 1.1 | 0 | 0 |
| BT474 | + | 1.3 | 0.6 | 0.0002 | 3 |

*** activity in Boyden chamber chemoinvasion assay, graded as percent of MDA-MB-231 activity. + 0-40%, ++ 40-80%, +++ >80% (after Sommers et al., Breast Cancer Research and Treatment 1994, 31: 325-335).**

To role of CCL2/CCR2 signaling on MO migration into Hs578T spheroids was directly tested via blocking the CCR2 receptors on MO using the DOC-3 antibody (analogically to experiments performed for TAF spheroids, see chapter 3.2.4.2). Interestingly, MO pre-incubation with DOC-3 antibody, did not affect MO infiltration of Hs578T breast tumor spheroids. This was revealed in three independent experiments, i.e. for MO from three different donors. The data indicate that factors influencing MO migration are cell line/cell type dependent and CCL2 is relevant for MO migration into TAF but not into Hs578T spheroids. This hypothesis is also supported by the observation that although TAF express higher levels of CCL2 (0.1-0.75 pg/cell) than Hs578T (0.05 pg/cell) MO infiltration is higher into Hs578T spheroids than into TAF spheroids, 26% and 16% respectively. As already discussed (see chapter 4.2.1) differences in kinetics of MO migration into TAF and Hs578T spheroids, confirm this hypothesis.

The analysis of MO migration into breast tumor cell lines, clearly shows that MO subpopulations infiltrating particular cell lines differ in size indicating that they cannot be considered as one and the same population. However, this hypothesis of subpopulations of MO with different infiltrative potential should be more deeply studied in order to describe these differences in details.

Macrophages isolated from tumor tissues may show a reduced response to CCL2 due to a “defective” expression of its receptor (Muller *et al.*, 1997; Sica *et al.*, 2000). In the experiment of the present thesis, MO were exposed for a maximum of 40 h to factors

secreted by tumor cells and an impact on expression of the receptor cannot be excluded since a significant decrease of receptor expression can occur in a very short time. *In vitro* treatment of macrophages with potent endotoxins such as LPS resulted in a dramatic decrease of the *ccr2* mRNA levels in only 2 h after LPS addition. It is unclear, however, how long it takes, until this change mRNA expression transfer to the protein level as this depends on translation processes and receptor turnover (Zhou *et al.*, 1999).

The current study and several other studies (Goede *et al.*, 1999; Ueno *et al.*, 2000; Salcedo *et al.*, 2000) focused on CCL2 as a protein that affects the recruitment of MO into breast tumor sites. However, as already mentioned, CCL2 is only one of several chemokines which are able to attract MO. In addition to CCL2, CCL5, another inflammatory chemokine which also possess potent monocyte-recruiting activity, attracted major alteration. A preliminary study provided data on constitutive expression of CCL5 by T47D and MCF-7 cells *in vitro* (Luboshits *et al.*, 1999). Additionally, it was demonstrated that CCL5 is over expressed by tumor cells including breast and ovarian cancer (Negus *et al.*, 1997; Soria and Ben-Baruch, 2008). Research on the expression of CCL5 and other chemokines by all five breast cell lines and MO migration mechanism into spheroids will thus shed more light into this phenomenon and will be required to verify which alternative or additional paracrine/autocrine modulators are of major relevance. Latest studies on this subject showed that from several chemokines implicated in MO migration, only IL-8 was spontaneously secreted by the Hs578T spheroid cultures (Kunz-Schughart – personal communication). IL-8 activates multiple intracellular signaling pathways downstream of two cell-surface, G protein-coupled receptors (CXCR1 and CXCR2) and was recently described to enhance MO migration (Gouwy *et al.*, 2008; Waugh and Wilson, 2008).

### 4.2.4 Migrating MO subpopulation

Tumor associated macrophages derive from blood MO, migrate into tumor tissue and undergo a process of differentiation determined by the tumor microenvironment. Recruited TAM have the potential to dramatically affect tumor development and progression. Since peripheral blood MO are the precursors of most tissue macrophages and also of TAM, the ability of MO to migrate is essential for their accumulation within the fibroblastic stroma surrounding tumor cell islets as shown in invasive ductal breast tumors (Mueller, 1992).

One of the aims of this thesis was to identify and characterize the migrating blood MO subpopulation capable of infiltrating TAF spheroids. Subpopulations of blood monocytes can be identified for example by surface antigens. First, we tested if the migrating MO subpopulation differ in CCR2A/B expression. DOC-3 antibody staining did not reveal any difference between migrating and non-migrating MO, which seems contradictory to the

results presented by Mizuno et al (Mizuno *et al.*, 2005). They simultaneously stained MO with anti-CD14, anti-CD16 and anti-CCR2 antibodies. This allowed to clearly distinguish two subpopulations of MO from which $CD14^{low}CD16^{high}$ expressed little CCR2, whereas $CD14^{high}CD16^{low}$ cells expressed high level of CCR2. Ziegler-Heitbrock and coworkers described, in addition to classical $CD14^{++}CD16^{-}$ MO, population of MO, which co express CD16 and low level of CD14 ($CD14^{+}CD16^{+}$). This subpopulation was described as proinflommatory because of its higher expression of proinflammatory cytokines and higher potency in antigen presentation. This subpopulations differs in expression of cell surface molecules including CCR2 which was not detected on $CD14^{+}CD16^{+}$ MO and highly expressed on $CD14^{++}CD16^{-}$ MO (Ziegler-Heitbrock, 2007). The difference may result from accuracy of staining or from the preparation of blood monocytes, in current thesis, for this step of research, simple one-color staining was employed.

Human blood MO can be analyzed using flow cytometry by employing multi-color immunofluorescence with antibodies directed against CD14 and CD16 antigens. Based on CD14 and CD16 expression four fractions were distinguished ($CD14^{++}CD16^{-}$, $CD14^{+}CD16^{++}$, $CD14^{++}CD16^{++}$, $CD14^{++}CD16^{+}$) although there are basically two to three populations described in the literature (Ziegler-Heitbrock, 1996; Ziegler-Heitbrock, 2007). The fractions were sorted by FACS and their migration activity was compared. None of the MO subpopulations significantly differed in the infiltrating potential into TAF spheroids. It is particularly interesting when comparing to already mentioned results of Ziegler-Heitbrock presenting differences of CCR2 expression in MO subpopulations. Anacuta et al. showed that $CD14^{+}CD16^{+}$ MO (which lack CCR2 and thus not respond to CCL2), migrate in response to CX3CL1 and CXCL12 (Anacuta *et al.*, 2003).

Since integrines play a role in cell adhesion and motility (Weerasinghe *et al.*, 1998; Mouse *et al.*, 2001) and therefore may have an impact on migration processes, blood MO were analyzed for differences in integrin expression. Integrines LFA-1 (CD11a), MAC-1 (CD11b) and VLA5 (CD49e) and their expression on MO, were taken under consideration. Multicolor stainings (CD14, CD49e, CD11a and CD14, CD49e, CD11b) did not indicate any subpopulation with discrete expression profile with respect to these surface antigens. It became clear that looking at random into molecules which could be theoretically involved in migration/adhesion mechanisms in cells of interest is not effective. Therefore, multigene screening of migrating versus non-migrating MO was performed. This experiment revealed a number of genes that is supposedly up-regulated in migrated MO compared to non-migrated and control ones. Among them, genes associated with cell adhesion, proteolysis, peptidolysis or cell motility were present. This experiment could be considered only as an introduction into complex analyses. Additional molecular studies like RT-PCR validation

of genes should be performed to further evaluate the identified up-regulated genes. Also, it has to be considered that the initial experimental set-up did not allow to discriminate between genes that differ in the migrating MO subpopulation before or as a result of the infiltration process.

Although a lot of effort has been put into the discovery of migrating MO subpopulation based on antigens suggested in the literature, no clear population was distinguished. However, the microarray analysis brought promising results that require further evaluation. It would be interesting to continue this line of research also because of few reports on this subject. In literature, with regard to TAM, mostly reports consider characterization of blood MO with respect to different pathological conditions (Finnin *et al.*, 1999; Li *et al.*, 2004; Takeyama *et al.*, 2007) not blood MO from healthy donors. Another line of research, present in literature is focused on mature macrophages, with expression pattern modulated by the specific tissue environment (Konur *et al.*, 1998; Sica *et al.*, 2000).

# 5. Summary

The majority of invasive-ductal breast tumors develop a desmoplastic reaction. The most abundant stromal host cell type in desmoplastic tumors are fibroblasts. In addition to tumor-associated/derived fibroblasts (TAF), the complex cellular tumor microenvironment comprises other host cell types including endothelial and immunocompetent cells, e.g. monocytes (MO) and macrophages (MAC). All of these cells are known to be influenced by tumor cells and vice versa have an impact on tumor progression. Invasive ductal breast cancer is characterized by a high MO/MAC content. These immune cells are predominantly located within the fibroblastic stroma surrounding tumor cell islets.

The objective of the current thesis was to get insights in the process of MO migration into fibroblastic tumor areas. A 3-D spheroid co-culture system in liquid overlay was used as a model to resemble the reciprocal interactions between fibroblasts and MO and between breast tumor cells and MO. A previous study had shown that TAF 3-D cultures are more efficiently infiltrated by blood MO derived from healthy donors as compared to normal skin and breast fibroblasts. The fraction of blood MO which infiltrated TAF spheroids ranged between 10% and 20% leading to the hypothesis that a particular MO subpopulation may show high infiltrative potential into TAF spheroids and fibroblastic tumor areas, respectively. Moreover, CCL2 levels were significantly higher in supernatants of TAF as opposed to normal fibroblast spheroids indicating that this chemokine may play a role in the process of MO migration. However, MO migration into TAF spheroids could not be inhibited by a CCL2 neutralizing antibody which was highly effective in a Boyden chamber assay.

In the present work numerous experiments were designed to

- strengthen the hypothesis that paracrine factors including CCL2 are responsible for the increased infiltration of MO into TAF spheroids.
- identify a potential MO subpopulations in the blood MO pool with enhanced infiltrative potential
- also monitor blood MO infiltration of breast tumor cell line spheroids.

The data reveal that 3-D spheroid cultures of both fibroblasts and carcinoma cells from breast tumor origin are infiltrated by MO. Five different breast tumor cell lines (Hs578T, BT549, T47D, MCF-7, BT474) were examined for MO infiltration and CCL2 release. The highly invasive Hs578T cell line showed highest levels of cellular CCL2 production and MO infiltration, while less invasive MCF-7 and BT474 cell lines, expressing very little or no CCL2 were poorly infiltrated. However, the hypothesized correlation between CCL2 expression and MO infiltration was not confirmed by linear regression analysis.

To verify the relevance of paracrine factors, particularly CCL2/CCL2R signaling, for MO migration into spheroids of breast tumor origin (especially TAF and highly infiltrated Hs578T breast tumor cells) several experimental series were performed. Washing out of paracrine factors including CCL2 in TAF spheroids resulted in delayed MO migration. Disruption of CCL2 gradient by adding recombinant CCL2 to the external milieu of TAF spheroids, almost entirely abrogated the infiltration of TAF spheroids by MO but it does not affect the low, basic migration of MO into normal skin fibroblast spheroids. This result indicates that basic MO migration may relate to mechanisms different from MO infiltration of TAF spheroids. The observation was encouraging to deeper study the paracrine factors signaling in TAF spheroids. Experiments to block downstream signaling from $G_{i/o}$ and $G_{\alpha s}$ protein coupled receptors by pertussis toxin (PTX) and cholera toxin (ChTX), respectively were performed. MO recruitment into TAF was inhibited by pre-exposure of MO to PTX and ChTX. However, in contrast to PTX, ChTX could not completely block MO migration. The strong inhibitory effect of PTX is consistent with described in literature involvement of $G_{i/o}$ proteins in CCL2 signaling, however other 7-transmembrane G protein coupled receptors may also be affected. Therefore, CCL2 receptor signaling was inhibited by pre-exposure of MO to the specific CCR2A/B blocking antibody DOC-3. This approach resulted in an almost complete loss of MO infiltration of TAF spheroids. Analogical experiments were performed for Hs578T spheroids (chosen because of their high infiltration rate and CCL2 release). Here, however, MO infiltration was unaltered by CCR2A/B receptor blockade. This indicates that the migration of MO and also the localization of TAM in tumor tissues are affected by the individual expression pattern of both stromal and tumor cell compartments. This is supported by the additional observation that MO subpopulation size and migration kinetics differ in TAF and Hs578T spheroids. Other chemokines implicated in MO migration such as CCL5, BRAK, or IL-8 are thus discussed and proposed for extended future studies.

In order to identify the migrating MO subpopulation, blood MO were stained for surface antigens CD14/CD16 that were described earlier to discriminate blood MO populations with different infiltrative potential. Staining and flow cytometric analysis allowed to distinguish four different MO fractions, however none of these fractions showed differences in migration capacity when isolated by fluorescence activated cell sorting and then added to TAF spheroids. Because the expression pattern of some other antigens relevant for cell-cell interactions did not indicate the presence of a particular subpopulation, the search for the blood MO population with high infiltrative potential was extended to a multigene screening approach of migrated *versus* non-migrated MO was performed. It revealed a number of genes which seem over expressed in migrated cells and which should be validated and further explored in the future..

In summary, CCL2/CCR2A/B signaling was shown to be important for MO infiltration into TAF but not Hs578T tumor spheroids. A particular high infiltrative blood MO populations according to those described in the literature could not yet be identified. It is concluded that paracrine factors from stromal fibroblasts are relevant to govern and/or at least fine tune the infiltration and location of blood MO in breast tumor tissue where they supposedly undergo abnormal differentiation to become tumor promoting, tumor-associated macrophages. The role of fibroblast-derived CCL2 in this scenario has to be emphasized in light of earlier evidence that the level of tumor derived CCL2 correlates with the abundance of TAM, poor prognosis and clinical outcome in breast tumors.

# 6. Reference List


1. al-Sarireh,B. and Eremin,O. (2000). Tumour-associated macrophages (TAMS): disordered function, immune suppression and progressive tumour growth. J. R. Coll. Surg. Edinb. *45*, 1-16.

2. Alfano,M., Schmidtmayerova,H., Amella,C.A., Pushkarsky,T., and Bukrinsky,M. (1999). The B-oligomer of pertussis toxin deactivates CC chemokine receptor 5 and blocks entry of M-tropic HIV-1 strains. J. Exp. Med. *190*, 597-605.

3. Amann,B., Perabo,F.G., Wirger,A., Hugenschmidt,H., and Schultze-Seemann,W. (1998). Urinary levels of monocyte chemo-attractant protein-1 correlate with tumour stage and grade in patients with bladder cancer. Br. J. Urol. *82*, 118-121.

4. Amatruda,T.T., III, Gerard,N.P., Gerard,C., and Simon,M.I. (1993). Specific interactions of chemoattractant factor receptors with G-proteins. J. Biol. Chem. *268*, 10139-10144.

5. Ancuta,P., Rao,R., Moses,A., Mehle,A., Shaw,S.K., Luscinskas,F.W., Gabuzda,D. (2003). Fractalkine preferentially mediated arrest and migration of CD16+ monocytes. J. Exp. Med. *7*, 311-317.

6. Azenshtein,E., Luboshits,G., Shina,S., Neumark,E., Shahbazian,D., Weil,M., Wigler,N., Keydar,I., and Ben-Baruch,A. (2002). The CC chemokine RANTES in breast carcinoma progression: regulation of expression and potential mechanisms of promalignant activity. Cancer Res. *62*, 1093-1102.

7. Bacon,K. *et al.* (2002). Chemokine/chemokine receptor nomenclature. J. Interferon Cytokine Res. *22*, 1067-1068.

8. Baggiolini,M. (1998). Chemokines and leukocyte traffic. Nature *392*, 565-568.

9. Baggiolini,M. and Dahinden,C.A. (1994). CC chemokines in allergic inflammation. Immunol. Today *15*, 127-133.

10. Balkwill,F. (2004). Cancer and the chemokine network. Nat. Rev. Cancer *4*, 540-550.

11. Banerjea,A., Li,M.J., Bauer,G., Remling,L., Lee,N.S., Rossi,J., and Akkina,R. (2003). Inhibition of HIV-1 by lentiviral vector-transduced siRNAs in T lymphocytes differentiated in SCID-hu mice and CD34+ progenitor cell-derived macrophages. Mol. Ther. *8*, 62-71.

12. Biber,K., Zuurman,M.W., Homan,H., and Boddeke,H.W. (2003). Expression of L-CCR in HEK 293 cells reveals functional responses to CCL2, CCL5, CCL7, and CCL8. J. Leukoc. Biol. *74*, 243-251.

13. Bingle,L., Brown,N.J., and Lewis,C.E. (2002). The role of tumour-associated macrophages in tumour progression: implications for new anticancer therapies. J. Pathol. *196*, 254-265.

14. Blachere,N.E., Li,Z., Chandawarkar,R.Y., Suto,R., Jaikaria,N.S., Basu,S., Udono,H., and Srivastava,P.K. (1997). Heat shock protein-peptide complexes, reconstituted in

vitro, elicit peptide-specific cytotoxic T lymphocyte response and tumor immunity. J. Exp. Med. *186*, 1315-1322.

15. Bodnar,A.G., Ouellette,M., Frolkis,M., Holt,S.E., Chiu,C.P., Morin,G.B., Harley,C.B., Shay,J.W., Lichtsteiner,S., and Wright,W.E. (1998). Extension of life-span by introduction of telomerase into normal human cells. Science *279*, 349-352.

16. Bokoch,G.M. (1995). Chemoattractant signaling and leukocyte activation. Blood *86*, 1649-1660.

17. Boring,L., Gosling,J., Chensue,S.W., Kunkel,S.L., Farese,R.V., Jr., Broxmeyer,H.E., and Charo,I.F. (1997). Impaired monocyte migration and reduced type 1 (Th1) cytokine responses in C-C chemokine receptor 2 knockout mice. J. Clin. Invest *100*, 2552-2561.

18. Bossink,A.W., Paemen,L., Jansen,P.M., Hack,C.E., Thijs,L.G., and Van,D.J. (1995). Plasma levels of the chemokines monocyte chemotactic proteins-1 and -2 are elevated in human sepsis. Blood *86*, 3841-3847.

19. Brigati,C., Noonan,D.M., Albini,A., and Benelli,R. (2002). Tumors and inflammatory infiltrates: friends or foes? Clin. Exp. Metastasis *19*, 247-258.

20. Brouty-Boye,D., Raux,H., Azzarone,B., Tamboise,A., Tamboise,E., Beranger,S., Magnien,V., Pihan,I., Zardi,L., and Israel,L. (1991). Fetal myofibroblast-like cells isolated from post-radiation fibrosis in human breast cancer. Int. J. Cancer *47*, 697-702.

21. Brown,D.L., Phillips,D.R., Damsky,C.H., and Charo,I.F. (1989). Synthesis and expression of the fibroblast fibronectin receptor in human monocytes. J. Clin. Invest *84*, 366-370.

22. Cambien,B., Pomeranz,M., Millet,M.A., Rossi,B., and Schmid-Alliana,A. (2001). Signal transduction involved in MCP-1-mediated monocytic transendothelial migration. Blood *97*, 359-366.

23. Carr,M.W., Roth,S.J., Luther,E., Rose,S.S., and Springer,T.A. (1994). Monocyte chemoattractant protein 1 acts as a T-lymphocyte chemoattractant. Proc. Natl. Acad. Sci. U. S. A *91*, 3652-3656.

24. Charo,I.F., Myers,S.J., Herman,A., Franci,C., Connolly,A.J., and Coughlin,S.R. (1994). Molecular cloning and functional expression of two monocyte chemoattractant protein 1 receptors reveals alternative splicing of the carboxyl-terminal tails. Proc. Natl. Acad. Sci. U. S. A *91*, 2752-2756.

25. Chen,C.S., Mrksich,M., Huang,S., Whitesides,G.M., and Ingber,D.E. (1997). Geometric control of cell life and death. Science *276*, 1425-1428.

26. Chou,C.C., Fine,J.S., Pugliese-Sivo,C., Gonsiorek,W., Davies,L., Deno,G., Petro,M., Schwarz,M., Zavodny,P.J., and Hipkin,R.W. (2002). Pharmacological characterization of the chemokine receptor, hCCR1 in a stable transfectant and differentiated HL-60 cells: antagonism of hCCR1 activation by MIP-1beta. Br. J. Pharmacol. *137*, 663-675.

27. Combadiere,C., Salzwedel,K., Smith,E.D., Tiffany,H.L., Berger,E.A., and Murphy,P.M. (1998). Identification of CX3CR1. A chemotactic receptor for the human CX3C chemokine fractalkine and a fusion coreceptor for HIV-1. J. Biol. Chem. *273*, 23799-23804.

28. Conti,I. and Rollins,B.J. (2004). CCL2 (monocyte chemoattractant protein-1) and cancer. Semin. Cancer Biol. *14*, 149-154.

29. Cukierman,E., Pankov,R., Stevens,D.R., and Yamada,K.M. (2001). Taking cell-matrix adhesions to the third dimension. Science *294*, 1708-1712.

30. Cullen,K.J., Allison,A., Martire,I., Ellis,M., and Singer,C. (1992). Insulin-like growth factor expression in breast cancer epithelium and stroma. Breast Cancer Res. Treat. *22*, 21-29.

31. Daly,C. and Rollins,B.J. (2003). Monocyte chemoattractant protein-1 (CCL2) in inflammatory disease and adaptive immunity: therapeutic opportunities and controversies. Microcirculation. *10*, 247-257.

32. De Wever, O., Demetter,P., Mareel,M., and Bracke,M. (2008). Stromal myofibroblasts are drivers of invasive cancer growth. Int. J. Cancer *123*, 2229-2238.

33. De Wever, O. and Mareel,M. (2002). Role of myofibroblasts at the invasion front. Biol. Chem. *383*, 55-67.

34. Devalaraja,M.N. and Richmond,A. (1999). Multiple chemotactic factors: fine control or redundancy? Trends Pharmacol. Sci. *20*, 151-156.

35. Dharmacon,I. (2004). RNA Interference, Technical Refrence and Application Guide, Dharmacon, Inc.

36. Dittmer,A., Schunke,D., and Dittmer,J. (2008). PTHrP promotes homotypic aggregation of breast cancer cells in three-dimensional cultures. Cancer Lett. *260*, 56-61.

37. Eeles,R.A. (1999). Screening for hereditary cancer and genetic testing, epitomized by breast cancer. Eur. J. Cancer *35*, 1954-1962.

38. Elbashir,S.M., Harborth,J., Lendeckel,W., Yalcin,A., Weber,K., and Tuschl,T. (2001). Duplexes of 21-nucleotide RNAs mediate RNA interference in cultured mammalian cells. Nature *411*, 494-498.

39. Elenbaas,B. and Weinberg,R.A. (2001). Heterotypic signaling between epithelial tumor cells and fibroblasts in carcinoma formation. Exp. Cell Res. *264*, 169-184.

40. Ernst,C.A., Zhang,Y.J., Hancock,P.R., Rutledge,B.J., Corless,C.L., and Rollins,B.J. (1994). Biochemical and biologic characterization of murine monocyte chemoattractant protein-1. Identification of two functional domains. J. Immunol. *152*, 3541-3549.

41. Ferlay,J., Bray,F., Parkin,D., and Pisani,P. (2001). Cancer Incidence and Mortality Worldwide, IARC Press, Lyon.

42. Ferlay,J., Autier,P., Boniol,M., Heanue,M., Colombet,M., and Boyle,P. (2007). Estimates of the cancer incidence and mortality in Europe in 2006. Ann. Oncol. *18*, 581-592.

43. Fingerle,G., Pforte,A., Passlick,B., Blumenstein,M., Strobel,M., and Ziegler-Heitbrock,H.W. (1993). The novel subset of CD14+/CD16+ blood monocytes is expanded in sepsis patients. Blood *82*, 3170-3176.

44. Finnin,M., Hamilton,J.A., and Moss,S.T. (1999). Characterization of a CSF-induced proliferating subpopulation of human peripheral blood monocytes by surface marker expression and cytokine production. J. Leukoc. Biol. *66*, 953-960.

45. Fishman,P.H. (1982). Internalization and degradation of cholera toxin by cultured cells: relationship to toxin action. J. Cell Biol. *93*, 860-865.

46. Frade,J.M., Mellado,M., del,R.G., Gutierrez-Ramos,J.C., Lind,P., and Martinez,A. (1997). Characterization of the CCR2 chemokine receptor: functional CCR2 receptor expression in B cells. J. Immunol. *159*, 5576-5584.

47. Frederick,M.J., Henderson,Y., Xu,X., Deavers,M.T., Sahin,A.A., Wu,H., Lewis,D.E., El-Naggar,A.K., and Clayman,G.L. (2000). In vivo expression of the novel CXC chemokine BRAK in normal and cancerous human tissue. Am. J. Pathol. *156*, 1937-1950.

48. Frenzel,K.R., Saller,R.M., Kummermehr,J., and Schultz-Hector,S. (1995). Quantitative distinction of cisplatin-sensitive and -resistant mouse fibrosarcoma cells grown in multicell tumor spheroids. Cancer Res. *55*, 386-391.

49. Friedrich,J., Ebner,R., and Kunz-Schughart,L.A. (2007). Experimental anti-tumor therapy in 3-D: spheroids--old hat or new challenge? Int. J. Radiat. Biol. *83*, 849-871.

50. Friedrich,J., Seidel,C., Ebner,R., and Kunz-Schughart,L.A. (2009). Spheroid-based drug screen: considerations and practical approach. Nat. Protoc. *4*, 309-324.

51. Fujimoto,H., Sangai,T., Ishii,G., Ikehara,A., Nagashima,T., Miyazaki,M., and Ochiai,A. (2009). Stromal MCP-1 in mammary tumors induces tumor-associated macrophage infiltration and contributes to tumor progression. Int. J. Cancer.

52. Futami,T., Miyagishi,M., Seki,M., and Taira,K. (2002). Induction of apoptosis in HeLa cells with siRNA expression vector targeted against bcl-2. Nucleic Acids Res. Suppl 251-252.

53. Gale,L.M. and McColl,S.R. (1999). Chemokines: extracellular messengers for all occasions? Bioessays *21*, 17-28.

54. Goede,V., Brogelli,L., Ziche,M., and Augustin,H.G. (1999). Induction of inflammatory angiogenesis by monocyte chemoattractant protein-1. Int. J. Cancer *82*, 765-770.

55. Gong,X., Gong,W., Kuhns,D.B., Ben-Baruch,A., Howard,O.M., and Wang,J.M. (1997). Monocyte chemotactic protein-2 (MCP-2) uses CCR1 and CCR2B as its functional receptors. J. Biol. Chem. *272*, 11682-11685.

56. Gonzalo,J.A. *et al.* (1998). The coordinated action of CC chemokines in the lung orchestrates allergic inflammation and airway hyperresponsiveness. J. Exp. Med. *188*, 157-167.

57. Gorrin-Rivas,M.J., Arii,S., Mori,A., Takeda,Y., Mizumoto,M., Furutani,M., and Imamura,M. (2000). Implications of human macrophage metalloelastase and vascular endothelial growth factor gene expression in angiogenesis of hepatocellular carcinoma. Ann. Surg. *231*, 67-73.

58. Gorsch,S.M., Memoli,V.A., Stukel,T.A., Gold,L.I., and Arrick,B.A. (1992). Immunohistochemical staining for transforming growth factor beta 1 associates with disease progression in human breast cancer. Cancer Res. *52*, 6949-6952.

59. Gottfried,E., Faust,S., Fritsche,J., Kunz-Schughart,L.A., Andreesen,R., Miyake,K., and Kreutz,M. (2003). Identification of genes expressed in tumor-associated macrophages. Immunobiology *207*, 351-359.

60. Gottfried,E., Kunz-Schughart,L.A., Andreesen,R., and Kreutz,M. (2006). Brave little world: spheroids as an in vitro model to study tumor-immune-cell interactions. Cell Cycle *5*, 691-695.

61. Gouwy,M., Struyf,S., Noppen,S., Schutyser,E., Springael,J.Y., Parmentier,M., Proost,P., and Van,D.J. (2008). Synergy between coproduced CC and CXC chemokines in monocyte chemotaxis through receptor-mediated events. Mol. Pharmacol. *74*, 485-495.

62. Grabbe,S., Bruvers,S., Beissert,S., and Granstein,R.D. (1994). Interferon-gamma inhibits tumor antigen presentation by epidermal antigen-presenting cells. J. Leukoc. Biol. *55*, 695-701.

63. Gregoire,M. and Lieubeau,B. (1995). The role of fibroblasts in tumor behavior. Cancer Metastasis Rev. *14*, 339-350.

64. Griffith,L.G. and Swartz,M.A. (2006). Capturing complex 3D tissue physiology in vitro. Nat. Rev. Mol. Cell Biol. *7*, 211-224.

65. Grimshaw,M.J. and Balkwill,F.R. (2001). Inhibition of monocyte and macrophage chemotaxis by hypoxia and inflammation--a potential mechanism. Eur. J. Immunol. *31*, 480-489.

66. Hackett,A.J., Smith,H.S., Springer,E.L., Owens,R.B., Nelson-Rees,W.A., Riggs,J.L., and Gardner,M.B. (1977). Two syngeneic cell lines from human breast tissue: the aneuploid mammary epithelial (Hs578T) and the diploid myoepithelial (Hs578Bst) cell lines. J. Natl. Cancer Inst. *58*, 1795-1806.

67. Hagemann,T., Wilson,J., Burke,F., Kulbe,H., Li,N.F., Pluddemann,A., Charles,K., Gordon,S., and Balkwill,F.R. (2006). Ovarian cancer cells polarize macrophages toward a tumor-associated phenotype. J. Immunol. *176*, 5023-5032.

68. Hamm,H.E. (1998). The many faces of G protein signaling. J. Biol. Chem. *273*, 669-672.

69. Hanahan,D. and Weinberg,R.A. (2000). The hallmarks of cancer. Cell *100*, 57-70.

70. Harborth,J., Elbashir,S.M., Bechert,K., Tuschl,T., and Weber,K. (2001). Identification of essential genes in cultured mammalian cells using small interfering RNAs. J. Cell Sci. *114*, 4557-4565.

71. Hauptmann,S., Zwadlo-Klarwasser,G., Jansen,M., Klosterhalfen,B., and Kirkpatrick,C.J. (1993). Macrophages and multicellular tumor spheroids in co-culture: a three-dimensional model to study tumor-host interactions. Evidence for macrophage-mediated tumor cell proliferation and migration. Am. J. Pathol. *143*, 1406-1415.

72. Hedrick,J.A. and Zlotnik,A. (1996). Chemokines and lymphocyte biology. Curr. Opin. Immunol. *8*, 343-347.

73. Heimdal,J.H., Aarstad,H.J., Olsnes,C., and Olofsson,J. (2001). Human autologous monocytes and monocyte-derived macrophages in co-culture with carcinoma F-spheroids secrete IL-6 by a non-CD14-dependent pathway. Scand. J. Immunol. *53*, 162-170.

74. Horgan,K., Jones,D.L., and Mansel,R.E. (1987). Mitogenicity of human fibroblasts in vivo for human breast cancer cells. Br. J. Surg. *74*, 227-229.

75. Iacovelli,L., Sallese,M., Mariggio,S., and De,B.A. (1999). Regulation of G-protein-coupled receptor kinase subtypes by calcium sensor proteins. FASEB J. *13*, 1-8.

76. Inamura,N., Sone,S., Okubo,A., Singh,S.M., and Ogura,T. (1990). Heterogeneity in responses of human blood monocytes to granulocyte-macrophage colony-stimulating factor. J. Leukoc. Biol. *47*, 528-534.

77. Ivascu,A. and Kubbies,M. (2007). Diversity of cell-mediated adhesions in breast cancer spheroids. Int. J. Oncol. *31*, 1403-1413.

78. Jakobsson,L., Kreuger,J., and Claesson-Welsh,L. (2007). Building blood vessels--stem cell models in vascular biology. J. Cell Biol. *177*, 751-755.

79. Jiang,X., Bruzewicz,D.A., Wong,A.P., Piel,M., and Whitesides,G.M. (2005). Directing cell migration with asymmetric micropatterns. Proc. Natl. Acad. Sci. U. S. A *102*, 975-978.

80. Jiang,X.R. *et al.* (1999). Telomerase expression in human somatic cells does not induce changes associated with a transformed phenotype. Nat. Genet. *21*, 111-114.

81. Jones,A.L. and Millar,J.L. (1989). Growth Factors in Haemopoiesis. In Clinical Haematology: Aplastic Anaemia, WB Saunders, London.

82. Katada,T., Tamura,M., and Ui,M. (1983). The A protomer of islet-activating protein, pertussis toxin, as an active peptide catalyzing ADP-ribosylation of a membrane protein. Arch. Biochem. Biophys. *224*, 290-298.

83. Katayose,Y., Kim,M., Rakkar,A.N., Li,Z., Cowan,K.H., and Seth,P. (1997). Promoting apoptosis: a novel activity associated with the cyclin-dependent kinase inhibitor p27. Cancer Res. *57*, 5441-5445.

84. Kawasaki,H., Tsunemi,M., Iyo,M., Oshima,K., Minoshima,H., Hamada,A., Onuki,R., Suyama,E., and Taira,K. (2002). A functional gene discovery in cell differentiation by hybrid ribozyme and siRNA libraries. Nucleic Acids Res. Suppl 275-276.

85. Keydar,I., Chen,L., Karby,S., Weiss,F.R., Delarea,J., Radu,M., Chaitcik,S., and Brenner,H.J. (1979). Establishment and characterization of a cell line of human breast carcinoma origin. Eur. J. Cancer *15*, 659-670.

86. Knight,J.F. *et al.* (2008). TEAD1 and c-Cbl are novel prostate basal cell markers that correlate with poor clinical outcome in prostate cancer. Br. J. Cancer *99*, 1849-1858.

87. Konur,A., Kreutz,M., Knuchel,R., Krause,S.W., and Andreesen,R. (1996). Three-dimensional co-culture of human monocytes and macrophages with tumor cells: analysis of macrophage differentiation and activation. Int. J. Cancer *66*, 645-652.

88. Konur,A., Kreutz,M., Knuchel,R., Krause,S.W., and Andreesen,R. (1998). Cytokine repertoire during maturation of monocytes to macrophages within spheroids of malignant and non-malignant urothelial cell lines. Int. J. Cancer *78*, 648-653.

89. Krause,S.W., Kreutz,M., and Andreesen,R. (1998). Isolation, characterization and cultivation of human monocytes and macrophages. Methods Microbiol. *25*, 663-684.

90. Kunkel,T.A. (1985). Rapid and efficient site-specific mutagenesis without phenotypic selection. Proc. Natl. Acad. Sci. U. S. A *82*, 488-492.

91. Kunz-Schughart,L.A. (1999). Multicellular tumor spheroids: intermediates between monolayer culture and in vivo tumor. Cell Biol. Int. *23*, 157-161.

92. Kunz-Schughart,L.A., Freyer,J.P., Hofstaedter,F., Ebner,R. (2004). The use of 3-D cultures for high throughput screening: the multicellular spheroid model. J. Biomol. Screen. *9*, 273-85.

93. Kunz-Schughart,L.A. and Knuechel,R. (2002a). Tumor-associated fibroblasts (part I): Active stromal participants in tumor development and progression? Histol. Histopathol. *17*, 599-621.

94. Kunz-Schughart,L.A. and Knuechel,R. (2002b). Tumor-associated fibroblasts (part II): Functional impact on tumor tissue. Histol. Histopathol. *17*, 623-637.

95. Kunz-Schughart,L.A., Kreutz,M., and Knuechel,R. (1998). Multicellular spheroids: a three-dimensional in vitro culture system to study tumour biology. Int. J. Exp. Pathol. *79*, 1-23.

96. Kunz-Schughart,L.A., Schroeder,J.A., Wondrak,M., van,R.F., Lehle,K., Hofstaedter,F., and Wheatley,D.N. (2006). Potential of fibroblasts to regulate the formation of three-dimensional vessel-like structures from endothelial cells in vitro. Am. J. Physiol Cell Physiol *290*, C1385-C1398.

97. Kurth,I., Willimann,K., Schaerli,P., Hunziker,T., Clark-Lewis,I., and Moser,B. (2001). Monocyte selectivity and tissue localization suggests a role for breast and kidney-expressed chemokine (BRAK) in macrophage development. J. Exp. Med. *194*, 855-861.

98. Kuziel,W.A., Morgan,S.J., Dawson,T.C., Griffin,S., Smithies,O., Ley,K., and Maeda,N. (1997). Severe reduction in leukocyte adhesion and monocyte extravasation in mice deficient in CC chemokine receptor 2. Proc. Natl. Acad. Sci. U. S. A *94*, 12053-12058.

99. Lasfargues,E.Y., Coutinho,W.G., and Redfield,E.S. (1978). Isolation of two human tumor epithelial cell lines from solid breast carcinomas. J. Natl. Cancer Inst. *61*, 967-978.

100. Leek,R.D., Lewis,C.E., Whitehouse,R., Greenall,M., Clarke,J., and Harris,A.L. (1996). Association of macrophage infiltration with angiogenesis and prognosis in invasive breast carcinoma. Cancer Res. *56*, 4625-4629.

101. Lefkowitz,R.J. (1998). G protein-coupled receptors. III. New roles for receptor kinases and beta-arrestins in receptor signaling and desensitization. J. Biol. Chem. *273*, 18677-18680.

102. Lelievre,S.A., Weaver,V.M., Nickerson,J.A., Larabell,C.A., Bhaumik,A., Petersen,O.W., and Bissell,M.J. (1998). Tissue phenotype depends on reciprocal interactions between the extracellular matrix and the structural organization of the nucleus. Proc. Natl. Acad. Sci. U. S. A *95*, 14711-14716.

103. Leonard,E.J. and Yoshimura,T. (1990). Human monocyte chemoattractant protein-1 (MCP-1). Immunol. Today *11*, 97-101.

104. Li,G., Hangoc,G., and Broxmeyer,H.E. (2004). Interleukin-10 in combination with M-CSF and IL-4 contributes to development of the rare population of CD14+CD16++ cells derived from human monocytes. Biochem. Biophys. Res. Commun. *322*, 637-643.

105. Lieubeau,B., Garrigue,L., Barbieux,I., Meflah,K., and Gregoire,M. (1994). The role of transforming growth factor beta 1 in the fibroblastic reaction associated with rat colorectal tumor development. Cancer Res. *54*, 6526-6532.

106. Lin,R.Z. and Chang,H.Y. (2008). Recent advances in three-dimensional multicellular spheroid culture for biomedical research. Biotechnol. J. *3*, 1172-1184.

107. Lu,Y., Cai,Z., Galson,D.L., Xiao,G., Liu,Y., George,D.E., Melhem,M.F., Yao,Z., and Zhang,J. (2006). Monocyte chemotactic protein-1 (MCP-1) acts as a paracrine and autocrine factor for prostate cancer growth and invasion. Prostate *66*, 1311-1318.

108. Luboshits,G., Shina,S., Kaplan,O., Engelberg,S., Nass,D., Lifshitz-Mercer,B., Chaitchik,S., Keydar,I., and Ben-Baruch,A. (1999). Elevated expression of the CC chemokine regulated on activation, normal T cell expressed and secreted (RANTES) in advanced breast carcinoma. Cancer Res. *59*, 4681-4687.

109. Luster,A.D. (1998). Chemokines--chemotactic cytokines that mediate inflammation. N. Engl. J. Med. *338*, 436-445.

110. Mahad,D. *et al.* (2006). Modulating CCR2 and CCL2 at the blood-brain barrier: relevance for multiple sclerosis pathogenesis. Brain *129*, 212-223.

111. Manome,Y., Wen,P.Y., Hershowitz,A., Tanaka,T., Rollins,B.J., Kufe,D.W., and Fine,H.A. (1995). Monocyte chemoattractant protein-1 (MCP-1) gene transduction:

an effective tumor vaccine strategy for non-intracranial tumors. Cancer Immunol. Immunother. *41*, 227-235.

112. Mantovani,A. (1994). Tumor-associated macrophages in neoplastic progression: a paradigm for the in vivo function of chemokines. Lab Invest *71*, 5-16.

113. Mantovani,A., Bottazzi,B., Colotta,F., Sozzani,S., and Ruco,L. (1992). The origin and function of tumor-associated macrophages. Immunol. Today *13*, 265-270.

114. Matsushima,K., Larsen,C.G., DuBois,G.C., and Oppenheim,J.J. (1989). Purification and characterization of a novel monocyte chemotactic and activating factor produced by a human myelomonocytic cell line. J. Exp. Med. *169*, 1485-1490.

115. Matuliene,J. and Kuriyama,R. (2002). Kinesin-like protein CHO1 is required for the formation of midbody matrix and the completion of cytokinesis in mammalian cells. Mol. Biol. Cell *13*, 1832-1845.

116. Mouse,U., Huwe,J., Mouse,R., Seeger,W., and Lohmeyer,J. (2001). Alveolar JE/MCP-1 and endotoxin synergize to provoke lung cytokine upregulation, sequential neutrophile and monocyte influx, and vascular leakage in mice. Am. J. Respir. Crit Care Med. *164*, 406-411.

117. Mellado,M., Rodriguez-Frade,J.M., Aragay,A., del,R.G., Martin,A.M., Vila-Coro,A.J., Serrano,A., Mayor,F., Jr., and Martinez,A. (1998). The chemokine monocyte chemotactic protein 1 triggers Janus kinase 2 activation and tyrosine phosphorylation of the CCR2B receptor. J. Immunol. *161*, 805-813.

118. Mellado,M., Rodriguez-Frade,J.M., Manes,S., and Martinez,A. (2001a). Chemokine signaling and functional responses: the role of receptor dimerization and TK pathway activation. Annu. Rev. Immunol. *19*, 397-421.

119. Mellado,M., Rodriguez-Frade,J.M., Vila-Coro,A.J., Fernandez,S., Martin de,A.A., Jones,D.R., Toran,J.L., and Martinez,A. (2001b). Chemokine receptor homo- or heterodimerization activates distinct signaling pathways. EMBO J. *20*, 2497-2507.

120. Mestdagt,M., Polette,M., Buttice,G., Noel,A., Ueda,A., Foidart,J.M., and Gilles,C. (2006). Transactivation of MCP-1/CCL2 by beta-catenin/TCF-4 in human breast cancer cells. Int. J. Cancer *118*, 35-42.

121. Miller,V.M., Xia,H., Marrs,G.L., Gouvion,C.M., Lee,G., Davidson,B.L., and Paulson,H.L. (2003). Allele-specific silencing of dominant disease genes. Proc. Natl. Acad. Sci. U. S. A *100*, 7195-7200.

122. Mizuno,K., Toma,T., Tsukiji,H., Okamoto,H., Yamazaki,H., Ohta,K., Ohta,K., Kasahara,Y., Koizumi,S., and Yachie,A. (2005). Selective expansion of CD16high. Clin. Exp. Immunol. *142*, 461-470.

123. Molino,M. *et al.* (2000). CXCR4 on human endothelial cells can serve as both a mediator of biological responses and as a receptor for HIV-2. Biochim. Biophys. Acta *1500*, 227-240.

124. Morales,C.P., Holt,S.E., Ouellette,M., Kaur,K.J., Yan,Y., Wilson,K.S., White,M.A., Wright,W.E., and Shay,J.W. (1999). Absence of cancer-associated changes in human fibroblasts immortalized with telomerase. Nat. Genet. *21*, 115-118.

125. Mueller,H. (1992). The Human Carcinoma: A Model For The Relations Between Growth Fractions, Tumor-Associated MAcrophages and Prognostic Factors., Gustaw Fischer Verlag.

126. Mueller-Klieser,W. (2000). Tumor biology and experimental therapeutics. Crit Rev. Oncol. Hematol. *36*, 123-139.

127. Mueller-Klieser,W. (1997). Three-dimensional cell cultures: from molecular mechanisms to clinical applications. Am. J. Physiol *273*, C1109-C1123.

128. Muhlbauer,M., Bosserhoff,A.K., Hartmann,A., Thasler,W.E., Weiss,T.S., Herfarth,H., Lock,G., Scholmerich,J., and Hellerbrand,C. (2003). A novel MCP-1 gene polymorphism is associated with hepatic MCP-1 expression and severity of HCV-related liver disease. Gastroenterology *125*, 1085-1093.

129. Muller,R., Zheng,M., and Mrowietz,U. (1997). Significant reduction of human monocyte chemotactic response to monocyte-chemotactic protein 1 in patients with primary and metastatic malignant melanoma. Exp. Dermatol. *6*, 81-86.

130. Murdoch,C. and Finn,A. (2000). Chemokine receptors and their role in inflammation and infectious diseases. Blood *95*, 3032-3043.

131. Murphy,P.M. (1994). The molecular biology of leukocyte chemoattractant receptors. Annu. Rev. Immunol. *12*, 593-633.

132. Murphy,P.M., Baggiolini,M., Charo,I.F., Hebert,C.A., Horuk,R., Matsushima,K., Miller,L.H., Oppenheim,J.J., and Power,C.A. (2000). International union of pharmacology. XXII. Nomenclature for chemokine receptors. Pharmacol. Rev. *52*, 145-176.

133. Nakagawa,H., Liyanarachchi,S., Davuluri,R.V., Auer,H., Martin,E.W., Jr., de la,C.A., and Frankel,W.L. (2004). Role of cancer-associated stromal fibroblasts in metastatic colon cancer to the liver and their expression profiles. Oncogene *23*, 7366-7377.

134. Nakashima,E., Mukaida,N., Kubota,Y., Kuno,K., Yasumoto,K., Ichimura,F., Nakanishi,I., Miyasaka,M., and Matsushima,K. (1995). Human MCAF gene transfer enhances the metastatic capacity of a mouse cachectic adenocarcinoma cell line in vivo. Pharm. Res. *12*, 1598-1604.

135. Namba,M., Nishitani,K., Fukushima,F., Kimoto,T., and Yuasa,Y. (1988). Multi-step neoplastic transformation of normal human fibroblasts by Co-60 gamma rays and Ha-ras oncogenes. Mutat. Res. *199*, 415-423.

136. Nathan,C.F. (1987). Secretory products of macrophages. J. Clin. Invest *79*, 319-326.

137. Neer,E.J. and Clapham,D.E. (1988). Roles of G protein subunits in transmembrane signaling. Nature *333*, 129-134.

138. Negus,R.P., Stamp,G.W., Hadley,J., and Balkwill,F.R. (1997). Quantitative assessment of the leukocyte infiltrate in ovarian cancer and its relationship to the expression of C-C chemokines. Am. J. Pathol. *150*, 1723-1734.

139. Negus,R.P., Turner,L., Burke,F., and Balkwill,F.R. (1998). Hypoxia down-regulates MCP-1 expression: implications for macrophage distribution in tumors. J. Leukoc. Biol. *63*, 758-765.

140. Nesbit,M., Schaider,H., Miller,T.H., and Herlyn,M. (2001). Low-level monocyte chemoattractant protein-1 stimulation of monocytes leads to tumor formation in nontumorigenic melanoma cells. J. Immunol. *166*, 6483-6490.

141. O'Boyle,G., Brain,J.G., Kirby,J.A., and Ali,S. (2007). Chemokine-mediated inflammation: Identification of a possible regulatory role for CCR2. Mol. Immunol. *44*, 1944-1953.

142. O'Hare,M.J. *et al.* (2001). Conditional immortalization of freshly isolated human mammary fibroblasts and endothelial cells. Proc. Natl. Acad. Sci. U. S. A *98*, 646-651.

143. Oishi,M., Nagasaki,Y., Nishiyama,N., Itaka,K., Takagi,M., Shimamoto,A., Furuichi,Y., and Kataoka,K. (2007). Enhanced growth inhibition of hepatic multicellular tumor spheroids by lactosylated poly(ethylene glycol)-siRNA conjugate formulated in PEGylated polyplexes. ChemMedChem. *2*, 1290-1297.

144. Olivotto,I., Gelmon,K., McCready,D., Pritchard,K., and Kuusk,U. (2006). Intaligent Patient Guide to Breast Cancer, Vancouver: Intelligent Patient Guide Limited.

145. Olumi,A.F., Grossfeld,G.D., Hayward,S.W., Carroll,P.R., Tlsty,T.D., and Cunha,G.R. (1999). Carcinoma-associated fibroblasts direct tumor progression of initiated human prostatic epithelium. Cancer Res. *59*, 5002-5011.

146. Osborne,C.K., Coronado,E.B., Kitten,L.J., Arteaga,C.I., Fuqua,S.A., Ramasharma,K., Marshall,M., and Li,C.H. (1989). Insulin-like growth factor-II (IGF-II): a potential autocrine/paracrine growth factor for human breast cancer acting via the IGF-I receptor. Mol. Endocrinol. *3*, 1701-1709.

147. Owen,C.A., Campbell,E.J., and Stockley,R.A. (1992). Monocyte adherence to fibronectin: role of CD11/CD18 integrins and relationship to other monocyte functions. J. Leukoc. Biol. *51*, 400-408.

148. Pampaloni,F., Reynaud,E.G., and Stelzer,E.H. (2007). The third dimension bridges the gap between cell culture and live tissue. Nat. Rev. Mol. Cell Biol. *8*, 839-845.

149. Proost,P., Wuyts,A., Opdenakker,G., and Van Damme,J. (1998). Monocyte Chemotactic Proteins 1, 2 and 3. In: Cytokines, ed. A.Mire-SLuis and R.Thorpe Academic Press, 494.

150. Rabin,R.L., Park,M.K., Liao,F., Swofford,R., Stephany,D., and Farber,J.M. (1999). Chemokine receptor responses on T cells are achieved through regulation of both receptor expression and signaling. J. Immunol. *162*, 3840-3850.

151. Rodriguez-Frade,J.M., Mellado,M., and Martinez,A. (2001). Chemokine receptor dimerization: two are better than one. Trends Immunol. *22*, 612-617.

152. Rodriguez-Frade,J.M., Vila-Coro,A.J., de Ana,A.M., Albar,J.P., Martinez,A., and Mellado,M. (1999a). The chemokine monocyte chemoattractant protein-1 induces

functional responses through dimerization of its receptor CCR2. Proc. Natl. Acad. Sci. U. S. A *96*, 3628-3633.

153. Rodriguez-Frade,J.M., Vila-Coro,A.J., Martin,A., Nieto,M., Sanchez-Madrid,F., Proudfoot,A.E., Wells,T.N., Martinez,A., and Mellado,M. (1999b). Similarities and differences in RA. J. Cell Biol. *144*, 755-765.

154. Rollins,B.J. (1997). Chemokines. Blood *90*, 909-928.

155. Rollins,B.J. and Sunday,M.E. (1991). Suppression of tumor formation in vivo by expression of the JE gene in malignant cells. Mol. Cell Biol. *11*, 3125-3131.

156. Ronnov-Jessen,L. and Petersen,O.W. (1993). Induction of alpha-smooth muscle actin by transforming growth factor-beta 1 in quiescent human breast gland fibroblasts. Implications for myofibroblast generation in breast neoplasia. Lab Invest *68*, 696-707.

157. Ronnov-Jessen,L., Petersen,O.W., and Bissell,M.J. (1996). Cellular changes involved in conversion of normal to malignant breast: importance of the stromal reaction. Physiol Rev. *76*, 69-125.

158. Rothe,G., Gabriel,H., Kovacs,E., Klucken,J., Stohr,J., Kindermann,W., and Schmitz,G. (1996). Peripheral blood mononuclear phagocyte subpopulations as cellular markers in hypercholesterolemia. Arterioscler. Thromb. Vasc. Biol. *16*, 1437-1447.

159. Saji,H., Koike,M., Yamori,T., Saji,S., Seiki,M., Matsushima,K., and Toi,M. (2001). Significant correlation of monocyte chemoattractant protein-1 expression with neovascularization and progression of breast carcinoma. Cancer *92*, 1085-1091.

160. Sakai,N. *et al.* (2006). MCP-1/CCR2-dependent loop for fibrogenesis in human peripheral CD14-positive monocytes. J. Leukoc. Biol. *79*, 555-563.

161. Salcedo,R., Ponce,M.L., Young,H.A., Wasserman,K., Ward,J.M., Kleinman,H.K., Oppenheim,J.J., and Murphy,W.J. (2000). Human endothelial cells express CCR2 and respond to MCP-1: direct role of MCP-1 in angiogenesis and tumor progression. Blood *96*, 34-40.

162. Sanchez-Madrid,F. and del Pozo,M.A. (1999). Leukocyte polarization in cell migration and immune interactions. EMBO J. *18*, 501-511.

163. Sanders,S.K., Crean,S.M., Boxer,P.A., Kellner,D., LaRosa,G.J., and Hunt,S.W., III (2000). Functional differences between monocyte chemotactic protein-1 receptor A and monocyte chemotactic protein-1 receptor B expressed in a Jurkat T cell. J. Immunol. *165*, 4877-4883.

164. Sanderson,R.J., Shepperdson,R.T., Vatter,A.E., and Talmage,D.W. (1977). Isolation and enumeration of peripheral blood monocytes. J. Immunol. *118*, 1409-1414.

165. Santini,M.T., Rainaldi,G., and Indovina,P.L. (2000). Apoptosis, cell adhesion and the extracellular matrix in the three-dimensional growth of multicellular tumor spheroids. Crit Rev. Oncol. Hematol. *36*, 75-87.

166. Santini,M.T., Rainaldi,G., and Indovina,P.L. (1999). Multicellular tumour spheroids in radiation biology. Int. J. Radiat. Biol. *75*, 787-799.

167. Schoppmann,S.F., Birner,P., Stockl,J., Kalt,R., Ullrich,R., Caucig,C., Kriehuber,E., Nagy,K., Alitalo,K., and Kerjaschki,D. (2002). Tumor-associated macrophages express lymphatic endothelial growth factors and are related to peritumoral lymphangiogenesis. Am. J. Pathol. *161*, 947-956.

168. Schor,A.M., Rushton,G., Ferguson,J.E., Howell,A., Redford,J., and Schor,S.L. (1994). Phenotypic heterogeneity in breast fibroblasts: functional anomaly in fibroblasts from histologically normal tissue adjacent to carcinoma. Int. J. Cancer *59*, 25-32.

169. Schroder,A.E., Greiner,A., Seyfert,C., and Berek,C. (1996). Differentiation of B cells in the nonlymphoid tissue of the synovial membrane of patients with rheumatoid arthritis. Proc. Natl. Acad. Sci. U. S. A *93*, 221-225.

170. Schurch,W. (1999). The myofibroblast in neoplasia. Curr. Top. Pathol. *93*, 135-148.

171. Seidl,P. Der Einfluss des Stromafibroblasten auf die RNA Expression im Mamma. Untersuchungen An Einem Dynamischen 3-D Co-Cultur Model. 2001. University of Regensburg.
Ref Type: Thesis/Dissertation

172. Sennerstam,R. and Auer,G. (1993). Polyploidization by means of endoduplication in a human breast cancer cell line. Anal. Quant. Cytol. Histol. *15*, 303-310.

173. Shao,Z.M., Nguyen,M., and Barsky,S.H. (2000). Human breast carcinoma desmoplasia is PDGF initiated. Oncogene *19*, 4337-4345.

174. Shay,J.W., Van Der Haegen,B.A., Ying,Y., and Wright,W.E. (1993). The frequency of immortalization of human fibroblasts and mammary epithelial cells transfected with SV40 large T-antigen. Exp. Cell Res. *209*, 45-52.

175. Sica,A. *et al.* (2000). Defective expression of the monocyte chemotactic protein-1 receptor CCR2 in macrophages associated with human ovarian carcinoma. J. Immunol. *164*, 733-738.

176. Silzle,T., Kreutz,M., Dobler,M.A., Brockhoff,G., Knuechel,R., and Kunz-Schughart,L.A. (2003). Tumor-associated fibroblasts recruit blood monocytes into tumor tissue. Eur. J. Immunol. *33*, 1311-1320.

177. Smith,H.S., Liotta,L.A., Hancock,M.C., Wolman,S.R., and Hackett,A.J. (1985). Invasiveness and ploidy of human mammary carcinomas in short-term culture. Proc. Natl. Acad. Sci. U. S. A *82*, 1805-1809.

178. Sommers,C.L., Byers,S.W., Thompson,E.W., Torri,J.A., and Gelmann,E.P. (1994). Differentiation state and invasiveness of human breast cancer cell lines. Breast Cancer Res. Treat. *31*, 325-335.

179. Soria,G. and Ben-Baruch,A. (2008). The inflammatory chemokines CCL2 and CCL5 in breast cancer. Cancer Lett. *267*, 271-285.

180. Sozzani,S., Molino,M., Locati,M., Luini,W., Cerletti,C., Vecchi,A., and Mantovani,A. (1993). Receptor-activated calcium influx in human monocytes exposed to monocyte chemotactic protein-1 and related cytokines. J. Immunol. *150*, 1544-1553.

181. Spoettl,T., Hausmann,M., Herlyn,M., Gunckel,M., Dirmeier,A., Falk,W., Herfarth,H., Schoelmerich,J., and Rogler,G. (2006). Monocyte chemoattractant protein-1 (MCP-1) inhibits the intestinal-like differentiation of monocytes. Clin. Exp. Immunol. *145*, 190-199.

182. Steffen,C.L., Ball-Mirth,D.K., Harding,P.A., Bhattacharyya,N., Pillai,S., and Brigstock,D.R. (1998). Characterization of cell-associated and soluble forms of connective tissue growth factor (CTGF) produced by fibroblast cells in vitro. Growth Factors *15*, 199-213.

183. Stewart,B.W. and Kleinhaus,P. (2003). Breast Cancer. In: World Cancer Report, ed. B.W.Stewart and P.KleinhausParis: IARC Press, lyon, 190.

184. Strieter,R.M., Koch,A.E., Antony,V.B., Fick,R.B., Jr., Standiford,T.J., and Kunkel,S.L. (1994). The immunopathology of chemotactic cytokines: the role of interleukin-8 and monocyte chemoattractant protein-1. J. Lab Clin. Med. *123*, 183-197.

185. Stryer,L. and Bourne,H.R. (1986). G proteins: a family of signal transducers. Annu. Rev. Cell Biol. *2*, 391-419.

186. Sugarman,B.J., Aggarwal,B.B., Hass,P.E., Figari,I.S., Palladino,M.A., Jr., and Shepard,H.M. (1985). Recombinant human tumor necrosis factor-alpha: effects on proliferation of normal and transformed cells in vitro. Science *230*, 943-945.

187. Sunderkotter,C., Steinbrink,K., Goebeler,M., Bhardwaj,R., and Sorg,C. (1994). Macrophages and angiogenesis. J. Leukoc. Biol. *55*, 410-422.

188. Szabo,G., Miller-Graziano,C.L., Wu,J.Y., Takayama,T., and Kodys,K. (1990). Differential tumor necrosis factor production by human monocyte subsets. J. Leukoc. Biol. *47*, 206-216.

189. Takeyama,N., Yabuki,T., Kumagai,T., Takagi,S., Takamoto,S., and Noguchi,H. (2007). Selective expansion of the CD14(+)/CD16(bright) subpopulation of circulating monocytes in patients with hemophagocytic syndrome. Ann. Hematol. *86*, 787-792.

190. Tamura,M., Nogimori,K., Murai,S., Yajima,M., Ito,K., Katada,T., Ui,M., and Ishii,S. (1982). Subunit structure of islet-activating protein, pertussis toxin, in conformity with the A-B model. Biochemistry *21*, 5516-5522.

191. Thomas,C.H., Collier,J.H., Sfeir,C.S., and Healy,K.E. (2002). Engineering gene expression and protein synthesis by modulation of nuclear shape. Proc. Natl. Acad. Sci. U. S. A *99*, 1972-1977.

192. Tsung,K., Dolan,J.P., Tsung,Y.L., and Norton,J.A. (2002). Macrophages as effector cells in interleukin 12-induced T cell-dependent tumor rejection. Cancer Res. *62*, 5069-5075.

193. Tsutsui,S., Yasuda,K., Suzuki,K., Tahara,K., Higashi,H., and Era,S. (2005). Macrophage infiltration and its prognostic implications in breast cancer: the relationship with VEGF expression and microvessel density. Oncol. Rep. *14*, 425-431.

194. Turpin,J., Hersh,E.M., and Lopez-Berestein,G. (1986). Characterization of small and large human peripheral blood monocytes: effects of in vitro maturation on hydrogen peroxide release and on the response to macrophage activators. J. Immunol. *136*, 4194-4198.

195. Ueno,T., Toi,M., Saji,H., Muta,M., Bando,H., Kuroi,K., Koike,M., Inadera,H., and Matsushima,K. (2000). Significance of macrophage chemoattractant protein-1 in macrophage recruitment, angiogenesis, and survival in human breast cancer. Clin. Cancer Res. *6*, 3282-3289.

196. Usui,I., Imamura,T., Huang,J., Satoh,H., and Olefsky,J.M. (2003). Cdc42 is a Rho GTPase family member that can mediate insulin signaling to glucose transport in 3T3-L1 adipocytes. J. Biol. Chem. *278*, 13765-13774.

197. Vaage,J. (1992). Fibrosis in immune control of mammary-tumor growth. Int. J. Cancer *51*, 325-328.

198. Valkovic,T., Fuckar,D., Stifter,S., Matusan,K., Hasan,M., Dobrila,F., and Jonjic,N. (2005). Macrophage level is not affected by monocyte chemotactic protein-1 in invasive ductal breast carcinoma. J. Cancer Res. Clin. Oncol. *131*, 453-458.

199. van den Hoff,A. (1991). The role of stromal cells in tumor metastasis: a new link. Cencer Cells *3*, 186-187.

200. van Ravenswaay,C, Clasen,H.H., Kluin,P.M., and Fleuren,G.J. (1992). Tumour infiltrating cells in human cancer. On the possible role of CD16+ macrophages in anti-tumor cytotoxicity. Lab. Invest. *67*, 166-174.

201. van Roozendaal,C.E., Klijn,J.G., van,O.B., Claassen,C., Eggermont,A.M., Henzen-Logmans,S.C., and Foekens,J.A. (1995). Transforming growth factor beta secretion from primary breast cancer fibroblasts. Mol. Cell Endocrinol. *111*, 1-6.

202. Van Damme,J., Decock,B., Lenaerts,J.P., Conings,R., Bertini,R., Mantovani,A., and Billiau,A. (1989). Identification by sequence analysis of chemotactic factors for monocytes produced by normal and transformed cells stimulated with virus, double-stranded RNA or cytokine. Eur. J. Immunol. *19*, 2367-2373.

203. Vaughan,M.B., Howard,E.W., and Tomasek,J.J. (2000). Transforming growth factor-beta1 promotes the morphological and functional differentiation of the myofibroblast. Exp. Cell Res. *257*, 180-189.

204. Visscher,D.W., Tabaczka,P., Long,D., and Crissman,J.D. (1995). Clinicopathologic analysis of macrophage infiltrates in breast carcinoma. Pathol. Res. Pract. *191*, 1133-1139.

205. Walker,R.A. (2001). The complexities of breast cancer desmoplasia. Breast Cancer Res. *3*, 143-145.

206. Walter,S., Bottazzi,B., Govoni,D., Colotta,F., and Mantovani,A. (1991). Macrophage infiltration and growth of sarcoma clones expressing different amounts of monocyte chemotactic protein/JE. Int. J. Cancer *49*, 431-435.

207. Wang,J.M., Deng,X., Gong,W., and Su,S. (1998). Chemokines and their role in tumor growth and metastasis. J. Immunol. Methods *220*, 1-17.

208. Waugh,D.J. and Wilson,C. (2008). The interleukin-8 pathway in cancer. Clin. Cancer Res. *14*, 6735-6741.

209. Weber,C., Belge,K.U., von,H.P., Draude,G., Steppich,B., Mack,M., Frankenberger,M., Weber,K.S., and Ziegler-Heitbrock,H.W. (2000). Differential chemokine receptor expression and function in human monocyte subpopulations. J. Leukoc. Biol. *67*, 699-704.

210. Weerasinghe,D., McHugh,K.P., Ross,F.P., Brown,E.J., Gisler,R.H., and Imhof,B.A. (1998). A role for the alphavbeta3 integrin in the transmigration of monocytes. J. Cell Biol. *142*, 595-607.

211. Weiser,W.Y., Pozzi,L.M., and David,J.R. (1991). Human recombinant migration inhibitory factor activates human macrophages to kill Leishmania donovani. J. Immunol. *147*, 2006-2011.

212. Wernert,N. (1997). The multiple roles of tumour stroma. Virchows Arch. *430*, 433-443.

213. Whitman,S.C., Daugherty,A., and Post,S.R. (2000). Regulation of acetylated low density lipoprotein uptake in macrophages by pertussis toxin-sensitive G proteins. J. Lipid Res. *41*, 807-813.

214. Williams,J.G. (1999). Serpentine receptors and STAT activation: more than one way to twin a STAT. Trends Biochem. Sci. *24*, 333-334.

215. Wong,L.M., Myers,S.J., Tsou,C.L., Gosling,J., Arai,H., and Charo,I.F. (1997). Organization and differential expression of the human monocyte chemoattractant protein 1 receptor gene. Evidence for the role of the carboxyl-terminal tail in receptor trafficking. J. Biol. Chem. *272*, 1038-1045.

216. Yasaka,T., Mantich,N.M., Boxer,L.A., and Baehner,R.L. (1981). Functions of human monocyte and lymphocyte subsets obtained by counter current centrifugal elutriation: differing functional capacities of human monocyte subsets. J. Immunol. *127*, 1515-1518.

217. Yee,D., Paik,S., Lebovic,G.S., Marcus,R.R., Favoni,R.E., Cullen,K.J., Lippman,M.E., and Rosen,N. (1989). Analysis of insulin-like growth factor I gene expression in malignancy: evidence for a paracrine role in human breast cancer. Mol. Endocrinol. *3*, 509-517.

218. Yoder,B.J., Wilkinson,E.J., and Massoll,N.A. (2007). Molecular and morphologic distinctions between infiltrating ductal and lobular carcinoma of the breast. Breast J. *13*, 172-179.

219. Yoshimura,T., Yuhki,N., Moore,S.K., Appella,E., Lerman,M.I., and Leonard,E.J. (1989). Human monocyte chemoattractant protein-1 (MCP-1). Full-length cDNA

cloning, expression in mitogen-stimulated blood mononuclear leukocytes, and sequence similarity to mouse competence gene JE. FEBS Lett. *244*, 487-493.

220. Young,H.A. and Hardy,K.J. (1995). Role of interferon-gamma in immune cell regulation. J. Leukoc. Biol. *58*, 373-381.

221. Youngs,S.J., Ali,S.A., Taub,D.D., and Rees,R.C. (1997). Chemokines induce migrational responses in human breast carcinoma cell lines. Int. J. Cancer *71*, 257-266.

222. Yu,J.L. and Rak,J.W. (2003). Host microenvironment in breast cancer development: inflammatory and immune cells in tumour angiogenesis and arteriogenesis. Breast Cancer Res. *5*, 83-88.

223. Zembala,M., Uracz,W., Ruggiero,I., Mytar,B., and Pryjma,J. (1984). Isolation and functional characteristics of FcR+ and FcR- human monocyte subsets. J. Immunol. *133*, 1293-1299.

224. Zhou,Y., Yang,Y., Warr,G., and Bravo,R. (1999). LPS down-regulates the expression of chemokine receptor CCR2 in mice and abolishes macrophage infiltration in acute inflammation. J. Leukoc. Biol. *65*, 265-269.

224. Ziegler-Heitbrock,H.W. (1989). The biology of the monocyte system. Eur. J. Cell Biol. *49*, 1-12.

225. Ziegler-Heitbrock,H.W. (1996). Heterogeneity of human blood monocytes: the CD14+ CD16+ subpopulation. Immunol. Today *17*, 424-428.

225. Ziegler-Heitbrock, L. (2007). The CD14+CD16+ blood monocytes: their role in infection and inflammation. J. Leukoc. Biol. *81*, 584-592.

# 7. Abbreviations

| | |
|---|---|
| 2-D | two-dimensional |
| 3-D | three-dimensional |
| α-SMA | alpha-Smooth Muscle Actin |
| Ab | antibody |
| ADP | adenosine triphosphate |
| APC | allophycocyanin |
| BRAK | Breast and Kidney-expressed Chemokine |
| *BRCA1* | Breast Cancer 1, early onset |
| *BRCA2* | Breast Cancer 2, early onset |
| BSA | Bovine Serum Albumine |
| Ca2+ | calcium |
| cAMP | cyclic adenosine monophosphate |
| CCL13 (MCP-4) | Monocyte Chemoattractant Protein-4 |
| CCL2 (MCP-1) | Monocyte Chemoattractant Protein-1 |
| CCL7 (MCP-3) | Monocyte Chemoattractant Protein-3 |
| CCL8 (MCP-2) | Monocyte Chemoattractant Protein-2 |
| CCR2 | Chemokine (C-C motif) receptor 2 |
| CD | cluster of differentiation |
| cDNA | complementary DNA |
| ChTX | Cholera Toxin |
| $CO_2$ | carbon dioxide |
| Cy3 | |

| | |
|---|---|
| Cy5 | |
| DAB | diaminobenzidine |
| DEPC | diethylpyrocarbonate |
| DMEM | Dulbecco’s Modified Eagle Medium |
| DMSO | dimethylsulfoxid |
| DNA | deoxyribonucleic acid |
| dNTP | deoksinucleotide triphosphate |
| dsRNA | double stranded RNA |
| DTT | dithiothreitol |
| ECM | extracellularmatrix |
| EDTA | ethylenediaminetetraacetic acid |
| ELISA | Enzyme-Linked ImmunoSorbent Assay |
| ER | estrogene receptor |
| F | fibroblasts |
| FACS | Fluorescent-Activated Cell Sorting |
| FCS | Fetal Calf Serum |
| FcγR | Fc gamma Receptor |
| FITC | fluorescein |
| Fn | fibronectin |
| FSC | forward scatter |
| fw | forward |
| GDP | guanosine diphosphate |
| GPCR | G protein-coupled receptors |

| | |
|---|---|
| GTP | guanosine triphosphate |
| $H_2O$ | dihydrogen monoxide |
| $H_2O_2$ | hydrogen peroxide |
| HRP | horseradish peroxidase |
| ICAM-1 | Inter-Cellular Adhesion Molecule 1 |
| IGF-I | Insulin-Growth-Factor I |
| IGF-II | Insulin-Growth-Factor II |
| IgG | Immunoglobulin G |
| IL-1 | Interleukin-1 |
| IL-10 | Interleukin-10 |
| IL-6 | Interleukin-6 |
| ITGA5 | Integrin alpha 5 (CD49e) |
| ITGAL | Integrin alpha L (CD11a) |
| ITGAM | Integrin alpha M (CD11b) |
| JAK | Janus kinase |
| JNK | c-Jun N-terminal kinase |
| LFA-1 | Lymphocyte Function-associated Antigen 1 |
| Lkn-1 (CCL15) | Leukotactin-1 |
| LPS | lipopolysaccharide |
| MAC | macrophages |
| MAC-1 | Macrophage-1 antigen |
| MAPK | Mitogen-activated protein kinase |

| | |
|---|---|
| MCS | multicellular spheroids |
| M-CSF | Macrophage Colony-Stimulating Factor |
| MCTS | multicellular tumor spheroids |
| MIP-1α (CCL3) | Macrophage Inflammatory Protein-1alpha |
| MIP-1β (CCL23) | Macrophage Inflammatory Protein-1betha |
| MNC | mononuclear cells |
| MO | monocytes |
| $N_2$ | nitrogen |
| NA | not available |
| NK | Natural Killer |
| nt | nucleotide |
| PBS | Phosphate Buffered Saline |
| PCR | Polymerase Chain Reaction |
| PDGF | Platelet-Derived Growth Factor |
| PE | R-phycoerythrin |
| PR | progesterone receptor |
| PTX | Pertussis Toxin |
| RANTES (CCL5) | Regulated upon Activation, Normal T-cell Expressed, and Secreted |
| rev | reverse |
| rhMCP-1 | recombinant human MCP-1 |
| RNA | ribonucleic acid |
| RNAi | RNA interference |
| rpm | round per minute |

| | |
|---|---|
| RPMI | Roswell Park Memorial Institute |
| RT | reverse transcription |
| SD | standard deviation |
| seRNA | sense RNA |
| siRNA | small interfering RNA |
| SSC | side scatter |
| STAT3 | signal transducer and activator of transcription 3 |
| TAF | tumor associated fibroblasts = tumor derived fibroblasts |
| TAM | tumor associated macrophages |
| TC | Tumor cells |
| TGF-β | Tumor Growth Factor beta |
| TMB | tetramethylbenzidine |
| TNF | Tumor Necrosis Factor |
| VCAM-1 | Vascular Cell Adhesion Molecule 1 |
| VEGF | Vascular Endothelial Growth Factor |
| VLA-4 | Very Late Antigen-4 |
| VLA5A | fibronectin receptor |

**Acknowledgments/Danksagung**

Zu aller erst moechte ich mich bei Frau Prof. Dr. Leoni Kunz-Schughart fuer die Aufnahme in ihre Arbeitsgruppe und fuer die Bereitstellung des interessanten Themas bedanken. Ich danke ihr fuer alle wertvollen Ratschlaege waehrend unserer Zusammenarbeit.
Herrn Prof. Dr. Armin Kurtz moechte ich danken fuer die Uebernahme der Betreuung dieser Dissertation.

Herrn Prof. Dr. Ferdinand Hofstaedter, dem Direktor des Institutes fuer Pathologie der Universitaet Regensburg, danke ich fuer die Moeglichkeit, die Arbeit an seinem Institut durchzufuehren.

Prof. Dr. Marina Kreutz und PD Dr. Michael Rehli, Abteilung für Hämatologie und Internistische Onkologie der Universitaet Regensburg, gilt mein Dank fuer ihre Unterstuetzung und ihre Anregungen, die zur Erweiterung meines Methodenspektrums und damit zur Verbesserung dieser Arbeit fuehrten.

Bei Frau Marit Wondrak, Herrn Frank van Ray und Frau Brigitte Krause moechte ich mich bedanken fuer die geduldige Einfuehrung in Welt der Zellkultur. Sie haben mich in der Kultivierung und der Analyse von humanen Zellen unterwiesen und mich darüber hinaus in vielfaeltiger Weise unterstuetzt.

Ein ganz herzliches Dank gilt meinen Kollegen Dr. Juergen Friedrich und Dr. Wolfgang Eder und ebenso der ganzen befreundeten „Brockhoff AG“: PD Dr. Gero Brockhoff, Marietta Bock, Dr. Simone Diermeier-Daucher, Rosi Kromas, Andrea Sassen, Elisabeth Schmidt-Bruecken, Dr. Arabel Vollmann-Zwerenz fuer ihre Hilfsbereitigkeit, Offenheit und gemeinsam verbrachte gute Zeiten.

Ganz besonders moechte ich mich bei meiner Freundin Magdalena Szewczyk bedanken, die in ihrer spaerlichen Freizeit Zeit gefunden hat, diese Arbeit sprachlich zu korrigieren, und mir viele gute Ratschlaege zu geben.

Ein lieber Dank geht an meine Familie and Freunde in Polen, besonders an meine Eltern, Wanda Kadlubek und Magdalena Spychalska. Ohne ihre Unterstuezung und Liebe hätte diese Arbeit nicht entstehen können.

Ich widme diese Arbeit meinen Kindern – Alicja und Tadeusz

**Erklaerung**

Hiermit erklaere ich, dass ich die vorligende Arbeit selbstaendig und ohne frede Hilfe verfasst habe, und nur die von mir angegebenen Quellen und Hilfsmittel verwendet haben.
Diese Arbeit war bisher nicht Bestandteil eines Pruefungsverfahrens. Andere Promotionsversuche wurden nicht unternommen.

Gdynia, 2009